$5

# QEX

INCLUDING:
COMMUNICATIONS QUARTERLY

**Forum for Communications Experimenters**

January/February 2005
Issue No. 228

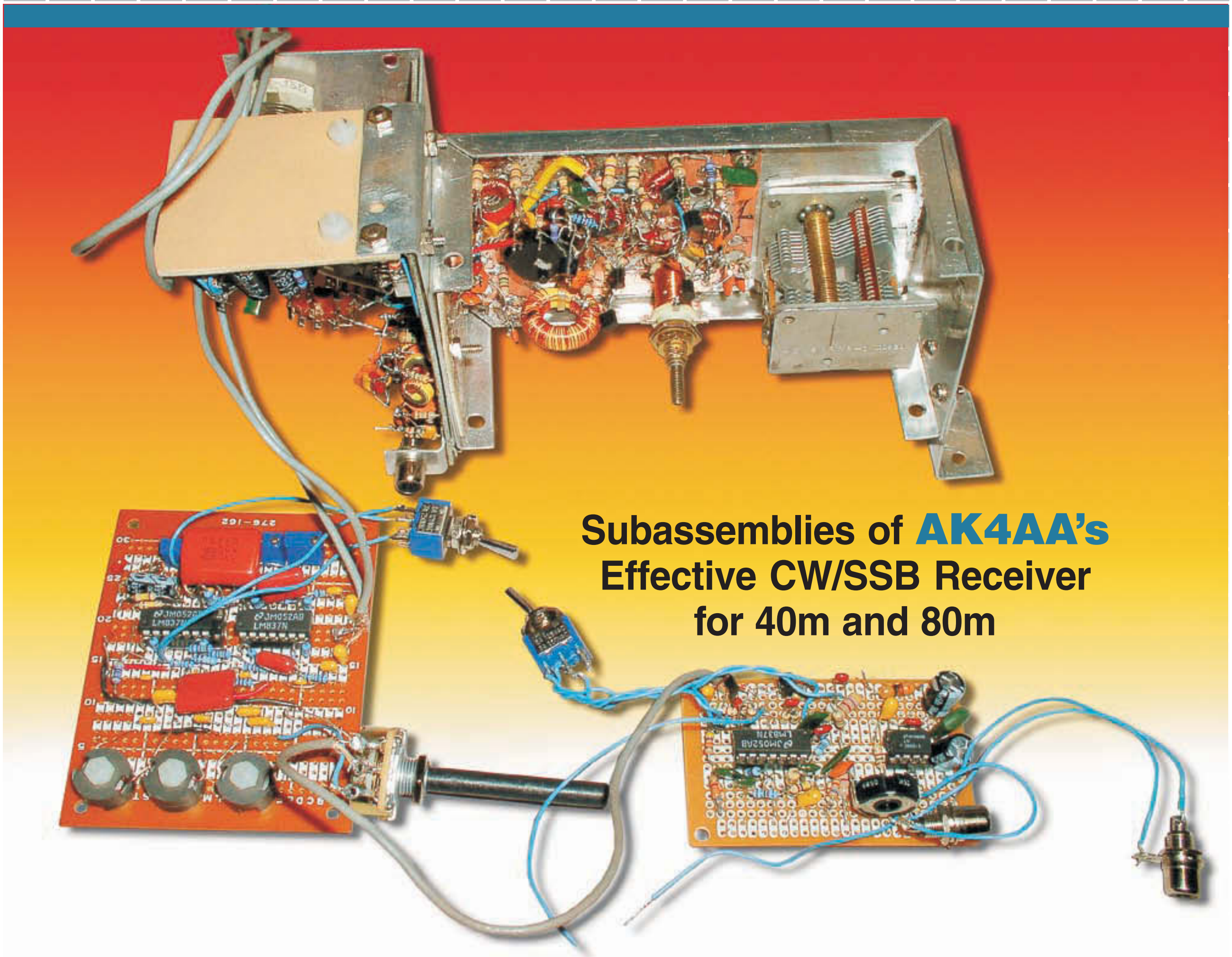

**Subassemblies of AK4AA's Effective CW/SSB Receiver for 40m and 80m**

ARRL The national association for AMATEUR RADIO
225 Main Street
Newington, CT USA 06111-1494

INCLUDING: COMMUNICATIONS QUARTERLY

*QEX* (ISSN: 0886-8093) is published bimonthly in January, March, May, July, September, and November by the American Radio Relay League, 225 Main Street, Newington CT 06111-1494. Periodicals postage paid at Hartford, CT and at additional mailing offices.

POSTMASTER: Send address changes to: QEX, 225 Main St, Newington, CT 06111-1494

Issue No 228



**Offices**

225 Main St, Newington, CT 06111-1494 USA
Telephone: 860-594-0200
Telex: 650215-5052 MCI
Fax: 860-594-0259 (24 hour direct line)
e-mail: **qex@arrl.org**

Subscription rate for 6 issues:

In the US: ARRL Member $24, nonmember $36;

US by First Class Mail: ARRL member $37, nonmember $49;

Elsewhere by Surface Mail (4-8 week delivery): ARRL member $31, nonmember $43;

Canada by Airmail: ARRL member $40, nonmember $52;

Elsewhere by Airmail: ARRL member $59, nonmember $71.

Members are asked to include their membership control number or a label from their *QST* when applying.

In order to ensure prompt delivery, we ask that you periodically check the address information on your mailing label. If you find any inaccuracies, please contact the Circulation Department immediately. Thank you for your assistance.




## About the Cover

**Dave Lyndon's (AK4AA) homebrew receiver starts on p 3.**

# Features



# Columns



# Jan/Feb 2005 *QEX* Advertising Index

## THE AMERICAN RADIO RELAY LEAGUE

The American Radio Relay League, Inc, is a noncommercial association of radio amateurs, organized for the promotion of interests in Amateur Radio communication and experimentation, for the establishment of networks to provide communications in the event of disasters or other emergencies, for the advancement of radio art and of the public welfare, for the representation of the radio amateur in legislative matters, and for the maintenance of fraternalism and a high standard of conduct.

ARRL is an incorporated association without capital stock chartered under the laws of the state of Connecticut, and is an exempt organization under Section 501(c)(3) of the Internal Revenue Code of 1986. Its affairs are governed by a Board of Directors, whose voting members are elected every two years by the general membership. The officers are elected or appointed by the Directors. The League is noncommercial, and no one who could gain financially from the shaping of its affairs is eligible for membership on its Board.

"Of, by, and for the radio amateur, "ARRL numbers within its ranks the vast majority of active amateurs in the nation and has a proud history of achievement as the standard-bearer in amateur affairs.

A bona fide interest in Amateur Radio is the only essential qualification of membership; an Amateur Radio license is not a prerequisite, although full voting membership is granted only to licensed amateurs in the US.

Membership inquiries and general correspondence should be addressed to the administrative headquarters at 225 Main Street, Newington, CT 06111 USA.

Telephone: 860-594-0200

FAX: 860-594-0259 (24-hour direct line)

**Officers**

***President:*** JIM D. HAYNIE, W5JBP
3226 Newcastle Dr, Dallas, TX 75220-1640
***Executive Vice President:*** DAVID SUMNER, K1ZZ

**The purpose of *QEX*** is to:
1) provide a medium for the exchange of ideas and information among Amateur Radio experimenters,
2) document advanced technical work in the Amateur Radio field, and
3) support efforts to advance the state of the Amateur Radio art.

All correspondence concerning *QEX* should be addressed to the American Radio Relay League, 225 Main Street, Newington, CT 06111 USA. Envelopes containing manuscripts and letters for publication in *QEX* should be marked Editor, *QEX*.

Both theoretical and practical technical articles are welcomed. Manuscripts should be submitted on IBM or Mac format 3.5-inch diskette in word-processor format, if possible. We can redraw any figures as long as their content is clear. Photos should be glossy, color or black-and-white prints of at least the size they are to appear in *QEX*. Further information for authors can be found on the Web at **www.arrl.org/qex/** or by e-mail to **qex@arrl.org**.

Any opinions expressed in *QEX* are those of the authors, not necessarily those of the Editor or the League. While we strive to ensure all material is technically correct, authors are expected to defend their own assertions. Products mentioned are included for your information only; no endorsement is implied. Readers are cautioned to verify the availability of products before sending money to vendors.


# *Empirical Outlook*

### Lies, Damned Lies and Statistics

With apologies to Benjamin Disraeli, our heading refers to precision and accuracy in measurement and estimation. After such a charged political cycle in the US, the foibles of pollsters provide a convenient start for discussion; but at the outset, let us agree to disagree. The question is: By how much?

*Precision* relates to the repeatability and consistency of measurements. We define *accuracy* as the degree to which measurements agree with some value of known precision. Those two terms apply to both political polling and electrical measurements, with some differences.

Imagine that we took a nationwide pre-election poll of registered voters to see how many votes each of two candidates was likely to get. Since we couldn't poll the entire electorate, we selected a sample of, say, 1200 at random. From that sample, we guessed how *all* national voters were going to vote. Because the sample was but 0.001% of the electorate, we declared a *margin of uncertainty* based on that sample size. We also guessed how many of those polled would change their minds between poll and election or simply not vote at all.

Through grungy statistical processes, we determined that our uncertainty was about ±3%. The two-man race seemed close but after the poll, however remote the chance, candidate A could have suddenly embraced some mortifying political position, and all 1200 in our sample would vote for candidate B, but the likelihood of that was virtually nil, especially if candidate A stuck to his advisors' (read *puppeteers'*) lines.

Then on Election Day, we take an exit poll. This time, we're sampling with higher inherent accuracy and precision, because we deem it quite unlikely that voters would lie to us about the choices they just made. Still, the size of the sample sets the margin of uncertainty when predicting the entire nation's vote.

At least one wag points out that if we combined the results of our polls with those of other pollsters, we'd get a larger sample size and less uncertainty. That's likely for truly random samples. In every case, though, we should really title our results, "Registered voters who respond to polls." Only a post-election tally reveals the accuracy of the polling and only then is the term *margin of error* appropriate.

In electronics, we rarely encounter precisely known quantities. Accordingly, a margin of uncertainty must accompany our measurements. Numerical results should appear with only as many significant figures as the margin of uncertainty supports.

For example, were we to state a receiver's noise figure as 7.1 dB, we'd imply that our uncertainty was ±0.1 dB; or if we announced a transmitter's power output to be 101 W, we'd tacitly claim an uncertainty of ±1 W or ±0.04 dB. That is, unless we explicitly stated a different margin!

Adherence to statistical rules is important politically and electronically, lest the results fall into the wrong category of this column's heading. It's just one of those many small improvements that might better our lot.

### In This Issue

Dave Lyndon, AK4AA, details his homebrew 80- and 40-m receiver. Dave takes a bit of the old and a bit of the new in his design.

Dennis Nendza, W7KMV, reports on building a messaging APRS tracker. He takes us through hardware, software, packaging and operation.

Bob Craiglow addresses some issues surrounding amplifier output impedance using nonlinear theory.

On the theoretical side of things, Stu Downs, WY6EE, contributes his look at why antennas radiate. Like the famous "Why is the sky blue?" question, getting a true understanding requires some study.

Randy Evans, KJ6PO, delivers ways to optimize phase-locked loop performance in frequency synthesis. His spreadsheets for type-1 and type-2 loops allow simulation beyond "cookbook" predictions of performance

Zack Lau, W1VT, presents a 10-GHz waveguide preamplifier in *RF*—
*Doug Smith, KF6DX, **kf6dx@arrl.org***

# An Effective 80 and 40 Meter SSB/CW Receiver

*Something old and something new in a homebrew dual-band receiver.*

By Dave Lyndon, AK4AA

There is no limit to the number of possible architectures for amateur-band receivers. This is yet another entry, an 80- and 40-meter SSB/CW receiver that uses modern technology (something new) to implement a high-performance design in a small package with its roots in the 1950s and 60s (something old). In addition, there's something borrowed, too. Although relying heavily on ARRL *Handbooks* and personal experience, much of the circuitry was borrowed from others without embarrassment. (I only steal from the very best! See the references at the end of this article for acknowledgements.) It has noise-figure, dynamic-range, and intermodulation performance as good as most high-quality commercial receivers, and it's better than many.

85 Woody Farm Rd
Hot Spring, NC 28743
**dlyndon@director.com**

The receiver is kept as simple as possible without sacrificing performance by foregoing optional bells and whistles. However, it is not a weekend project, nor a task for the faint-hearted. It will take some time and patience to duplicate, but the result will be rewarding—and relatively inexpensive, too. New parts are readily available from various sources on the Internet and can be purchased for less than $200. A well-endowed junk box will reduce that considerably. You will also need some test equipment to make various adjustments. My test bench is quite modest: an inexpensive digital multimeter, a 20 kΩ/V analog multimeter, an old Heathkit audio signal generator, an even-more-ancient Heathkit RF signal generator, a "bottom-of-the-line" frequency counter, a vintage 20 MHz dual-channel oscilloscope and a homebrew inductance meter described in Reference 8. You can get through this project with less equipment, but I found the scope and counter invaluable. It's amazing what can be accomplished with reasonably simple tools.

Fig 1 is a photograph of the completed receiver, and Fig 2 is the block diagram. The antenna is connected to the first mixer through passive filters that select either the 80- or 40-meter band. The local oscillator is a VFO, tunable from 5.2 to 5.7 MHz.

Signals either from 3.5 to 4.0 MHz or 6.9 to 7.4 MHz (7.0 to 7.3 MHz is the 40-meter amateur band) are down-converted to a common intermediate frequency of 1.7 MHz depending on which input filter is selected. A low-noise IF amplifier with manual gain control provides sufficient amplification to compensate for the losses of the first and second mixers, thus establishing a noise figure suitable for these bands, which are dominated by atmospheric rather than receiver noise. Consequently, there is no need for an RF preamplifier, which, if present, would very likely reduce the dynamic range and increase inter-modulation distortion.

From this point forward, the design is that of a 1.7-MHz direct-conversion receiver using the phasing method of sideband selection. The output of the IF amplifier is in phase simultaneously to two mixers. The local oscillator for those mixers is a 1.7-MHz oscillator that tunes ±3 kHz. In earlier ham parlance, we would have called this the beat frequency oscillator (BFO), and we shall use that terminology here. Once a signal is tuned in with the VFO, a very-fine tuning adjustment can be made with the BFO tuning control if desired. After isolating amplifiers, a hybrid phase shifter provides two LO signals in phase quadrature (90° out of phase) to the I (in phase) and Q (quadrature) second mixers.

The resulting low-level I and Q channel baseband (audio) signals, 90° out of phase, are amplified by nearly identical low-noise amplifiers, and then fed to I and Q audio phase-shift networks that have a 90° phase difference over the band of interest, 300-3000 Hz. By adding or subtracting the resulting phase shifted audio signals in an opamp, we select the upper or lower sideband.

Once the I and Q baseband signals have been combined, the SSB bandwidth is established by 3000 Hz low pass and 300 Hz high pass passive filters. Since there is no automatic gain control, a manual audio-gain control sets the level prior to further processing to use the full dynamic range of the preceding circuitry without overloading subsequent stages. For CW, a three-pole active filter with a 600-900 Hz passband may be switched into the signal path. Another circuit mutes the receiver during transmit periods, and an optional reed relay protects the first mixer from strong transmit/receive relay leakage. Line-level audio output is available for further external audio processing, and a minimal IC audio amplifier is included with sufficient power to drive headphones or a speaker. It is preceded by a secondary audio level control that does not affect the line output level.

One of the obstacles to building a receiver with a manually tuned VFO is a suitable mechanical tuning mechanism for the variable capacitor. Hard to find today, they were once ubiquitous in various forms (more something old), but not to worry. With hand tools and a soldering iron you can build your own from a coffee can, an old potentiometer, a spare tuning knob, a small spring, and a bit of dial cord. Don't laugh. Historically scorned by hams, this dial drive provides a 16 to 1 turns ratio with exceptionally smooth tuning, rock-solid positioning, and absolutely no discernable backlash. Its construction is described in the Appendix for the adventuresome.

The circuitry was arranged in functional groups on five circuit boards:


**Fig 1—The completed receiver.**

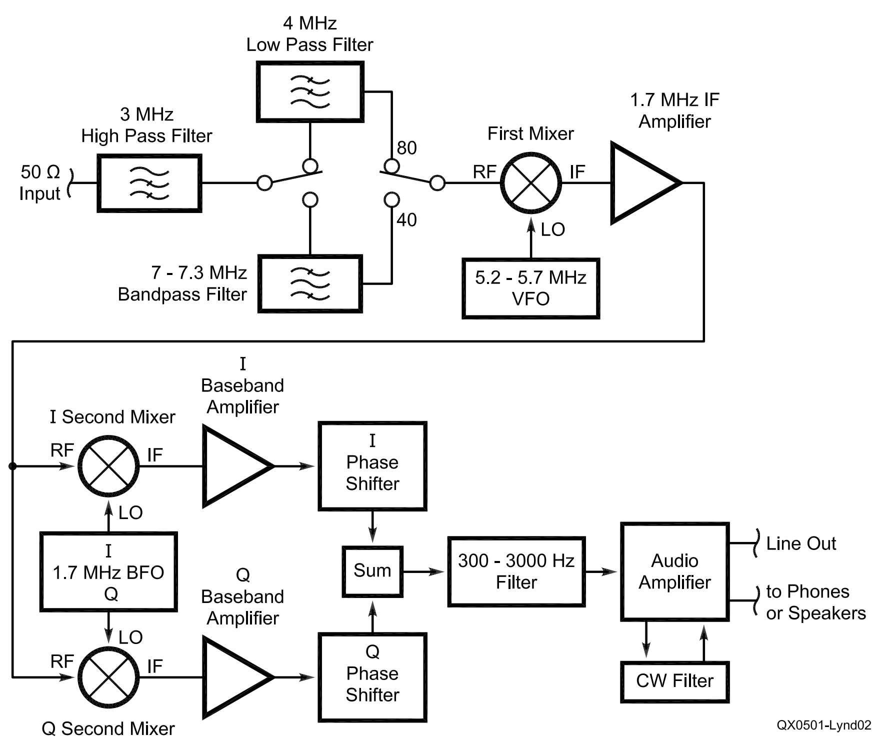


**Fig 2—The receiver block diagram.**

(1) the RF/IF Board, (2) the Oscillator Board in its own minibox, (3) the Baseband Amplifier Board, (4) the Phase Shifter/Filter Board, and (5) the Audio Board. Details of each board and its associated chassis components follow; you can look to the references for further elaboration. Since there are many toroidal inductors in the receiver, you should read my suggestions on winding toroidal inductors with magnet wire in the sidebar, "Toroid Winding Tips."

**RF/IF Board (Fig 3)**

This board was constructed on a single-sided circuit board using "ugly" and "dead-bug" methods. The copper foil is a ground plane to which ground connections can be made directly. Other connections are supported by standoffs (1 MΩ resistors with one end soldered to the ground plane) where required.

The first filter section is a 50-Ω high-pass filter with its cutoff just below the 80-meter band. It rejects strong broadcast-band signals below 3 MHz in all but the most severe environments, and it remains in the signal path when switching to the 40-meter band for that same purpose. A 50-Ω low-pass filter (cutoff just above 4 MHz) is switched in for the 80-meter band. This eliptical filter has a sharp cutoff to reject the image frequencies between 6.9 and 7.4 MHz. The insertion loss in the passband of the first and second filter sections in series is about 1 dB.

The 40-meter filter consists of a high-pass eliptical filter with a 6.9 MHz cutoff (needed to reject the 80-meter image) followed by two capacitively coupled parallel-tuned circuits. The inductors are tapped to obtain 50-Ω input and output impedances, while retaining the high Q needed for good

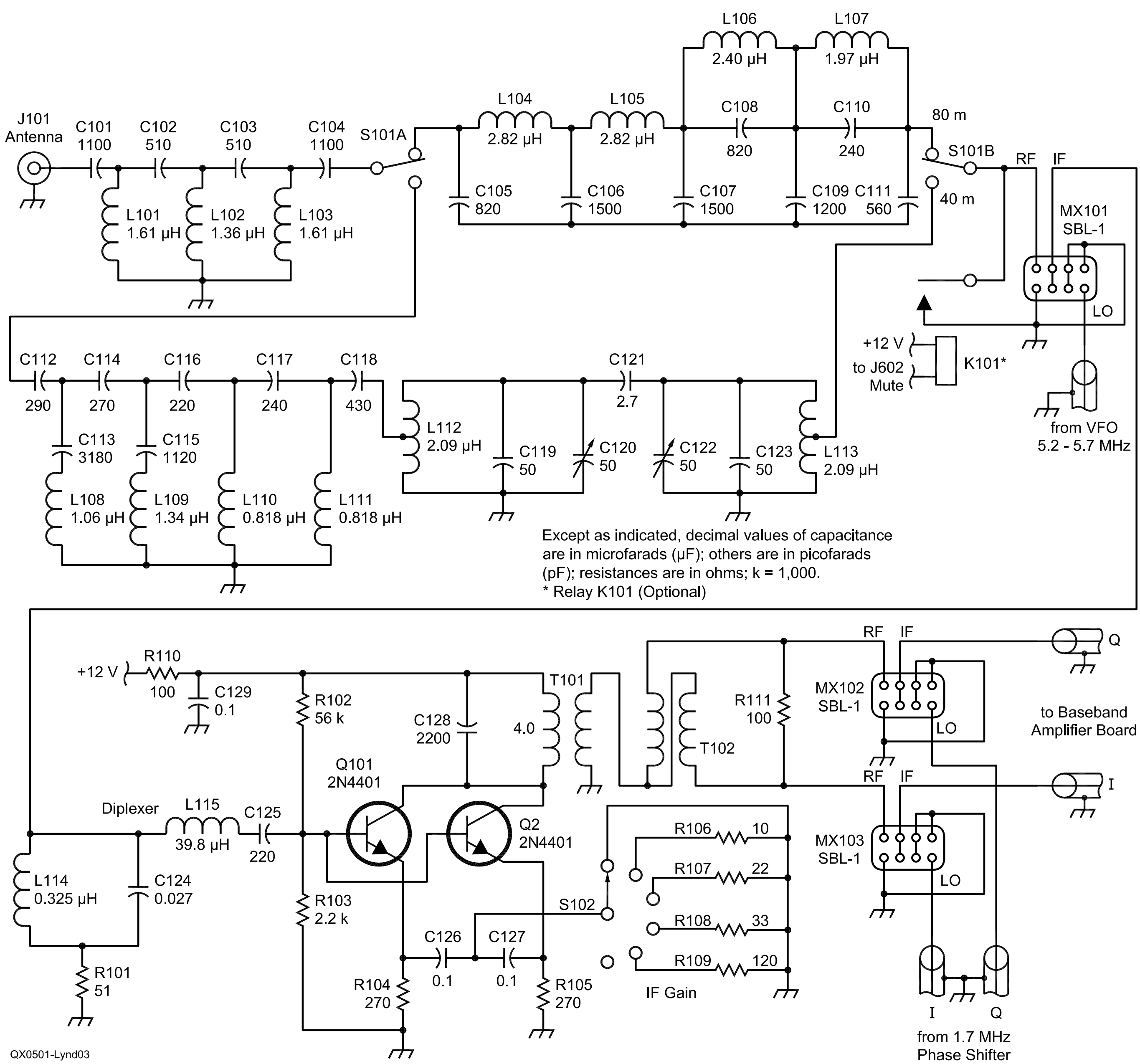


Fig 3—The RF/IF board.

selectivity. The circuits are stagger-tuned with their variable capacitors set for flattest response over the 7.0-7.3 MHz range. When properly adjusted, the image frequencies for either band are rejected by at least 60 dB (good enough) and theoretically 80 dB. I don't have the equipment to confirm that level of rejection was achieved, but my crude measurements were encouraging. The sharp-cutoff elliptical filters make this possible, so Table 1 includes the design resonant frequencies for the eliptical sections of the filters, and it is advisable to measure them before connection.

The SBL-1 doubly balanced diode first mixer down-converts the selected-input signal band to the 1.7-MHz IF when mixed with the VFO local oscillator. The LO level is +7 dBm, adjusted as described in the "Oscillator Board" section. Higher-order mixing products are safely outside this IF, so spurious "birdies" are absent. This small device is held in place on the board in dead-bug style by soldering bare wire from two opposite-end ground pins directly to the ground plane. A TUF-1 mixer could be used instead of the SBL-1, and it is quite a bit smaller.

The 1.7-MHz IF amplifier is two low-noise NPN transistors wired in parallel with some shunt feedback, and it provides the low input impedance necessary to properly terminate the first mixer. Proper termination insures the low intermodulation distortion needed to detect weak signals in the vicinity of strong signals, so a diplexer is used to send frequencies below and above 1.7 MHz to a 50 Ω resistive load and to pass 1.7 MHz to the 50-Ω amplifier input. The 1.7-MHz series-resonant frequency of L115 and C125 should be verified by measurement. Inexpensive 2N4401 transistors are ideal for this application, and 2N2222s are almost as good. Very narrow bandwidth is not required here, so the output load is a single parallel-tuned circuit, the primary of an RF transformer. The untuned secondary of this RF transformer drives a bifilar power divider that feeds two equal, in-phase signals to the I and Q SBL-1 mixers. Each winding presents a 50-Ω output impedance in combination with the 100-Ω isolating resistor, R111.

The IF gain can be reduced manually for very strong signals prior to baseband detection and audio amplification, thus increasing the dynamic range. The gain is changed by switching in resistors that change the emitter degeneration for RF without affecting the dc bias. Higher resistances provide more degeneration and lower the gain. With the resistance values shown, the gain is adjustable from about +23 dB to 0 dB in roughly 5 dB steps. The conversion loss and noise figure of each mixer when properly terminated. The IF gain is sufficient to overcome those losses while adding less than 2 dB to the overall receiver noise figure. Lacking suitable measurement equipment to confirm it absolutely, I estimate the Noise Figure of the receiver to be about 12 dB, more than adequate for these environmentally noisy bands.

The SBL-1 I and Q doubly balanced diode mixers receive their independent LO signals from the BFO phase shifter described in the "Oscillator

**Table 1**
**Coil-Winding Data**

| *SYMBOL* | *VALUE* | *FORM* | *TURNS* | *WIRE SIZE (AWG)* | *REMARKS* |
|---|---|---|---|---|---|
| L101 | 1.61 µH | T37-6 | 22 | 26 | |
| L102 | 1.38 µH | T37-6 | 19 | 26 | |
| L103 | 1.61 µH | T37-6 | 22 | 26 | |
| L104 | 2.82 µH | T50-6 | 25 | 24 | |
| L105 | 2.82 µH | T50-6 | 25 | 24 | |
| L106 | 2.40 µH | T50-6 | 22 | 24 | Resonates with C108 at 11.4 MHz |
| L107 | 1.97 µH | T50-6 | 20 | 24 | Resonates with C110 at 7.44 MHz |
| L108 | 1.06 µH | T37-6 | 16 | 26 | Resonates with C113 at 2.74 MHz |
| L109 | 1.34 µH | T37-6 | 18 | 26 | Resonates with C115 at 4.10 MHz |
| L110 | 0.818 µH | T30-6 | 15 | 28 | |
| L111 | 0.818 µH | T30-6 | 15 | 28 | |
| L112 | 2.09 µH | T30-6 | 22/4 | 28 | 22 turns tapped at 4 turns |
| L113 | 2.09 µH | T30-6 | 22/4 | 28 | 22 turns tapped at 4 turns |
| L114 | 0.325 µH | T25-2 | 3 | 24 | Resonates with C124 at 1.7MHz |
| L115 | 39.8 µH | T68-2 | 84 | 30 | Resonates with C125 at 1.7MHz |
| T101 | 4.0 µH | T50-2 | 28 & 16 | 24 | Primary resonates with C128 at 1.7MHz |
| T102 | 6.72 µH* | FT37-43 | 4 & 4 | 24 | 4 turns, bifillar-wound transformer |
| L201 | 11.2 µH | Slug Tuned | 40 | 26 | 1/2-inch OD ceramic slug-tuned coil form |
| L202 | 1000 µH* | FT37-43 | 48 | 32 | broadband RF choke |
| L203 | 18.3 µH | T80-6 | 60/15 | 28 | 60 turns tapped at 15 turns |
| T201 | 168 µH* | FT37-43 | 20 & 4 | 28 | Broadband transformer |
| T202 | 82.3 µH* | FT37-43 | 14 & 14 | 28 | 14 turns bifillar transformer |
| T203 | 4.70 µH* | T50-2 | 31 & 31 | 30 | 13 turns bifillar hybrid transformer |
| L301 | 47 mH | PC-1408-77 | 155 | 36 | 2 required, matched |
| L302 | 1.2 mH | FT37-77 | 35 | 30 | 2 required, matched |
| L401 | 137 mH | PC-1408-77 | 260 | 36 | |
| L402 | 40.5 mH | PC-1408-77 | 144 | 36 | |
| L403 | 40.5 mH | PC-1408-77 | 144 | 36 | |

*Use the number of turns given. The inductance value is approximate, not critical.

Board" section. These levels, too, are + 7 dBm for best performance. These devices are held in place as dead-bugs also by soldering bare wires from two opposite-end ground pins directly to the ground plane. The outputs of the I and Q mixers are fed directly to matched amplifiers on the Baseband Audio Board.

**Oscillator Board (Fig 4)**

This board is also ugly construction on a single-sided board. The series-tuned Colpitts VFO (remember those?) uses an MPF102 JFET operating from + 6 V regulated by a Zener diode. Output level is sacrificed for the frequency stability for which this circuit is noted. All capacitors in this circuit are zero-temperature-coefficient (NP0) ceramics. The tuning capacitor is an old-fashioned 15 to 365 pF non-linear capacitor with good mechanical stability (again, something old). Its characteristic (approximately capacitance squared versus rotation) provides a reasonably linear dial in this circuit. Such capacitors are available from Internet suppliers or possibly through junk-box trading. The one I used was a small two-section type, wired in parallel to give the required capacitance. The VFO inductor is the only slug-tuned inductor in the receiver; use a high-quality ceramic coil form. For best temperature stability, the number of turns is such that the slug is just barely into the winding, thus minimizing its contribution to temperature drift while providing sufficient adjustment to set the VFO frequency. Alternatively, a toroidal inductor could be used here. Type-6 powdered-iron material has the best temperature stability, although not as good as the tunable coil inductor. A trimming capacitor would be needed in that case; but since most miniature trimmers are not very stable, the slug-tuned inductor with fixed capacitors (other than the tuning capacitor) seems a better choice.

The frequency range is established by the fixed capacitors in parallel with the variable capacitor. Select the fixed capacitors for a bandspread just slightly wider than the required 5.2-5.7 MHz.

An MPF-102 JFET source follower isolates the oscillator from subsequent load variations. The output level needed from the subsequent transistor amplifier is +7 dBm into 50 Ω. Adjust the level by changing the small coupling capacitor from the source follower to the amplifier. Temporarily connect a 50-Ω resistive load, and once the level is set, remove the 50-Ω load and connect the output to the first mixer's

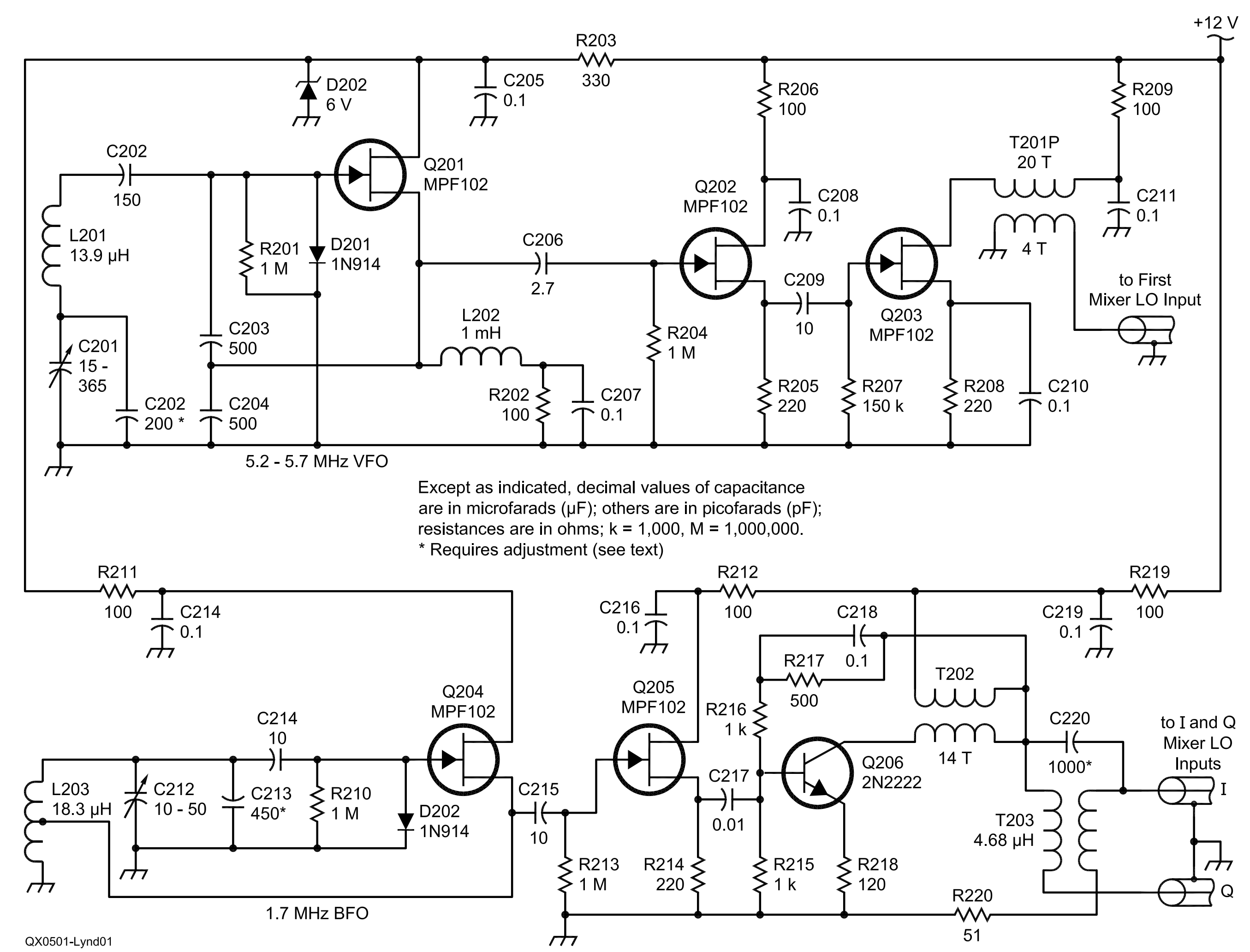


Fig 4—The Oscillator board.

LO terminal. Lacking a power meter, I adjusted the level to 1.4 $V_{P-P}$ with a broadband oscilloscope (1.4 $V_{P-P}$ = 0.7 $V_{Pk}$ = 0.49 $V_{RMS}$ = 4.8 mW into 50 Ω = +6.9 dBm.) The frequency variation from cold start to operating temperature in 70° F ambient was less than 500 Hz in the first half hour. After that, it was less than 50 Hz over a considerable period. Long contacts will not require retuning. That's not too bad for mostly junk-box parts!

The 1.7-MHz BFO is a conventional Hartley oscillator also using an MPF-102 JFET operating from the +6 V Zener. In this case, a type-6-material toroid is suitable. (The 1.7-MHz frequency is a smidge lower than recommended for high Q.) It is held securely in place upright by a plastic tie-wrap inserted through a small hole in the circuit board, looped through the toroid, routed back through the hole, and pulled taught through the locking slot of the tie-wrap. At 1.7 MHz, the frequency drift is as good as the VFO and tends to be in the opposite direction. The total drift is quite acceptable for both SSB and CW. Again, NP0 ceramic capacitors were used throughout, except for a small front-panel-mounted variable capacitor, C212, that is connected to the oscillator tank via a miniature shielded coaxial cable. The capacitance of the cable, 10 pF or so for about 4 inches, becomes a part of the tuned circuit, so it must be stable. I used a short length of one of the two small 72-Ω coax cables in an S-video cable. With the variable capacitor at its center position, the BFO center frequency is set to 1.7 MHz by selecting fixed NP0 capacitors and a small trimmer included for final adjustment. At this lower frequency, it is stable enough. The approximate values shown provided front-panel tuning of ±3 kHz after removing a couple of rotator plates from the capacitor I had on hand to get the required range.

The oscillator is followed by a JFET source follower for load isolation then an NPN transistor amplifier. The amplifier is a widely used low-output-impedance broadband circuit. Its gain is established by the ratio of resistors R217 and R216; the former is bypassed for RF, the latter is not. A larger R216 reduces RF feedback and increases the gain; a smaller R216 increases the RF feedback and lowers the gain. The total series resistance of R217 and R216 must be kept the same to properly bias the transistor. We need about +10 dBm of output (2.0 $V_{P-P}$ on the oscilloscope feeding a temporary 50-Ω resistor) to

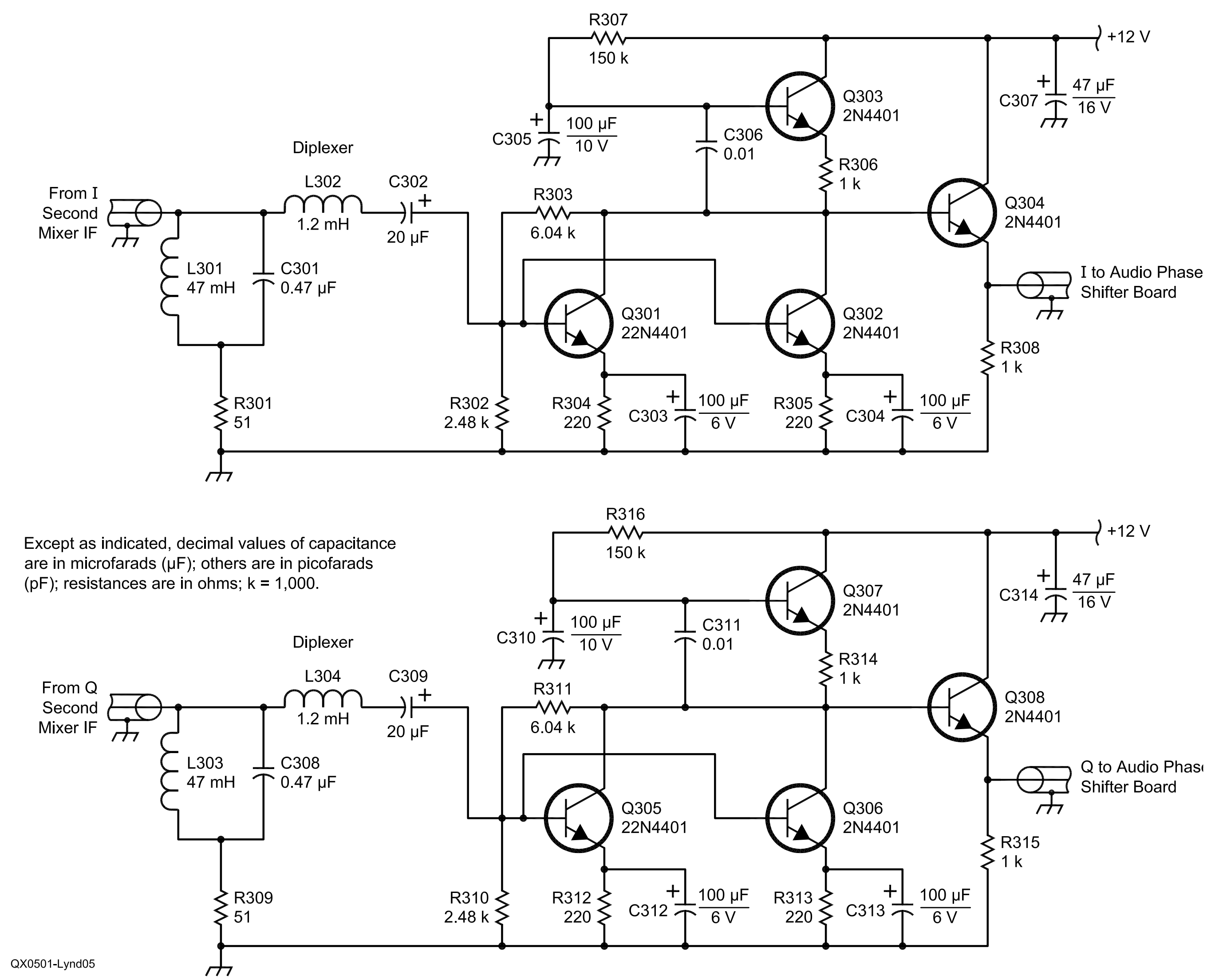


**Fig 5—The baseband (audio) board.**

provide +7 dBm LO signals out of the hybrid phase shifter to each of the two baseband mixers, and the component values shown should yield that result approximately.

A twisted-wire hybrid phase shifter, described in Reference 4, was used to divide the +10 dBm signal into two +7 dBm signals in phase quadrature. There are several possible RF phase-shift networks; but this circuit, while analytically mysterious, is simple to construct and requires no adjustment over a wide frequency range. This variant uses a single capacitor rather than two but is electrically equivalent to the original described in the reference. Precise 90° phase shift can be achieved by adjustment of the capacitance as described below. Its output levels change with frequency but remain 90° apart to enable excellent sideband rejection. With the values shown, the two outputs near 1.7 MHz will be nearly equal, about +7 dBm (1.4 $V_{P\text{-}P}$) when terminated with individual 50-Ω resistors. Once the levels are set by adjusting the gain of the amplifier, remove the terminating resistors and connect the outputs to the I and Q baseband mixers' LO terminals.

**Baseband Audio Board (Fig 5)**

This is the third ugly construction board. This board and part of the following board are stolen from the excellent designs of Glen Leinweber, VE3DNL, noted in Reference 4. Much of this work was based on the earlier work of Rick Campbell, KK7B, as cited in the references.

As Campbell and Leinweber have so eloquently informed us, the I and Q mixers must be properly terminated at all frequencies to provide the desired performance. For this purpose we use a diplexer that routes signals below 300 Hz and above 3000 Hz to a 50-Ω terminating resistor, while signals of interest are sent to an audio amplifier with 50-Ω input impedance. We need a lot of low-noise audio gain because the weakest signals from the I and Q mixers will be in the microvolt range. Furthermore, the diplexers and audio amplifiers in the I and Q channels must match each other as closely as possible to achieve good unwanted-sideband rejection. For that reason, we use 1%-matched components in the two channels. We can compensate for minor gain imbalance downstream, but phase-shift balance of 1° or better is required for good sideband rejection.

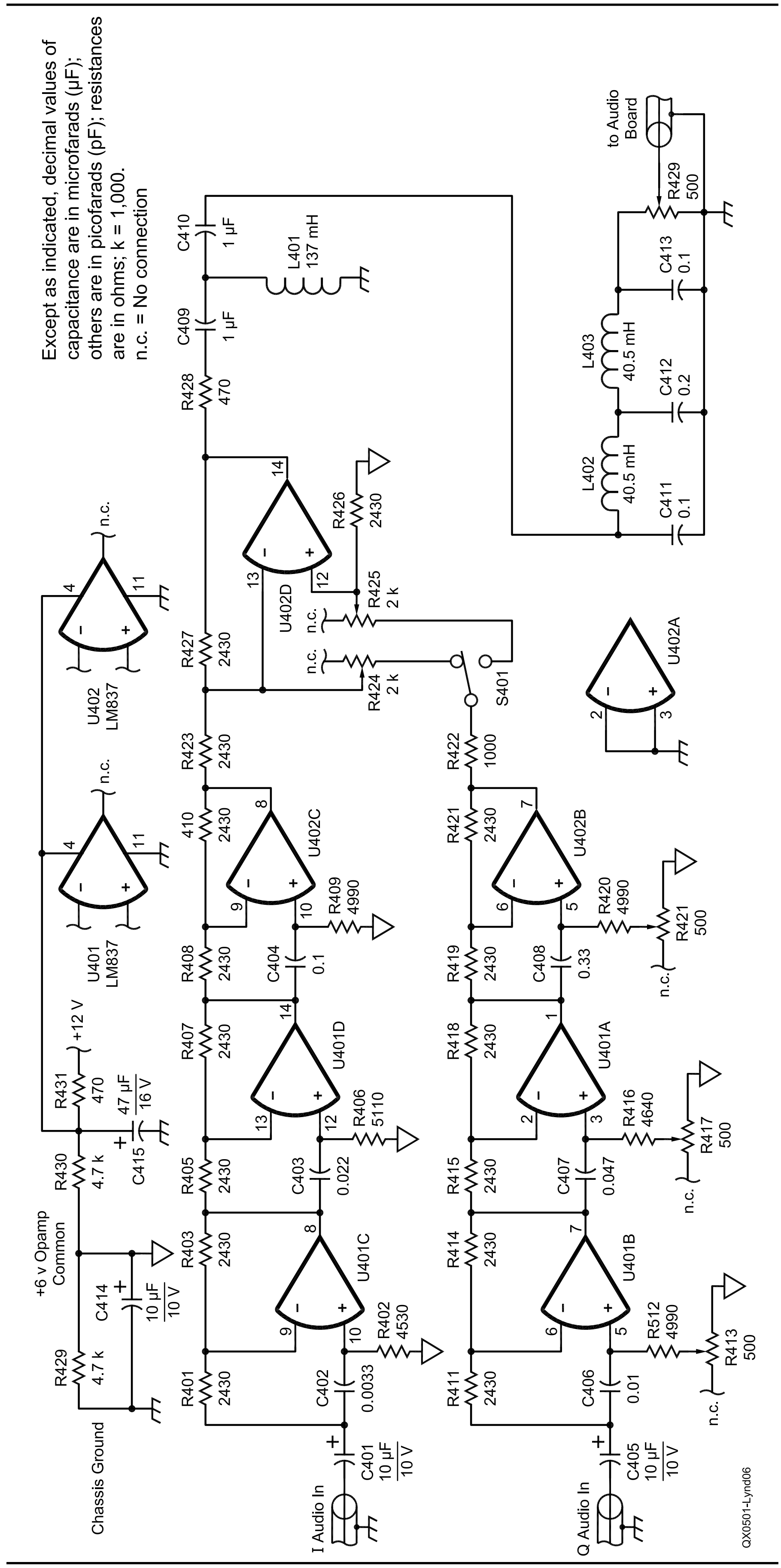


**Fig 6 (Right) —The phase shifter/filter board.**

On the advice of Leinweber, I used PC1408-77 pot cores available from Amidon to get high inductance with reasonable Q. Careful attention to equal turns count and equal plastic mounting-screw pressure will yield the desired result. Be careful not to over tighten the hardware because the cores are fragile, as I discovered to my regret. The exact inductance value is less important than is matching (equal values). If suitable test equipment is available, the inductor values should be measured. The most phase-critical components in the diplexers, however, are the series-tuned LC circuits that pass the audio frequencies to the amplifiers. You can check the amplifiers' phase shift by driving both channels with the same 1000-Hz audio signal at the diplexer inputs and observing the sum of the amplifier outputs on a dual-channel scope, with one channel inverted and the scope channel gains adjusted for the best null. Then check for nulls at 300 Hz and 3000 Hz with the same signal connected to both inputs. If there is not a good null at both frequencies, there is a phase difference in the channels, and it is more than likely caused by imbalance in the diplexers. In that case, you must adjust the inductance, capacitance or both in one channel or the other. The phase shift at 300 Hz is affected mostly by the series capacitance, so adding capacitance to one channel or the other will improve the low-frequency null. Similarly, the series inductor will dominate the phase shift at 3000 Hz, and it may be necessary to unwind a few turns on one inductor or the other to get a good high-frequency null. A final check using a Lissajous pattern (if your scope is so endowed) will show a straight line at 45° with no ellipticity (separation) over the audio range.

**Phase Shifter/Filter Board (Fig 6)**

This board and the Audio Board are built on prefabricated integrated-circuit experimental boards. Sockets were used for the integrated circuits although the devices could be soldered in directly at the risk of damaging them. Perfboard may even be preferable because the pads on prefab circuit boards are difficult to solder and may lift off. For the ambitious, a custom printed circuit board could be developed. Perhaps I would do that (for all the boards) if there is sufficient interest.

The I and Q audio phase shifters are implemented with quad low-noise op amps. The theory of operation is beyond the scope of this article; but with careful adjustment, the receiver is capable of at least 40 dB of unwanted sideband rejection. With extra care and patience 50 dB is possible, and 60 dB can be achieved with realizable components.

It is important to use stable 1%-tolerance capacitors in this network, and several types are available. I used polystyrene capacitors, although they are pricey and undesirably large. Trimming resistors in the Q network are used to finely adjust the phase shift. Leinweber describes a method for adjusting these trimmers using a homebrew quadrature square-wave oscillator; I shall suggest a simpler method below.

The entire receiver operates from a single +12-V power supply, but the op amps require both positive and negative supply voltages. To avoid the complexity and expense of dual power supplies, an artificial signal common is established +6 V above chassis ground using a "stiff" voltage divider. Thus, voltages +6 V above and -6 V below the signal common potential are established.

Outputs of the I and Q phase shifters are summed in an op amp to reject one sideband. By switching the Q output to the non-inverting input—in effect shifting its phase 180°—the opposite sideband is rejected. The resulting SSB signal is then filtered by a 500-Ω passive network consisting of a five-pole 3000-Hz low-pass filter and a three-pole 300-Hz high-pass filter implemented with pot-core inductors and stable capacitors. A 500-Ω potentiometer terminates the network and is the audio gain control.

Adjustment requires a pair of audio signals in phase quadrature at 3400, 715, and 295 Hz, in turn. The Leinweber method uses a homebrew circuit to create these signals as square waves (see Reference 4), but harmonic filtering is required to observe the fundamental only. Another method is to use the front end of the receiver itself to generate the quadrature audio signals. I found that both methods give nearly the same result. It relies on the 1.7 MHz hybrid phase shifter's correct LO phase relationships, so initially we must trust in that circuit's performance prior to final adjustment.

Insert a low-level 80-meter signal from an RF signal generator or test oscillator at the antenna input. While monitoring the signal at the audio-gain control with the scope, tune the receiver to obtain an audio output. That audio frequency can be measured with a frequency counter or by comparison with an accurate audio oscillator us-

### Toroid Winding Tips

The enamel must be removed from the wire, of course, for solder connections where required, either chemically or by scraping with a sharp knife. I prefer the latter method. For mechanical stability I recommend that the first and last turn on each inductor be "tucked under" itself and pulled taught, taking care not to damage the enamel, which would short the turn. The inductance of these toroids can be adjusted over a range of ±5% or so by spreading or compressing the turns. The number of turns and their spacing is more important than the wire size, so one should generally use the largest wire that will fit comfortably on the core and allow for some adjustment. For maximum Q, the winding should cover only about 3/4 of the core circumference. Turns-versus-inductance formulas for these toroids are approximations. It may be necessary to add or remove turns to achieve the desired inductance. I have found the formulas generally call for too many turns, so inductance measurement is required. One method for doing this was described in my *QEX* article (Reference 8). For the bifilar windings specified, twist two lengths of magnet wire together with about eight turns per inch. This insures that the two windings are closely coupled, of the same length and same number of turns. Once the inductance is correct, generously apply coil dope to prevent winding movement. Clear nail polish works very well for this purpose. Table 1 provides the turns and wire sizes actually used for the inductors and RF transformers in the receiver.

The receiver uses several pot-core inductors, available from Amidon, for the higher inductances values required in the audio circuits. Many turns (hundreds) of very fine magnet wire must be wound on the plastic bobbin provided with the cores. That fine wire is fragile and difficult to connect externally. Borrow a technique used in transformers: Strip and wind an inch or so of each fine-wire end over the stripped end of a larger-diameter insulated wire, solder the joint, coat the connection with coil dope (nail polish) for insulation and wind the last few coil turns with the larger wire, which seves as a lead for the transformer. To prevent slippage of the winding, the final turn is "looped under" and pulled taught as is done for the toroids. Apply a coat of dope over the winding.

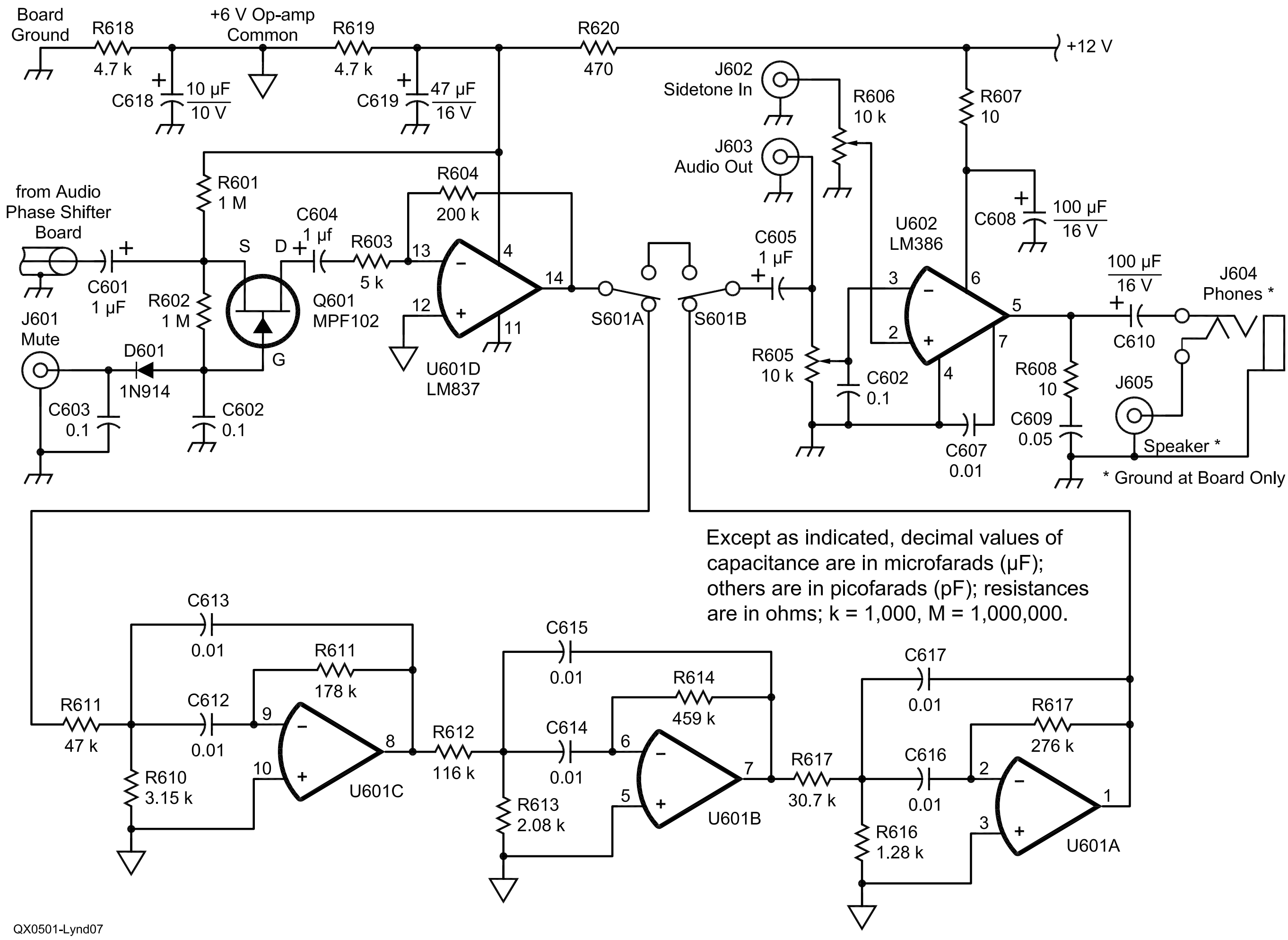


**Fig 7—The audio board.**

ing a Lisajous presentation on the scope, or it can be estimated by using the scope's time base. Tune the receiver to obtain a 3400-Hz audio signal (the BFO tuning will come in handy here), and then switch the sideband selector. The opposite sideband amplitude should be significantly lower. First, adjust the balance control, R424 or R425, whichever has an effect, for a null, increasing the scope gain as necessary to observe the weak signal at null. Next, adjust R406 for a null, and then adjust these two controls alternately for best null. Now retune the receiver slightly to the opposite sideband and obtain a 3400-Hz signal in the sideband previously rejected. Switch the sideband selector and adjust the other balance control, R425 or R424, for a null in the new rejected sideband. Similarly, obtain signals at 715 and 295 Hz by retuning the receiver and adjust R406 and R409, respectively, without disturbing the

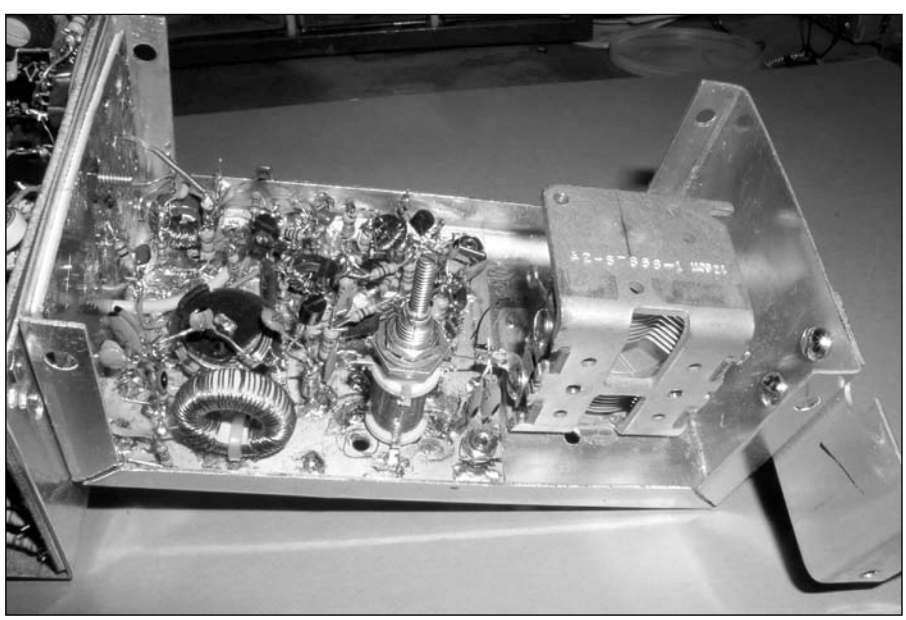

**Fig 8—The VFO tuning capacitor inside, mounted on the front of the more-rigid box section that has the folded tabs.**

amplitude-balance controls. With generous portions of care and patience, iteration of these five adjustments will yield optimum performance.

If good nulls of approximately equal rejection cannot be obtained on both upper and lower sidebands using the sum and difference balance adjustments only with common audio phase shifter adjustments, the 1.7-MHz hybrid phase shifter may not be providing signals exactly 90° out of phase. Add (or subtract) a bit of capacitance to C 220 in increments of about 50 pF and try again at 4300 Hz. When the hybrid's outputs are in phase quadrature, it should be possible to get both upper and lower sideband rejection of at least 40 dB (100:1 voltage ratio between sidebands) with the same set of phase adjustments in the audio phase shifter. I got 46 dB without much trouble, and 50 dB with a little patience.

**Audio Board (Fig 7)**

Another stiff voltage divider is used to establish an artificial signal common at +6 V for this board's op amps. The signal passes first through a JFET transistor used to mute the receiver during transmit by grounding the cathode of diode D601 to bias the transistor off. The following stage is an op amp with 26 dB gain to raise the signal to a line level suitable for external audio processing.

The three-pole band-pass active filter may be switched into the signal path for CW reception. It has a 3-dB bandwidth of 400 Hz centered on 750 Hz. The resistor values were chosen such that all capacitors in the filter are the same value, 0.01 µF. They need not be this exact value, but their values should match within 3% for best filter performance. The non-standard resistance values are series/parallel combinations of resistors as measured with a DMM. Notice that each stage's input signal is attenuated; these band-pass stages have considerable gain that must be compensated to avoid downstream overload. The overall gain of the filter is about 10 dB, and that provides a reasonable balance of audible signal level when switching the narrow filter in and out. A secondary audio-gain control is provided to set the level for the optional IC headphone and speaker amplifier that follows. This amplifier will also accept an input for a CW sidetone if desired.

**Power Supply**

A single external +12 V source is required. It must supply about 100 mA, but if the on-board audio power amplifier is used to drive a speaker, the current will peak to twice that value at full volume. Obviously, the receiver is well suited for field or emergency operation since it can be operated from a 12 V battery.

**Construction (Figs 8 through 11)**

The receiver is housed in a 5×10×3 inch aluminum chassis (Bud BPA-1591 or equivalent) with the 5×10 inch surface as the front panel. A window in the front panel allows viewing a portion of the rotary dial. Of course, a more exotic (and expensive) enclosure could be used, and a bit more space would be a welcome luxury. Nevertheless, this is a description of the receiver as actually constructed.

The phase shifter/filter board is mounted inside the chassis on one end and the audio board on the bottom, both with ¼-inch standoff hardware to hold the boards' underside wiring off the chassis. They are positioned to allow clearance for the minibox assembly described below. The SIDEBAND selector switch and the main AUDIO GAIN control are the front panel controls associated with the phase shifter/filter board, and they are mounted on the front panel near that board. Similarly, the headphone/speaker VOLUME control, the ungrounded speaker and headphone jacks, and the CW filter switch are mounted on the front panel

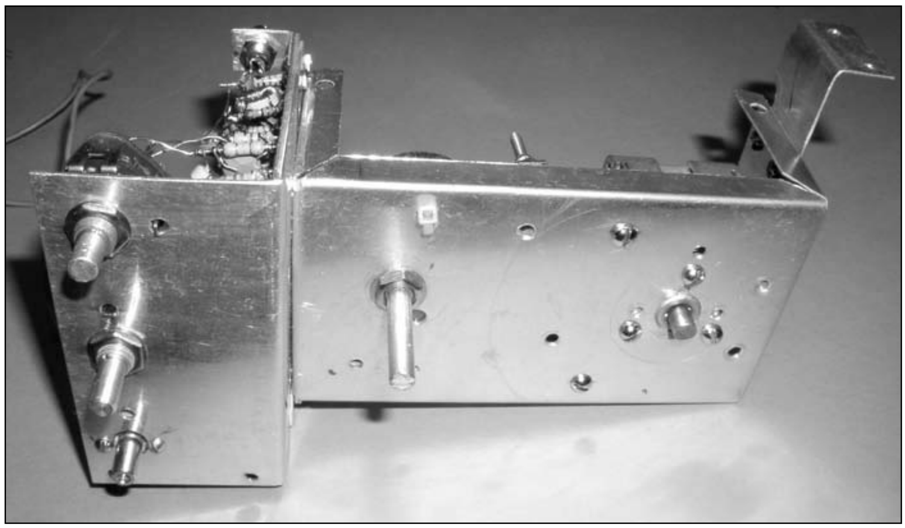

Fig 9—The rotary dial drive outside the front of the more-rigid box section.

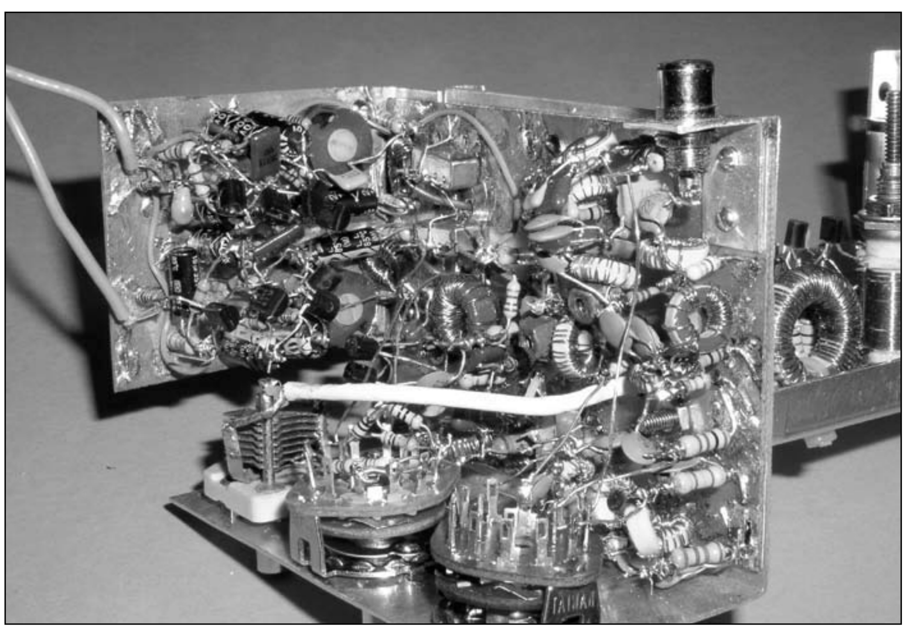

Fig 10—The RF/IF board is mounted outside the minibox on an L-shaped aluminum bracket attached to one end of the oscillator minibox.

near the audio board. These front-panel controls are wired to the boards before mounting them inside the chassis, and they must be positioned to leave space for the rotary dial.

The oscillator board is mounted in a separate aluminum "minibox." Figs 8 and 9 show the VFO tuning capacitor inside and rotary dial drive outside, mounted on the front of the more-rigid box section that has the folded tabs. The box itself is secured ¾ inch behind the receiver front panel to allow space for the rotary dial. The dial driveshaft is long enough to pass through a clearance hole in the front panel for fitting of the main tuning knob. Since the VFO frequency may be affected slightly when the rear cover is installed, a hole in the cover provides access to the VFO inductor for final adjustment.

An L-shaped aluminum bracket attaches to one end of the oscillator minibox as shown in Fig 10, and the RF/IF board is mounted outside the minibox on this bracket with the same mounting screws. Small holes are drilled through the board, bracket and minibox through which pass wires from the oscillators to the mixers, to the VFO via small coax and to the BFO with short insulated wires. The oscillator board receives +12 V through a small hole, bypassed with a 0.1-µF capacitor at the entry point. The front face of the bracket supports the BFO tuning capacitor, the IF GAIN switch, and the band switch. A small aluminum corner bracket at the top of the L-shaped bracket (as shown) attaches the baseband amplifier board to the assembly.

Once wiring is completed, the assembly is mounted inside the larger chassis, and the hardware for the front-panel controls attaches the assembly to the front panel. Another small aluminum bracket attaches the opposite end of the box to the bottom of the chassis for stability. The minibox assembly will, with care and patience, fit inside the larger chassis even though the rotary dial is slightly larger than the back opening and must be inserted at an angle until inside the chassis.

Because the receiver has more than 100 dB of audio gain available, good shielding, adequate power supply decoupling and careful grounding are required to prevent feedback when all controls are set for maximum gain. Use high-quality shielded cable for audio connections, and connect grounds of the baseband amplifier, phase shifter, and audio boards only via the shields of these cables. The headphone and speaker leads are twisted-pair, grounded only at the audio board, so insulated jacks are required. Using only these ground connections will avoid potentially troublesome ground loops and microphonics. The interconnecting cables are intentionally made long so that the units may be prewired and tested together prior to mounting them inside the chassis, as shown in Fig 11.

Back-panel connectors are mounted on the lower lip of the chassis at the rear. These are 12 V dc input, mute control, line-level audio out, sidetone in, and speaker. When all wiring is complete, an optional back panel with

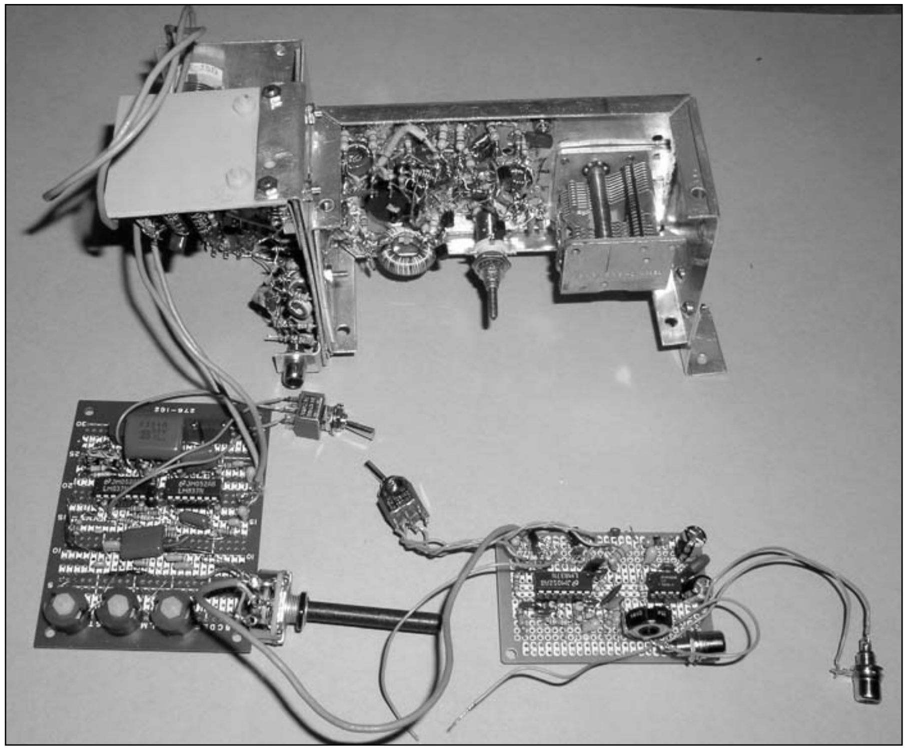

**Fig 11—The receiver units prewired and tested together prior to mounting them inside the chassis.**

**Fig 12—The position of the brass fitting soldered to the bottom of the dial-drive drum. A ½-inch-long cutout in the cylinder completes the drum.**

## Appendix I – A Homebrew Dial Drive

You can build the dial mechanism shown here from a coffee can, a potentiometer, a tuning knob, a small spring, and about 18 inches of radio-quality dial cord. From the coffee can and tuning knob you construct a dial drum that fits onto the variable capacitor shaft and supports the rotary dial. You modify the potentiometer to create a tuning shaft. The spring maintains tension on the dial cord that connects the shaft to the drum. The drum is 4 inches in diameter and the tuning shaft is ¼-inch diameter, so the mechanical advantage (turns ratio) is 16:1, slow enough to tune SSB or CW signals without difficulty.

The dial drum is fashioned from the top and bottom of a 4 inch-diameter tin can. Do not use aluminum or paper since soldering is required. Use the kind that is vacuum packed with a removable foil top under a plastic cover. This type of can has a support ring inside the open end that keeps it circular. Not to advertise, but at least one variety of Yuban coffee has that feature, and I'm sure there are others. If there is paint on the cylinder, remove it for about the first half inch below the rim using fine sandpaper or paint remover. The top end of the can must be carefully severed about ¼ inch below the rim around the circumference of the cylinder. The plastic cover comes in handy for marking the cut line. I used a Dremel tool with a fine cutting disk to make that cut after it was carefully marked, but you could use tin snips. The important thing is that the cut edge must fit flush on a flat surface. The bottom end of the can is cut away from the cylinder just at its rim and filed smooth. You then have a disk with a rim that adds to its rigidity.

These two parts must be soldered together to form a narrow drum with rims that keep the dial cord in place as the drum rotates. Place the convex side of the bottom disk against the cut cylinder of the top end, and hold them in place temporarily with spring-type wooden clothespins. Then solder-tack the joint at several points inside the cylinder after which the clothespins may be removed. Finally, melt a light coat of solder continuously and smoothly around the joint on the outside, filling the joint and any small cracks resulting from an imperfect fit. Then use a fine file or sandpaper to smooth the solder joint. The dial cord must ride on the surface of the cylinder without binding.

A plastic tuning knob with a setscrew is the source of the ¼-inch ID brass fitting needed to attach the drum to the capacitor shaft. First remove the setscrew and set it aside for future use. Then crush the plastic knob in a vice or cut the plastic away until the brass fitting is free. (*Wear eye protection.*) Apply pressure only along the axis of the knob to avoid damaging the brass fitting. That fitting is now soldered to the drum bottom, facing away from the drum. It will extend sufficiently to provide about $^1/_8$ inch clearance between the drum and the capacitor mounting surface.

First, locate the exact center of the drum. The unused plastic cover may have a tiny molding protrusion at its center that can be used for that purpose. Starting with a small pilot drill and as accurately as possible, drill a ¼-inch hole at the center for alignment with the brass fitting. Prepare the solder surfaces of both parts by sanding them clean and tinning them with a thin coat of solder on the surfaces to be attached. To hold the parts in place during soldering, I used a jig consisting of a short ¼-inch dowel inserted in a perpendicular ¼-inch hole made with a drill press in a flat block of wood. Press the parts together over the jig and solder them securely. It takes some time to heat the parts sufficiently for solder to flow freely around the joint. Be careful to keep solder from getting into the setscrew hole. Fig 12 shows the position of the brass fitting soldered to the bottom of the drum.

To complete the drum, we need a ½-inch long cutout in the cylinder as shown in Fig 12. First, drill a hole as wide as the cylinder between the rims. Then, cut slits at both rims about ¼ inch in each direction from the hole. A Dremel tool or a sharp knife can be used to make those cuts. This creates two tabs that can be bent down into the cylinder so that the cord will pass harmlessly over rounded surfaces at the bends. Finally, install two $^1/_4$-inch-long machine screws in holes drilled in the bottom surface of the drum opposite the slot just created. The ends of the dial cord and spring will be attached to those screws. The completed drum may now be mounted on the variable capacitor shaft and locked in place with the setscrew. Use some leftover nail polish to prevent the setscrew from turning. (Glyptol is the mil-spec chemical of choice, but nail polish will do.)

The potentiometer must be modified to become a smooth-turning drive shaft. First, remove the back cover, then remove the stationary wafer that contains the resistor surface and connectors by chipping it away with side cutters or pliers. Retain the plastic rotary wafer at the end of the shaft as an end stop for the shaft. Remove the metal wiper that previously contacted the resistor surface by pulling it away carefully without damaging the plastic wafer. The remaining parts are a smoothly rotating shaft in a bushing that will be mounted an inch or so from the rim of the dial drum. Potentiometers are lubricated with a viscous jell that offers slight resistance to rotation so that the shaft does not rotate unintentionally. Do not remove that lubricant. It is harmless (it will not leak onto the external part of the shaft), it prevents wear, and it allows the dial to turn smoothly but hold its position when released. No, you can't spin the dial as some like to do, but that luxury will not be necessary in this application.

To prevent slippage of the dial cord, use a sharp tool to scribe parallel scratches in the direction of the shaft from the bushing about ¾ inch forward all around the shaft where the cord will engage it. Then lightly sand the surface to remove any sharp edges while leaving the scribed grooves for friction.

With the shaft and dial drum mounted securely, the dial cord can be installed. Fig 13 shows how the cord is routed: $1^1/_2$ turns around the drive shaft, 2 turns around the drum with the ends through the slot. Thus, the cord is tangential to the drum throughout the 180° rotation of the variable capacitor. One end of the cord is attached to one of the machine screws opposite the slot in the drum cylinder, and the other end is tied to a spring attached to the other screw. Adjust the length of the cord for sufficient spring tension to prevent slipping on the drive shaft. As the dial is rotated, the cord will travel about ½ inch along the shaft length, over the prepared non-slip surface, while the spring keeps the tension constant.

To support the dial face, epoxy a $^1/_2$-inch-wide ring of cardboard inside the dial drum resting on the narrow inner ring as shown in Fig 14. A circular dial face may then be glued to the cardboard ring with rubber cement. This allows it to be removed or repositioned. Before the plastic window is mounted inside the chassis front panel, temporarily install the oscillator/RF/IF assembly with the dial drum attached. Temporary markings can be made on a trial dial face at convenient frequency increments. Using the trial dial face as a template, make a final dial face on glossy paper by hand or with a computer graphics program and attach it to the cardboard ring with rubber cement. Fig 1 shows a computer-printed dial with major marks every 100 kHz from 0 to 5 with frequencies for 80 and 40 meters. Minor marks are placed at 25-kHz increments. In this particular configuration, the indicated frequency decreases from left to right as the tuning capacitor is rotated clockwise from maximum to minimum capacitance. If you wish, cross over the dial cord between the tuning shaft and the dial drum for opposite rotation. A clear plastic "window" is attached to the inside of the chassis over the dial opening with masking tape. A thin magnet wire, also held in place with tape inside the chassis, becomes the dial index line.

While it certainly does not approach digital accuracy, this drive tunes smoothly with no discernable backlash. If constructed with care, it will rival an expensive anti-backlash gear drive and outperform a planetary drive, assuming they could be found. A companion transmitter section is now in development, and it will share the receiver's oscillators for transceive operation. I'm planning for digital frequency readout in that unit because transmitter frequency must be more carefully controlled.

**Fig 13—The dial-cord routing: 1½ turns around the drive shaft, 2 turns around the drum with the ends through the slot. One end of the cord attaches to one of the machine screws opposite the drum cylinder slot. The other end ties to a spring attached to the other screw.**

**Fig 14—A ½-inch-wide cardboard ring glued inside the dial drum rests on the narrow inner ring.**

necessary cutouts to clear the connectors may be attached. Self-adhesive plastic "feet" are mounted on the bottom of the receiver.

For appearance only, a front-panel was produced with a drawing program and printed on heavy photo-quality paper. After a few coats of clear Krylon spray were applied, it was attached to the front of the chassis with rubber cement and a bit of transparent tape at the edges.

## Performance

I am well pleased with the performance of this relatively simple receiver. Its principal drawbacks are the lack of automatic gain control and a precise frequency display. In practice, however, these are minor inconveniences. A two-handed tuning procedure with one hand on the tuning knob and one on the audio gain is easily accommodated. Audio AGC in external processing would make that unnecessary for all but the strongest signals.

Theoretically, the receiver should have excellent dynamic range and third-order intercept performance, but I don't have the test equipment required for precise measurements. Nonetheless, my anecdotal observations are as follows. The receiver will dig weak CW or SSB signals out of the 80 and 40 meter "mud" as well as any I have used, and extremely strong amateur signals nearby do not produce the slightest evidence of blocking. (Of course, the 80 dB over S-9 nighttime broadcast signals on 40 meters are another matter.) Unwanted-sideband rejection is entirely adequate for SSB and single-signal CW reception in a crowded band. In fact, the effective SSB filtering is so good that zero-beat is barely audible when spot tuning the transmitter to get on frequency. The audio quality when fed to an external power amplifier and a good speaker provides natural and pleasant voice reception, and there is no ringing when the CW filter is switched in.

Something old, something new, something borrowed, but thankfully, nothing blue.

### References


[1] R. Fisher, W2CQH, "Twisted-wire Quadrature Hybrid Directional Couplers," *QST* Jan 1978, pp 21-23

[2] R. Campbell, KK7B, "High Performance, Direct-Conversion Receivers," *QST*, Aug 1992, pp 19-28.

[3] R. Campbell, KK7B, "High Performance, Single-Signal, Direct-Conversion Receivers," *QST*, Jan 1993, pp 32-40.

[4] G. Leinweber, VE3DNL, "The R2 Single Sideband Direct Conversion Receiver, Revisited: The R2a," *QRP Quarterly*, Oct 1996, pp 19-21

[5] B. Blanchard, N1EKV, "RF Phase Shifters for Phasing-type SSB Rigs," *QEX*, Jan 1998, p 34-39.

[6] R. Campbell, KK7B, "A Binaural I-Q Receiver," *QST* Mar 1999, pp 44-48.

[7] Diplexer configuration from Fig 15-31 of *The ARRL Handbook for Radio Amateurs*, 2001 (Newington: ARRL, 2000).

[8] D. Lyndon, AK4AA, "Accurate Measurement of Small Inductances," *QEX*, Jan/Feb 2004, pp 47-50.

# Anatomy of a Homebrew Messaging APRS Tracker

*Tracker, noun—A device to record or transmit the path of a moving object such as a person or vehicle.*

By Dennis Nendza, W7KMV

It's difficult to imagine anyone who has been a ham for more than a few years who hasn't wanted to design a useful piece of gear and build it. Sometimes a less than perfect technical proficiency in circuit design, soldering, construction techniques and component knowledge holds us back. Well, I'm here to tell you that all you need is curiosity, *The ARRL Handbook for Radio Communications*, access to the Internet and a desire to learn. You can turn out some useful items for the shack or for the road. You may not be interested in APRS, but I think you'll find the process I followed to create a useful piece of equipment applies to many other radio projects.

I've been a ham since the eighth grade, which for me was way back in 1962. My interest started with a desire to use radio to reach a friend a block away. I was encouraged by visits to my great-uncle Emil (8AYH, W8AYH, W3LKM) who had shelves of homebrew equipment in his shack. I built lots of Heathkits and repackaged some other equipment to work for Amateur Radio purposes. As a high-school student I managed to set the back seat of the family car on fire (quickly extinguished) with some faulty wire routing for my Heathkit Twoer . So I've had my share of things gone wrong mixed with the successes.

One of the big satisfactions of Amateur Radio is completing a project and giving it the "smoke test"—applying power for the first time and finding that it works. Now, each of us brings our own expertise to the radio art. For me it is a lot of computer programming knowledge and a modicum of digital circuit understanding. Maybe that is why the digital modes, such as Packet radio, seem so intriguing. It's also why I was drawn to experimenting with APRS, the Automatic Position Reporting System devised by Bob Bruninga, WB4APR. [1] There are a lot of thrills to be had using APRS in its many applications, and a big one for me was building a self-contained APRS tracker to my own specifications.

Commercial versions of trackers exist.[2] They give you the ability to attach a GPS (or include a built-in model) and a radio to transmit your

1970 W Magee Rd #12102
Tucson, AZ 85704
520-829-4591
**w7kmv@arrl.net**

[1]Notes appear on page 28.

position using the APRS format. The shortcomings of most available systems are that they are not fully programmable, do not include any messaging capability and can cost a great deal. Here is how I began creating my own tracker.

Several years ago I took up paragliding, and of course my handheld went with me. Our paragliding organization included many licensed hams and one of the flying coordination frequencies was in the 2-meter band. Just as instruments are used in sailplanes to indicate altitude and vertical rates of climb/descent, most paragliding and hang gliding enthusiasts carry a multipurpose instrument to do just that. It has also become very popular to fly with a GPS that can record the flight track as well as indicate ground speed and distance to the goal. This set me to thinking about packaging an APRS tracker that would take the GPS information and transmit it through my HT on an APRS frequency.

My first crude experiments with paraglider tracking began in early 2002. I packaged a Kantronics KPC-3 Plus with a Garmin GPSII and my Alinco DJ-580 handheld. I "borrowed" my daughter's perfectly sized soft CD player carry case and lashed it to a safe area of the paraglider harness. It actually worked, which encouraged me to use it a number of times with various beaconing settings to see the effect on throughput and tracking resolution. I soon became dissatisfied with the limitations of fixed time interval beaconing and the difficulty of changing the beacon rates in the field, which required a terminal or computer.

**A Smaller Solution**

The cables I had originally built for use on the KPC-3 Plus in the shack proved to be heavier and bulkier than the TNC itself. This, combined with the push-on push-off power button on the front and cable connection on the rear made it difficult to operate inside the CD-player carry case and certainly not something I wanted to grapple with in flight to enable or disable. I was already looking for a smaller solution and it seemed like the TinyTrakII was just the item. It was under $40 and designed to provide the TNC tracker function. I quickly built the kit the day it arrived, and together with the accompanying *Windows* program that sets up a call sign and other parameters, it was operational in no time. I packaged it with a 9-V battery in a small plastic project box complete with a DB-9 connector for the GPS and a stereo mini-jack for the radio's audio connections. I mounted a toggle switch for power between the two connectors for protection from inadvertent switching while packed away.

Several tests conducted while driving around indicated that the speed and turn-based triggering for position reporting worked effectively. I did notice an occasional tendency to send several rapid-fire reports when I didn't expect them. It wasn't until I used the unit in flight that I found out there was a big problem with the installation. Upon landing one day, I switched the handheld off and it was too hot to hold. The transmit indicator was displayed on the handheld LCD and disappeared as soon as I pulled the audio/keying plug from the radio. Obviously, the equipment had been locked in transmit mode for some time. Thankfully, the radio was set to low power. I belatedly apologize to APRS users in the San Bernardino, California area for wiping out the channel for up to 30 minutes.

Back on the workbench, it soon became obvious that a strong RF field adversely affected the unshielded TinyTrakII. While flying, all the equipment is in very close proximity and the RF field is extremely intense for the nearby electronics. Short of repackaging the device in a metal box, I added ferrite beads to all the wires leading to the outside world and placed a big clamp-on ferrite over several turns of the GPS data cable. This vastly reduced the lock-up events, but did not always prevent them.

That creeping sense of dissatisfaction started coming back, and rather than attempt to RF-proof the TinyTrakII further, I decided to see what I could do to package my own solution.

**Blue-Sky Syndrome**

I remember sitting in meetings (not employment related) with my notepad, scribbling down ideas for the tracker I'd like to have. I must have seemed a pretty diligent attendee with all that pencil activity. I drew block diagrams of modules, cabling requirements, lists of functions and the beginnings of a computer program flow chart. Five years earlier I had picked up a Basic Stamp[3] "single chip" computer. It's called the "Stamp" since it is about the size of a large postage stamp. While it is contained on a 24-pin carrier that plugs into a regular 24-pin IC socket, this computer actually is an assembly

Fig 1—The complete Messaging BXTracker station. Teaming up with the VHF transceiver is a round magnetic active (preamplified) GPS antenna, the BXTracker and a Cybiko hand-held "pda" employed as a terminal. A Palm Pilot or Pocket PC can also be used as a terminal. The terminal is not required for normal or non-messaging use. Background Apollo 16 photo, courtesy NASA and the NSSDC.

of several chips and other components. It is a phenomenal little device that is easy to program from a *Windows* based system. It appeared that this device might be able to serve as the control center for the tracker I had begun to diagram. I investigated the programming others had done to parse or interpret GPS output sentences with the Basic Stamp and it soon became clear that it had been taxed to its limit by the simplest of GPS work. Surely, I thought, there must be another processor that is somewhat more capable, but not so complex as to require a board full of support chips and the attendant high price.

The Internet never ceases to amaze me with the wealth of information that I can bring to my desktop. After a few searches with well-chosen keywords I was looking at a description of a stamp-like computer made by NetMedia, Inc[4]. The BX-24, built to be pin-compatible with the Basic Stamp, ran programs ten to fifteen times faster and had sixteen times more memory for program storage. More importantly, it had a much larger data or variable work area necessary for a program with the capabilities I planned. All this could be had for the same retail price as the Basic Stamp. Pin compatibility was great, as it meant I could use the same development board I had purchased with the Basic Stamp. I bought a BX-24.

The BASIC language used by the BX-24 is a sub-set of *Visual BASIC* as implemented by Microsoft, with extensions to make optimal use of the single chip computer possible. This subset is very easy to learn by anyone who has some programming experience and is not very difficult for those desiring to get started in programming. Because the program for this project is modifiable by anyone and may serve as a basis for derivative projects by those wishing to use this processor, I'll comment extensively on its development and considerations that I made along the way.

Once I settled on the BX-24, I began to program in earnest. The biggest unknown was whether the processor speed and temporary variable work area would be sufficient to measure up to my blue-sky plans. To develop and test the controlling program I had to set up a hardware test bed with which I could hook up the GPS, a TNC, a display device and the computer used to feed the program to the chip. A solderless breadboard is the ideal solution and I used one that has been my companion for nearly 30 years, a Heathkit Digital Design Experimenter. Lots of similar solderless breadboards with or without all the switches and built-in LEDs can be had today for a reasonable cost.

**Absolutely Amazing**

I began the breadboard experiment by installing the chip and very carefully wiring it to the ground and appropriate voltage. This is a time to double-check everything, as it is far too easy to push a wire into a nearby hole and watch $50 of miniature electronics curl up toward the ceiling in a little wisp of smoke. Actually, most breadboard power supplies aren't capable of generating smoke as they destroy a miswired component, but sometimes a battery and a one-amp or higher regulator are used in lieu of a more modest supply, and that can cause some serious heat in small parts.

The cables for the GPS and TNC that I had been using terminated in the customary DB-9 connectors, which called for mating connectors with soldered solid-wire leads that could be inserted into the breadboard. I also tried a flat cable that had an insulation displacement DB-9 on one end and an insulation displacement 14-pin dip plug on the other. That made for a tidy connection to the breadboard as well. At this point I had the connectors complete and installed on the breadboard. I then had an "oh-oh" moment. These devices communicated electrically using the RS-232 standard which specifies a plus and minus swing for the signaling voltage. The programming port of the BX-24 was happy with RS-232, but what would happen to the other input pins of the chip if a –12 V dc pulse occurred as allowed by the RS-232 specification?

This question sent me off to check the electrical specifications on the chip that did all the work in the BX-24, which can be exposed to the "outside world" through the pins on the chip carrier. I found the electrical specifications for the Atmel AT90S8535 processor and the maximum allowed negative voltage proved to be –1Vdc. Hey, I didn't want to worry about all this messy stuff. I just wanted to connect everything and get to work programming a nifty tracker. Well, in the interest of keeping it simple I tried to find a way to avoid an RS-232-to-logic level conversion chip. They seem to be way too big and expensive for what they do.

Thank you, Mr. Zener for discovering the effect that gave us Zener diodes. It seemed I could use a Zener diode to tame the input signals from RS-232 devices. Basically, I used the diodes to block negative voltage swings by shunting them to ground (forward biased) and limit positive voltage swings on the same line by using a diode with a 4.3 V dc reverse biased threshold. One Zener diode and two functions—neat.

Now, sending a logic level (0 or 5 V dc) signal to an RS-232 device seems to work fine. There may be equipment that doesn't recognize 0V as a low RS-232 level, since it is technically not in the negative range, but I haven't experienced any modern devices that refused to cooperate.

Okay, now I could get on to programming. I typically like to test out ideas by taking small parts of the problem and working out the details before moving on to the next higher level of complexity. The first task was to have the chip simply read whatever data was coming in from the TNC and write it back out on a serial line connected to my PC which was running a terminal program listening for data. I studied a few sample programs that worked with the serial communications on the BX-24 and put together my own. After a few iterations of debugging the program I saw the TNC data appear on the computer screen. Absolutely amazing!

**The Obsession**

Writing computer programs turns some of us into late-night obsessive tinkerers, a pretty well understood feeling among the ham radio community. Heartened by my success in dealing with serial data I began to expand the program to read the NMEA[6] sentences flowing out of the Garmin GPS and turn the latitude and longitude data into APRS messages indicating my station's location. This process occurred over a year as a part-time effort—the success of the whole project always lay in doubt as I pushed the BX-24 to accomplish additional work. Using a much more capable computing device with it's larger memory, faster processor and a more sophisticated operating system definitely would have accelerated the task by removing many constraints that required creative solutions. It probably would have resulted in a bulkier tracker with the attendant requirement for a larger battery.

While programming this device, I began to tune the program code, providing a balance between speed required to keep up with the data streams and a modicum of organization and maintainability.

If you haven't done much programming, this trade-off of time to execute, space required for the code and maintainability or understandability might not be apparent. It is simply the result of working with a small computer limited in many resources.

The BX-24 has a relative abundance of program memory (not working memory), so I chose to consume additional program space by duplicating certain functions within different routines, so that critical time and working memory was not consumed sending data off to common routines.

Once I had the basic APRS tracking function coded, I left the breadboard haywire assembly to run for days to see how robust the program was.

After chasing down problems caused by the use of too much working memory for variables, and unusual data arriving from the TNC, I figured I had a working tracker project. That wasn't good enough. I needed to obtain a dedicated TNC board that could be integrated into the same box with the processor. I recalled a November, 2000 *QST* article about a simple build-it-yourself TNC board designed by John Hansen, W2FS.[7] It looked to be the right size. After a few e-mail exchanges with John about the board, I ordered the kit.

In short, the W2FS TNC went together quickly in one evening and worked at first power-up when I tested it using a PC-based APRS program. It's well designed and perfect for this project. A completely new version is now available and it is less expensive. No doubt it would work as well. I deleted the LEDs and audio connector from the board anticipating reduced power consumption and the use of a smaller connector later. The selection of this TNC made it necessary to change my program. While using the Kantronics KPC-3 TNC, I had been dealing with the verbose terminal mode familiar to me. The W2FS TNC communicated strictly in the KISS[8] mode, a big difference in format. So I learned about the KISS mode and made the changes to the program, deleting the code that talked to the KPC-3 in terminal mode. KISS turned out to be much easier to handle.

Having obtained a great TNC for the project, I started to wonder what was available in a small GPS board that wouldn't break the bank. My previous research indicated these boards were expensive. What a surprise when I visited E-Bay. I found a credit card sized GPS board for sale. After reading the specifications and visiting the manufacturer's site I slowly became convinced that I could get my program to talk to it. For a total of $50 I had it delivered, and within a day that little board was full of clip-on test leads to check it out.

The µ-blox (Micro-Blox) PS1 GPS[9] is an incredible device. The on-board processor takes the raw GPS data from the very small RF section and turns it into a wide variety of useful positioning data. This small package is clearly visible on the right side of the rightmost board in Fig 2.

Fortunately, an extremely complete test and evaluation program for the device can be downloaded from the manufacturer to run on a PC. It accelerates the learning curve immensely. There are many similar GPS boards available and it is important to note that obtaining this specific model may not be possible. It is one of a class of components available from various manufacturers that can be used for the GPS function. The process I used to integrate it would certainly be similar for boards from other manufacturers. The important consideration is the availability of good documentation that allows you to figure out how to make it work. It is not necessary to have an *in-box* GPS for the tracker. A hand-held unit with a data cable attached to the tracker would work as well—just a small design change.

I added a piezo speaker so that certain events such as sending a position report would generate a sound. I found it necessary to check the miniature speaker for frequency response as many beep tones sent to it from the BX-24 did not sound very loud. Using an audio generator I found a pronounced peak near 3800 Hz. After that discovery I used the computer's "FreqOut" command to send tones near the 3800 Hz audio peak. If you don't have an audio generator on the bench, consider using a computer to generate tones from the audio card.[10] An alternate method is to use a SSB/CW transceiver tuned to a broadcast carrier and compute the frequency response by how far you are away from, zero beat of the station. Hook the piezo speaker to the headphone output. You may need to select a broad filter response or shift the IF to pass tones greater than 2 kHz.

With the haywire halo growing around my prototype, I connected all the modules together to see how well they would talk to each other. I had also purchased an amplified GPS antenna on E-Bay for about $20. I chopped off the coax connector because I needed a different one. This allowed me to clip the coax to the GPS board antenna connector for testing. With it needing just a few changes here and there, I could finally see that the whole project could work.

### It's All In the Packaging

Making a project look good is often one of the design goals. Certainly,

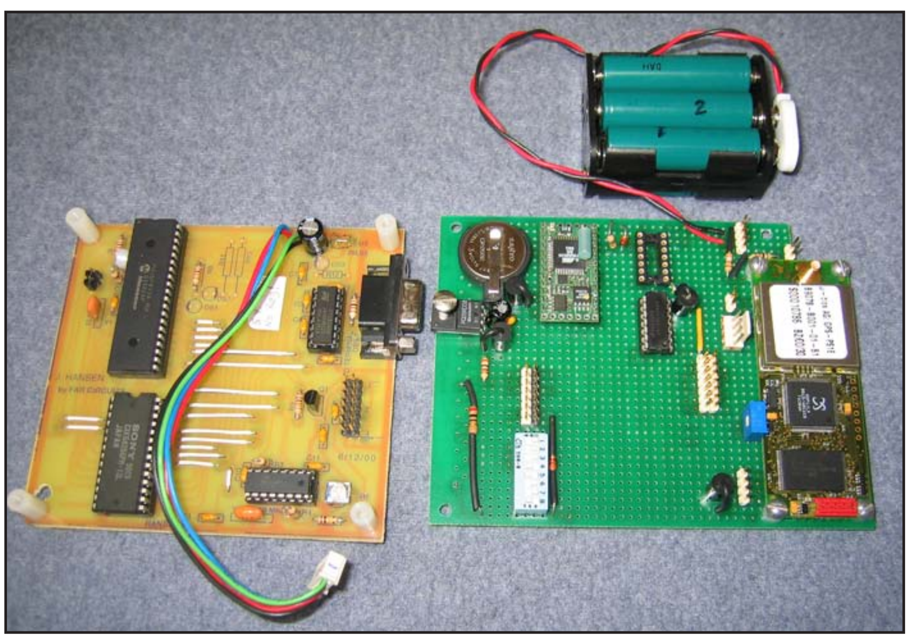

**Fig 2—The TNC board on the left is from the Hansen, W2FS, kit referenced in the article text. The GPS receiver is the small circuit board mounted on the right side of the perf-board. Note the room for expansion that remains on the perf-board. In operation, the two boards are piggybacked and connected with a data and power cable. The internal six-cell battery is shown attached.**

companies such as Apple Computer and Bose Corporation have this as one of their highest priorities. I figured that I couldn't spend this much time working on my tracker without making it look "ham radio attractive". Now that I had nearly all the components to complete the project, it was time to work out just how I could shoehorn them into a solid enclosure that still allowed for further development and tinkering.

The first item of business involved the collection of all sockets, buttons, switches and hardware that would be mounted to the enclosure. My goal was to have everything connect to one side panel. This would make access while flying, driving or on the shelf much easier and eliminate protrusions on all other sides. I toyed with several layouts and soon had some working ideas. I cut thin cardboard of the variety found in a shoebox or tablet backing and formed an extended corner of a typical enclosure that measures 4×7×2 inches.

The enclosure under consideration has a removable 4×7 inch side plate. I poked holes in the cardboard and mounted the components closely together to conserve space. I then removed the components and scanned the cardboard. With the scanned image in *Photoshop*, I drew horizontal and vertical lines through all the component holes and made some minor cosmetic alignments so the mounting wouldn't look so random. This became a template that I printed out and cut to size. After rechecking the actual component layout on this template, I was very close to the final location of the panel mounted parts.

The size of the Hansen TNC board dictated a minimum of 4 inches for one dimension of the enclosure. A prototyping circuit perf-board that I picked up measured 4×6 inches and I thought I could get the BX-24, GPS board and other components and connectors on it with room to spare. I decided that stacking the boards looked pretty slick and certainly conserved space.

The problem was that neither board had matching holes for mounting standoffs to hold them together. A close look indicated that I could drill the TNC board safely to obtain the hole spacing required. I also wanted to have a component layout that worked well on the prototype perf-board.

*Photoshop* allows for a great deal of image manipulation. It seemed that I could visualize a virtual copy of the prototype board with virtual components on it for a pre-build check of spacing and layout. Beginning with a scan of both sides of the board, I re-oriented the scan of the "copper" side so that it would look as if I x-rayed the perf-board from the top side. I then registered the holes of the top scan with the holes of the flipped bottom scan. I did this in *Photoshop* by making the top scan layer a bit transparent—like laying tracing paper with a drawing on it over another image. Such a combination allows you to perform a virtual build from the top, but easily see the copper pattern on the bottom for correct component placement. The rest that followed was the rather laborious scanning of most components by placing them on the scanner's glass and then taking the resulting scan and cleaning up the image of the separate components. I even imaged the GPS board since it would be mounted to the proto-board as well. I moved the virtual components into place on the virtual board. The virtual board can be seen in Fig 3. All dimensions remain nearly constant as the scanner is very linear when imaging items close to the glass. I learned that 3-D objects can become distorted if imaged as much as a fraction of an inch off the glass.

Things were looking good as I built up the virtual image of the board and it allowed me to decide that the enclosure I proposed to use was going to do the job. I took this virtual building technique a step further by scanning the enclosure's long side and open side and "placed" the virtual board in the virtual enclosure along with several virtual connectors on the enclosure side panel to check clearance. The real test was in placing three DB9 connectors on the side panel in an area where the circuit boards had only a little clearance from the panel wall. The virtual model indicated enough room for

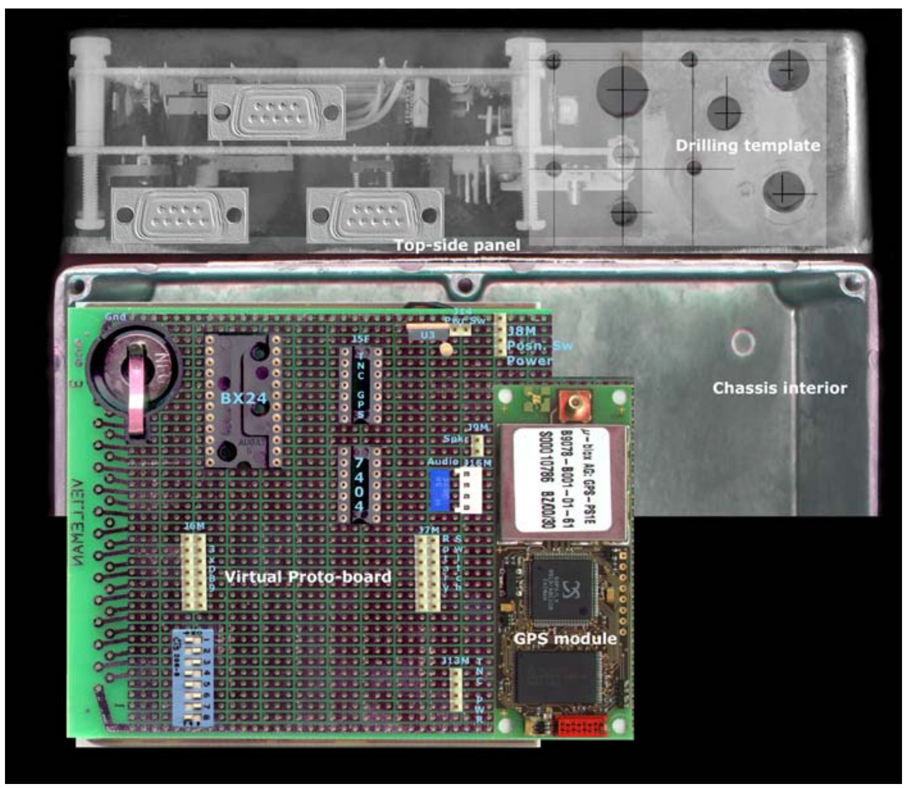


**Fig 3—This is a composite image of approximately 20 different scans. The chassis topside panel image is aligned with an image of its open interior. Overlaid on the panel is the template that was printed for hole drilling. The apparent "x-ray view" of the interior assembly layered beneath the drilling template came from a scan of the side of the assembled boards that was then digitally faded in to allow visualization of where the boards would rest relative to the panel. The DB9 connector template images could then be placed for best clearance. Before I attempted any drilling or assembly of the interior components, I made the "virtual" layout of the proto-board, which appears to sit in the open chassis. This allowed for initial placement of the major components. I moved the individual components around on the computer screen, not on the actual board. I then printed this layout to be a guide during assembly. Note that the circuit board lands are visible here but not when looking at the top of the actual board. Compare this with Fig 2 that shows the board as built.**

the connectors and holding the actual parts in place seemed to confirm it. Figure 3 is a composite of multiple scans assembled to show fit and placement. It was getting scary now, because the only thing left to do was to solder the components to the board, make the internal connecting cables and drill the enclosure. I say scary because I have so many projects where the holes are not in a straight line and daylight peeks in around the DB9 connectors mounted on a chassis. This enclosure cost nearly $20 and I was determined not to make it conform to the Swiss-cheese model.

I suppose it was my desire to get the holes nicely done that caused me to buy that drill press. It sure made the process a lot easier. What also helped was printing out the virtual panel as a template that I taped to the side of the enclosure to guide my drilling. That was worth the trouble as it made the task straightforward with no need to mark the aluminum and check alignments. The template also included outlines of the three DB9 connections so that I could file the openings very close to size before doing the final sizing of the holes and mounting of the connectors.

I'll mention another construction idea that appears to have worked well and that is the application of hot glue to the off-board components with soldered leads. The DB9 connectors, as well as the rotary switch with 14 delicate flat wire cable solder connections, would soon begin to lose their wires as they flex and fatigue due to removal and replacement of the main boards. By applying hot glue to the finished work and binding the wires together or to the base connector, they become much more resistant to flexing and damage. You can see a detail of the rotary switch with the glued (after soldering) flat cable in Fig 4.

**Hardware and Software Details**

In the earlier sections, I talked at length about the process that led me to design and create the tracker. Now, we will take a close look at the schematic and programming which makes this device rather unique. Many of the techniques and shortcuts described here are useful in other projects.

The schematic (Figs 5A, B, C) is not very complex, electrically. As a prelude to understanding the circuit, it is important to follow what the four-position, three-pole switch (SW4) accomplishes.

Beginning at the most counterclockwise position we have all internal circuits energized. Pole A of the switch distributes the regulated voltage. Poles B and C route data to and from the external DB9 (J2) connector pins 2 and 3 respectively. This first position could be called normal operation. It's possible to monitor TNC output at J2 and GPS output at J3 during normal operation. A data terminal may also be connected to J4 to communicate with the tracker and display the status.

Moving to the second switch position, we have regulated voltage supplied only to the BX-24 computer chip,. The input/output pins along with the always-connected ATN (attention) line for the chip are coupled to J2 so that the device may be programmed by an external computer. I thought this necessary, as I will probably never be satisfied just leaving the program alone.

Position three of the switch energizes only the TNC while connecting its input/output pins to J2. This allows the tracker's internal TNC to be used in conjunction with a more capable external computer running a more sophisticated APRS or packet communication program.

The fourth switch position energizes only the GPS. Once again, this is to allow an external computer to use the GPS for position data or to actually re-configure the GPS by running the manufacturer supplied test program. These four modes may be used while a PC is connected to J2. There is no need to change cables to move from TNC monitoring to BX-24 programming to TNC use or to GPS use. Fig 6, a block diagram of the project, shows the switching another way without all the clutter of a schematic.

Now, if you look closely at the schematic you will see that the TNC input and output are always connected to the BX-24 output and input respectively. By performing a little testing I discovered that if one of these devices is de-energized it does not significantly degrade the performance of the other while the pins remain connected. We do not have to switch the data lines to break the connection between the devices when allowing an external signal to communicate with either the energized BX-24 or the energized TNC. The same is true of the GPS connection to the computer chip. This discovery avoided the need for a more complex switching arrangement.

Returning to the voltage distribution for a moment, notice diodes D1, D2 and D3 are used to prevent back feed of the regulated voltage to the other components when we only wish to power a certain part of the tracker. All diodes have a forward voltage drop, and if we use a typical diode to distribute 5 V power we will end up with about 4.3 V due to the usual 0.7 V drop. This is not good, and the devices in this project would fail to work. I did a bit of investigation and found low forward-drop Schottky diodes. In the low-current regime inside the tracker they only drop about .2 V which is acceptable. You must look closely at the forward drop curves when selecting these devices as the drop varies significantly with the amount of current being passed. Generally, the lower the current the lower the drop. I decided to give the tracker active electronics a little more distance from their low voltage limits and raised the voltage regulator ground reference about 0.15 V with a simple voltage divider referenced to the regulated side. This applies 5.15 V when all devices are energized—still well below their high voltage limits and it keeps each one around 5 V when energized separately. The voltage

**Fig 4—In this enclosure box corner image you can see the hot glue securing the soldered flat cable wiring on the rotary switch. The black "button" shape to the left of the switch is the piezo transducer (speaker). It is held to the panel with two mating Velcro stick-on pads. There is a small hole drilled in the panel to allow the sound to exit the box.**

regulator was also chosen for its low drop-out characteristics, which means that the battery voltage can get within about 0.1 V of the desired voltage before it loses regulation. This allows for maximum utility of the internal 6-AA cell 1500 mAhr battery. Currently, Ni-MH AA cells as high as 2300 mAhr capacity are available.

The Zener diodes, D4 and D5, are used as described previously to tame the RS-232 ±12 V input signals that are possible from different external devices connected to the tracker. They avoid the necessity for the often-used RS-232 level converters found in many designs that "go by the book" to interface with these data signals. Notice that the BX-24 can handle standard RS-232 voltages only on the serial port, pins 1,2 and 3.

The GPS board is included in the schematic rather indirectly, represented by the connector that mates to it. Different suppliers of GPS modules each have their own special connectors and signal requirements. The μ-blox PS1 GPS has modest requirements. It takes 5 V for power and speaks and listens to inverted TTL logic. This inversion of the signals could have been handled without the interface inverter chip I chose to include since the BX-24 can perform input and output logic inversion on its data pins, but I wanted the GPS to be able to talk to the outside world as well, and the inverter chip accomplishes two functions in this regard. In concert with the Zener diodes, it acts as a bodyguard protecting the GPS from external out of bounds volt-

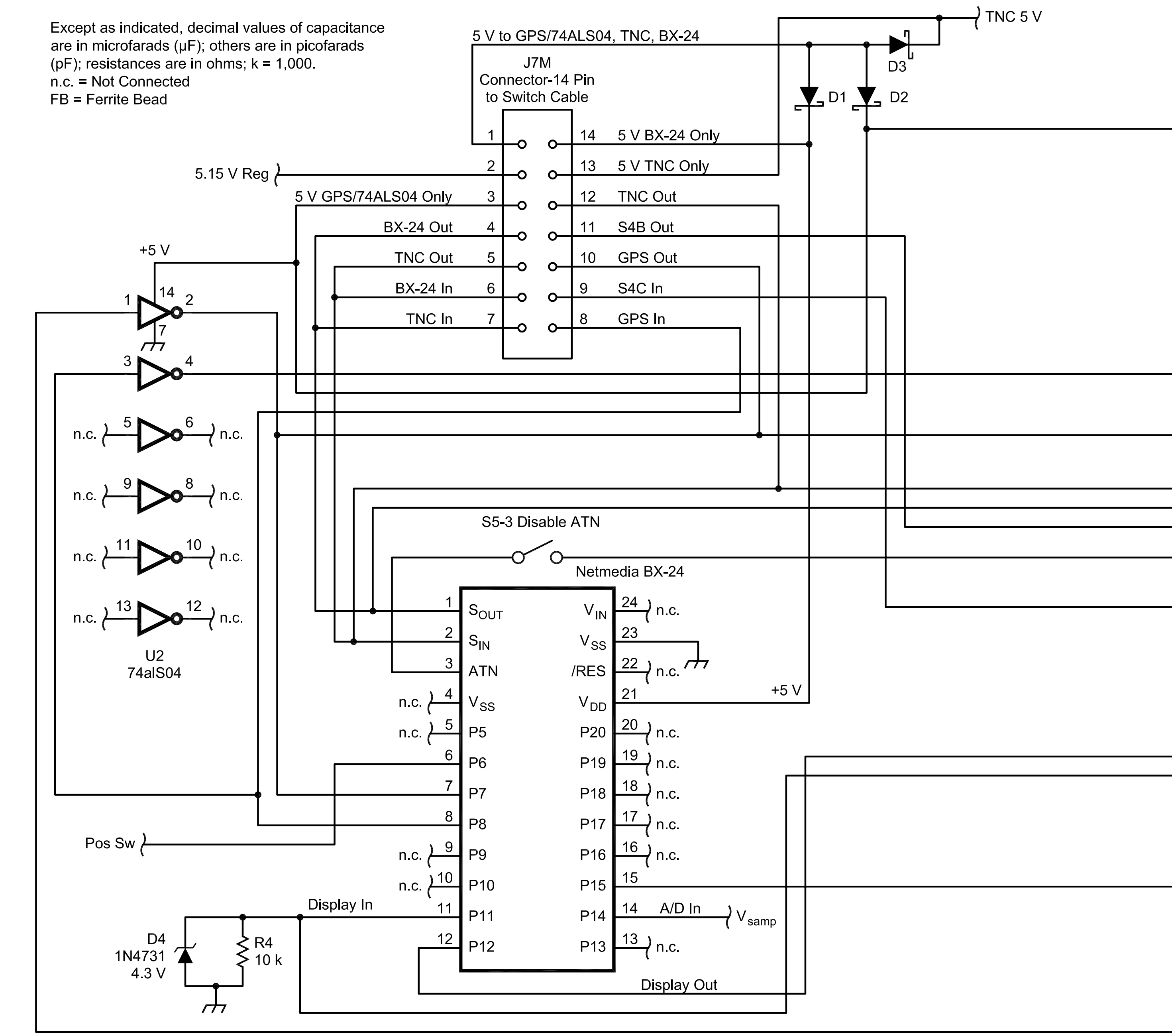


Fig 5(A)—Schematic diagram.

ages, and it also performs the necessary signal inversion.

Likewise, the TNC board is shown only as a reference to its signal connections.

This is a good place to explain the choice of some connectors. The Hansen TNC was originally designed with three connectors in mind: One for a battery connection, another for the computer data and a third for the radio audio. To minimize the wiring and reduce the connectors by one I looked at the DB9 connector on the TNC board and discovered that several pins were unused. It turns out that there were just enough pins left to add the analog audio and keying signals to that connector. I was concerned about the possibility of crosstalk in the ribbon cable that connected the data and analog signals to the prototype board, but it proved to work without any reduction of audio quality. I removed the TNC on-board voltage regulator and connected the V-in to V-out pads together since regulated power is centrally supplied.

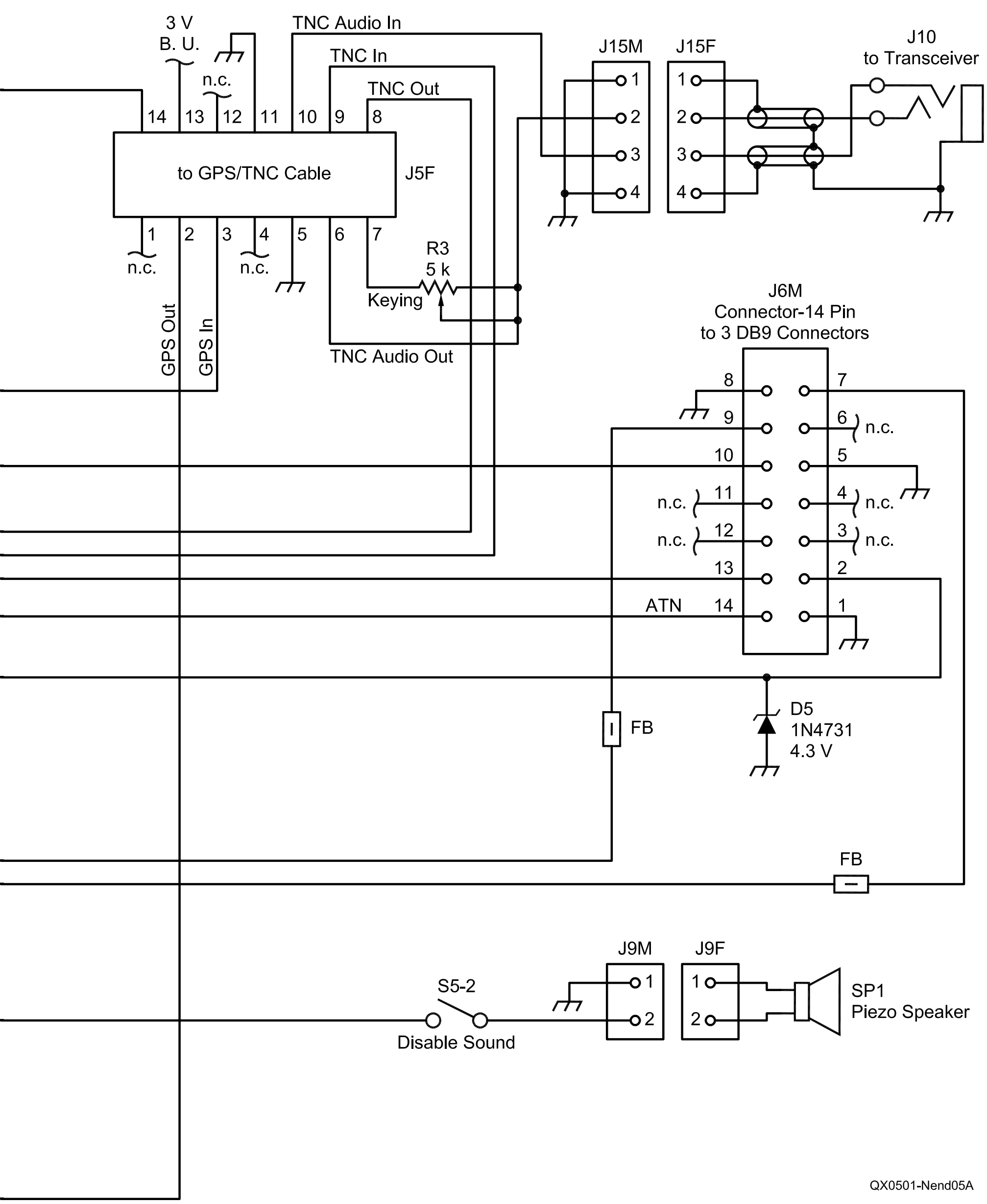


Too much drive from the TNC audio output for my particular transceiver, an Alinco DJ-580, caused a very touchy trimpot drive level adjustment. This may require changing the trimpot on the TNC or lowering the drive-level ahead of the capacitor that feeds the trimpot on the TNC board. I padded down the drive level.

**The Invisible Part**

There are three little computers running inside this tracker. Two of them are performing dedicated functions. The TNC's functions are orchestrated by a PIC16F877 microcontroller and the GPS depends on an internal Hitachi SH-7020. The third processor is one that we can easily access and use to make the tracker behave as we wish. A look at Fig 7 might bring back old memories for those involved in programming in years past. It seems that few modern self-made programmers tackle a flowchart before undertaking the programming of a project today. This chart is very instructive for anyone wishing to dig into the program and modify it. It gives an overall sense of the logic of the approach to making the tracker work.

In the lower half of the flowchart, notice a "loop" (connecting the bottom to the mid-section). This is where the tracker program spends most of its time once it is initialized and running. If no data is arriving from the GPS, TNC or terminal, this loop may be performed several thousand times per second. Data arrives in spurts and as soon as a piece of data, in the form of a character or byte, arrives from one of these devices, the program follows up on the event by reading more characters from the device. Many assumptions allow the program structure to remain relatively simple. These assumptions turn out to be true *most* of the time and the program works great. Understanding the limitations resulting from these assumptions is also necessary.

*Fact*—There is only so much that this small processor can do per unit of time, and it's a lot less than that PC sitting on your desk.

*Assumption*—If we pay attention to non-repeating or low repetition events first, the others can be handled later when they repeat. Occasionally, something will be missed.

*Case in point 1*—Data begins arriving from the TNC and the GPS starts to provide position data. Since this is a messaging tracker we may be receiving a message, which is more important than getting the latest position. We have also set up the GPS to tell us

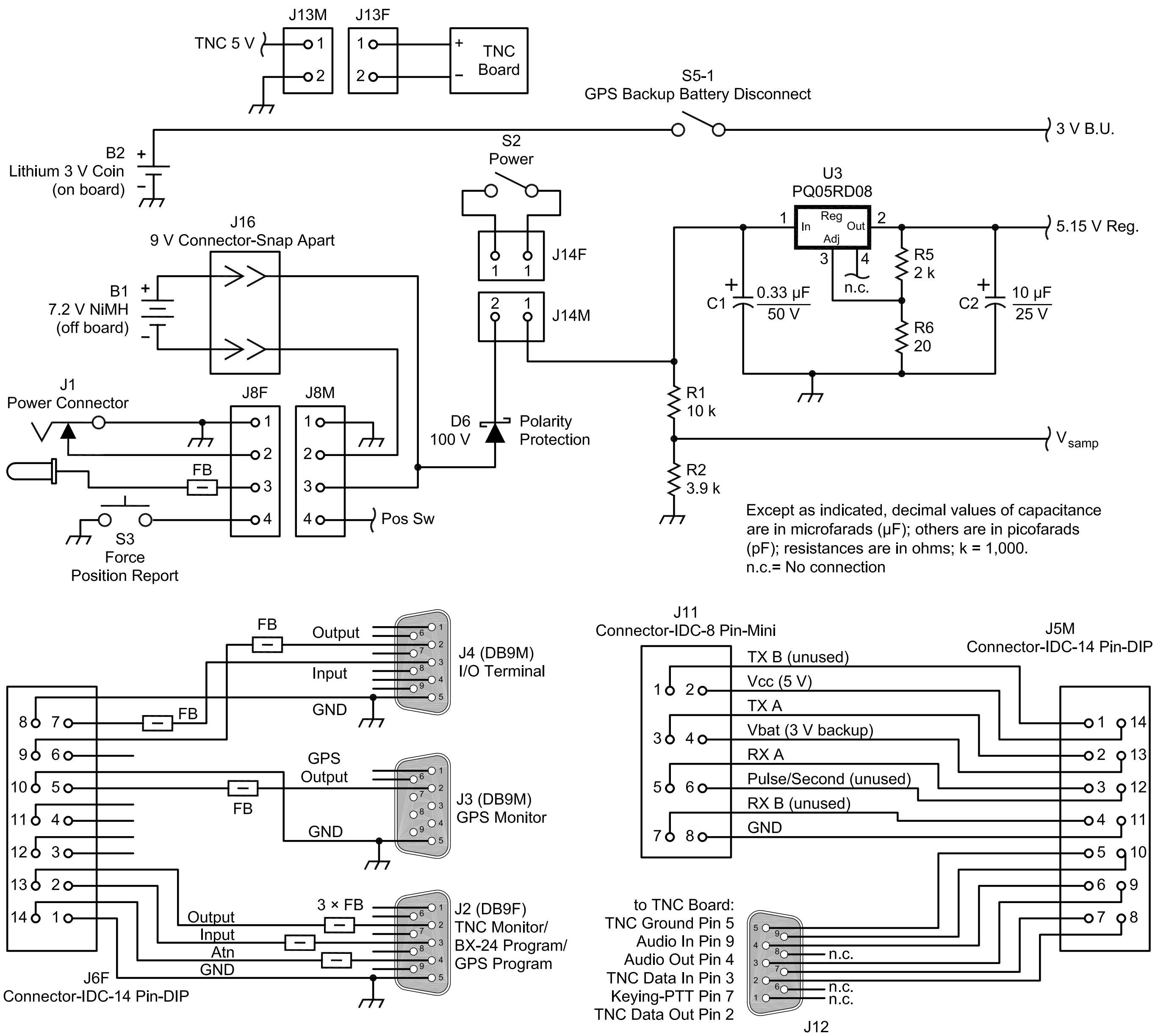


Fig 5(B)—Schematic diagram.

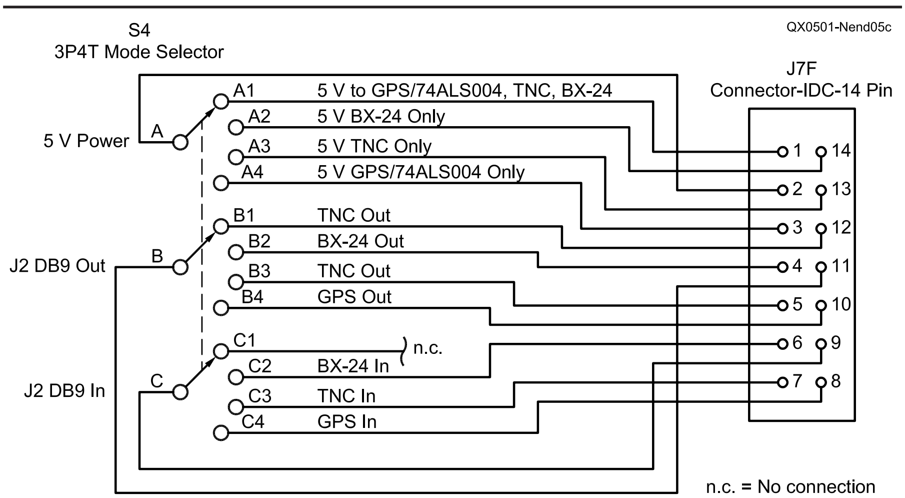


Fig 5(C)—Schematic diagram.

where we are every 10 seconds, so if we miss the position information this time around we can probably catch it next time. Whichever device sends the first character to the BX-24 wins, however, the TNC is always checked just before the GPS, giving it some priority.

*Case in point 2*—The user wants to send a message and has interrupted the normal program operation to compose the message. The processor is not fast enough and does not have enough memory to take care of other business while it assembles the typed message. You could also view this as the programmer not wishing to deal with the complexity of trying to make this happen. The result may be that we miss an incoming message. Also, we are not able to send position reports while composing a message.

*Case in point 3*—In the normal course of execution, this program may miss an incoming message if it is received at a critical time. Since all communication between devices within the tracker is at 4800 bps we can say that data is arriving at the rate of approximately 480 characters per second and can come from the TNC or the GPS. To help deal with this blast of data we use storage areas called buffers or queues that are filled up by the processor's underlying "operating system". Memory is at a premium and these buffers are minimal, maybe 20 characters long in the case of the TNC input. The simple necessity is that we process information from the buffer before it overflows. The TNC buffer can overflow in as little as a twenty-fourth of a second. It takes longer than that to complete the handling of the GPS data that arrives every 10 seconds and it also takes much longer than that to assemble a screen update for the attached display device which is also set at a 10- second interval. Thus, the tracker is blind to the TNC for a fraction of a second every 10 seconds.

Fortunately, APRS is predicated on the notion of running in an imperfect transmission environment. Messages may be automatically or manually sent several times to destinations

| | |
|---|---|
| Chassis | 4×7×2 inch (Mar Vac Electronics LMB KAB-3742) |
| Perf-Board | Velleman Eurocard 3-Hole Island 3.9×6.3 inch (All Electronics ECS-3) |
| SP1 | Piezo Speaker (All Electronics—variable similar stock) |
| B1 | Six cell AA holder (Mouser 12BH361) |
| B2 | Lithium 3 V coin cell (Mouser 639-CR2032) |
| | Coin cell holder (Mouser 534-103) |
| C1 | 10 µF, 25 V electrolytic |
| C2 | .33 µF, 50 V tantalum |
| D1,D2,D3 | Diode-Schottky 15 V, 9 A (DigiKey 95SQ015-ND) |
| D4,D5 | 1N4731 4.3 V, 1 W Zener (All Electronics 1N4731) |
| D6 | Diode-Schottky 100 V, 5 A (DigiKey 50SQ100-ND) |
| FB | Ferrite bead (#43 material for best 144 MHz attenuation) |
| J1 | Power connector-chassis mount (Mouser 163-4305) |
| | Male mate for J1 (Mouser 1710-0725) |
| J2 (DB9F) | |
| J3 (DB9M) | |
| J4 (DB9M) | |
| J5F,U2 | 14 pin IC socket (Mouser 575-193314) |
| J5M | 14 pin IDC DIP (Digikey CDP14G-ND) |
| J6F,J7F | 14 pin header socket (Digikey CSC14G-ND) |
| J6M,J7M | 2×7 row of 0.1 inch header pins. See header note. |
| J8F&M,J15F&M | 4-wire cable with connector and header( All Electronics CON-244) |
| J9F,J13F,J14F | 2-pin female (All Electronics CON-230P) |
| J9M,J13M,J14M | 2-pin (0.1 inch spacing) header |
| J10 | Mini stereo jack (Radio Shack 274-246A) |
| J11 | 8 pin IDC mini for uBlox GPS (refer to specific GPS manufacturer's documentation) |
| J12 | DB9M IDC (Mar Vac Electronics PAN IDC-9MA-P) |
| J16 | 9 V Connector-snap apart battery type (Mouser 123-7020) |
| R1 | 10 kΩ, 1/4 W resistor |
| R2 | 3.9 kΩ, 1/4 W resistor |
| R3 | 5 kΩ, 1/2 W trimmer resistor (Digikey 490-2133-ND) |
| R4 | 10 kΩ, 1/4 W resistor |
| R5 | 2 kΩ, 1/4 W resistor |
| R6 | 20 Ω, 1/4 W resistor |
| SW2 | SPST Toggle switch |
| SW3 | SPST Momentary pushbutton switch (Radio Shack 275-1571b) |
| SW4 | 3-pole 4-position rotary switch (Mouser 10WA166) |
| SW5-1 | SW5-2,SW5-3—8 section DIP switch |
| U1 | Netmedia BX-24 computer (**www.phanderson.com/basicx/index.html** ) |
| U2 | 74ALS04 Hex Inverter (Mouser DM74ALS04BN) |
| U3 | PQ05RD08 5 V, 0.8 A low drop out reg. (DigiKey 425-1593-5-ND) |

24 pin IC socket (Mouser 575-193324)

40 Pin strip header (Mouser 517-6111TG) Break segments as needed

Also required: A KISS TNC (4800 bps serial) and a GPS data source (4800 bps serial) with antenna

Header note: Several connections on the perf-board are made with headers that have been snapped off a longer strip of header pins. Generally, any connection scheme that fits will work. I chose from available pre-made connecting cables or insulation displacement flat cable terminations and installed a matching number of header pins.

**Fig 5(A-C)—Parts list.**

before an acknowledgement is received. This is a helpful property. In the BXTracker any received message is acknowledged if required. As for a message originated from the tracker, it is sent only once with a request for acknowledgement. There simply is not enough memory to keep the message body around and try again while allowing normal tracking operations to proceed. If an acknowledgement to a sent message is received, it is noted on the display and aurally as well.

**Configuring the Program**

Each user of the program must change at least one aspect of it before running it while connected to a transmitter, and that is the call sign embedded in the program. Fig 8 shows a code snippet in which this is done. Several additional places in the program contain references to the call sign as well. A note at the beginning of the program code describes how to find them. There are many other variables that can be changed to alter the performance of the program. For some of these we have two ways of accomplishing this. The program can be altered or we can set them through a configuration menu. When the unit is powered up a startup screen image is sent to any attached terminal. Within two seconds of the display appearance any character typed at the terminal will signify a desire to change some of the default variables.

The most likely settings to require changing are:

- Vehicle type and speed
- SSID number attached to the call sign
- Digipeater addresses
- Reporting-frequency limits

These items may be selected once the configuration screen has been invoked. If you would like other options to show up on the configuration screen, just follow the programming technique in the existing routines and add your own.

I made a choice to include a few features that have shown up in other trackers. There is a slightly modified version of the *SmartBeaconing* algorithm[11] developed by the inventors of HamHUD, another tracker solution. This varies the position reporting timing according to tracker speed and turns. I've also re-invented the *re-beaconing* feature published earlier by those same folks. I say *re-invented* since I came up with the idea independently and later found that others had already implemented it. This is simply the tracker's ability to listen on the channel and see if it hears any digipeat of its beacon within a given interval. In the BXTracker the default for this is set at a maximum of three repeats at ten second intervals if it does not detect a digipeat. This is particularly helpful for low power beaconing as the probability of getting stepped on by stronger or more distant stations is considerable.

**Operating the BXTracker**

With everything plugged in, the mode selector set to Normal and the GPS antenna's ability to see clear sky, all we have to do is turn the power on and hear the initial long beep. The startup screen appears on the attached display and we wait for the GPS to be initialized. Within approximately 30 seconds, and a few progress beeps, we hear a three-tone increasing pitch sound that signifies that the GPS has been initialized. Soon the display screen is formatted with the fixed fields that surround the variable data. Nearly simultaneously, an APRS status message is sent. This is accompanied by three short beeps, an "s" in Morse code, to indicate status sent. A glance at Fig 7 shows the appearance of the screen with live data displayed. It is quite easy to see what the tracker status is when viewing this screen. You might ask what happens when the GPS doesn't find satellites at startup, such as when we are under a metal roof? Well, we have no outside world time reference, so the clock is set to midnight UTC and all the GPS-related data is blanked. I designed the program to continue with the beaconing function, which it will perform at the slowest rate preprogrammed since speed would default to zero. It seemed to me that allowing remote monitoring to determine that the GPS wasn't providing data, rather than no beacons at all could be helpful. Eventually, the GPS will establish a lock on the satellites if the antenna is moved to where it can see a mostly unobstructed sky. A quicker way to get it to do so is to cycle the power on the unit.

At any time during normal operation we can interrupt the tracking function to do several other functions. And here is where we start to feel a few tradeoffs in using a small and limited processor. You may need to tap a key on the input keyboard a few times to get the tracker to notice you want its attention. Sometimes it is busy doing something and misses the keystrokes. As insurance against an inadvertent keystroke halting the whole process until an option is selected, I built in a five-second timeout. The letter "t" must be entered to proceed or operation will revert to normal. I chose the letter "t" because it is an interior key of the keyboard and less likely to be accidentally pressed if something is 'leaning" on the keyboard. When we have the unit's attention we can send a message, send status, send position, reconfigure or restart the tracker program. In the messaging department, we can send a canned message or one we type in ourselves. Since a custom message may be up to 67 characters in length, I had to re-use some of the working RAM memory employed by other functions. Usually, after one cycle of reading the GPS data (nominally, 10 seconds), these variables are restored to their original value. All messages sent request an "ack" (acknowledgement). The ack will display on the screen and cause a beep if it is detected. Otherwise, we have no

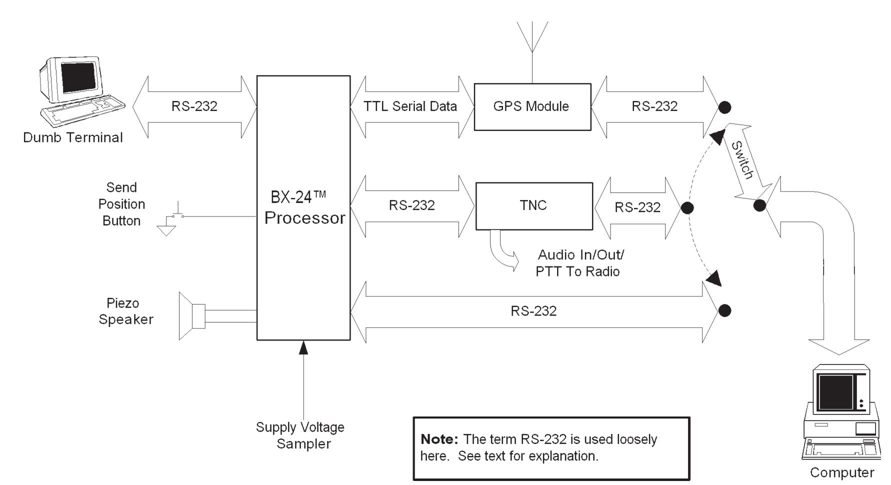


**Fig 6—BXTracker circuit block diagram.**

indication that our message was received by the other station. However, not receiving an ack is not a clear indication the message didn't make it. Maybe we didn't catch the ack due to a signal collision with another station. To be really sure our message got through we would need to send it again manually and get an ack.

When in the normal tracking mode we are able to receive messages and a few other queries/alerts. All received messages are "acked" according to the APRS specification. The tracker will also respond to the following upper case messages automatically:

?APRSS—sends status

?APRSP—sends position

?PING—(non-standard APRS) sends PONG back to sender

?VOLTS—(non-standard APRS) sends battery voltage (in mV) back to sender

?ALERT—(non-standard APRS) makes a EURO-style emergency beep at the tracker and posts the alerter's callsign on the screen on the "A:" line.

**Now What?**

One thing is clear to me, an inveterate tinkerer—I will probably never finish working on the program for the BX-24. It is so easy to make a change, upload it and try it out. I want to add more message and data logging memory in the form of a Ramtron FRAM[12] that can be added to the circuit. I would also like to charge the internal battery pack when a suitable external voltage is connected and extend the utility of the device. To enable its use as a simple local area digipeater seems like a worthwhile programming add-on, as well.

I hope my experience in designing and building this project has given you a few extra tools to employ in your own projects. Even if you never undertake the construction of a tracker, you may be intrigued by what can be done with a simple programmable controller and decide to incorporate one in a project you've been itching to put together. All you need is curiosity, *The ARRL Handbook for Radio Communications*, access to the Internet and a desire to learn and you can turn out some useful items for the shack or for the road.

*Dennis Nendza obtained his Novice license in 1962 while in eighth grade. He has always been interested in mobile operation since installing a Heathkit Twoer transceiver in the family car, adorned with a homemade turnstile antenna. Moving to Tucson, Arizona in 1974 he traded in his K3WOJ call for W7KMV. A few years later, he became involved in the personal-computer revolution by building an early system with 16 k of memory and a 2 MHz eight bit processor. In 1978 he programmed it to send and receive CW and RTTY. The next twelve years were consumed run-*

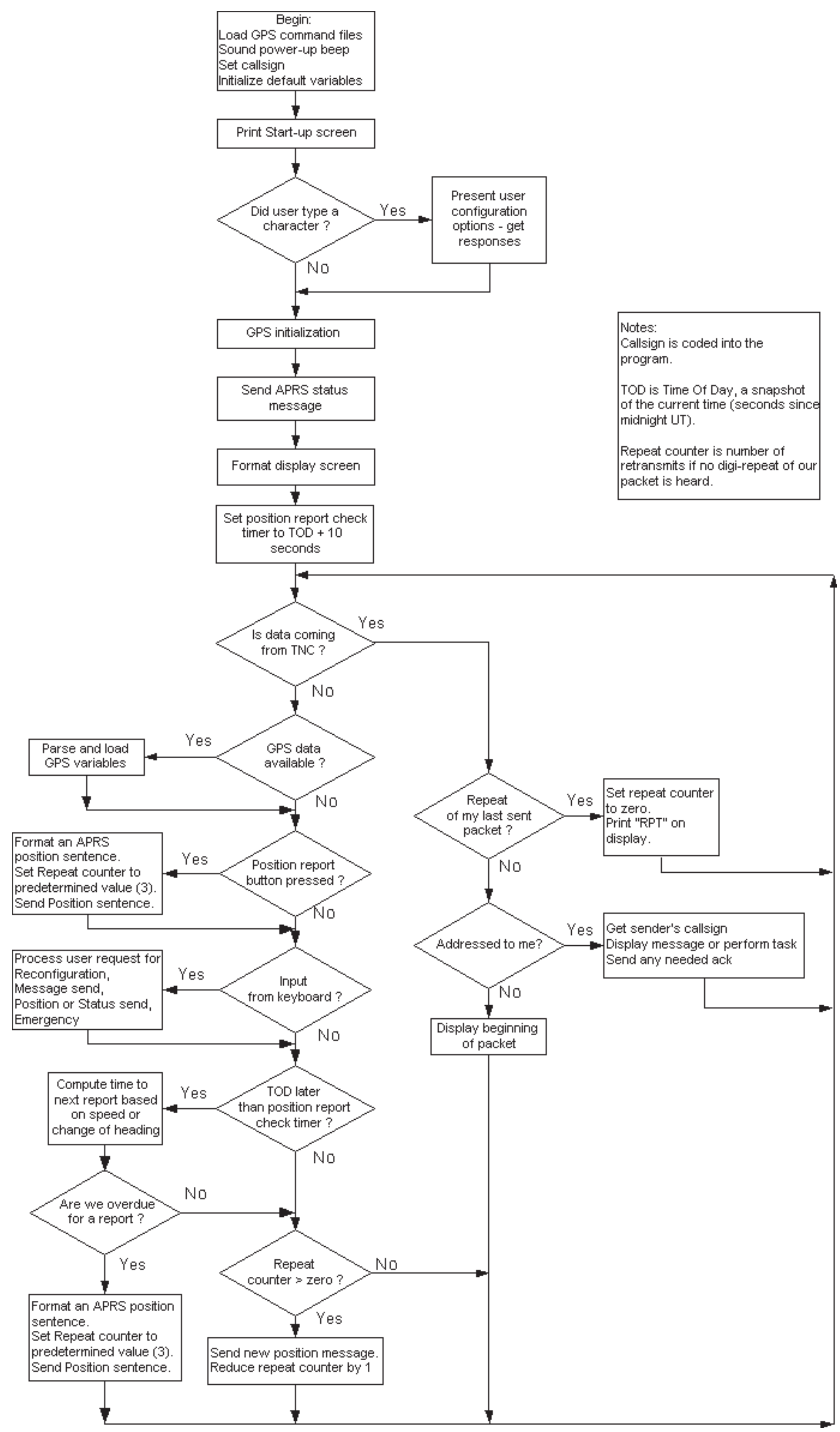


**Fig 7—Flowchart. The flow of program execution can be seen as a series of tests and operations. When examining the program code to make modifications or to learn how the processor is made to do the tracking function, this general overview of the program will help. A flow chart is the first step in creating a reliable and well-organized program.**

## Establishing A Callsign In The Program

```
MyCall(1)=ASCII_CW              'Set this unit's call sign(6 bytes + SSID) Ex: W7KMV-9
MyCall(2)=ASCIISeven            '  See the constant table at the beginning of the program
MyCall(3)=ASCII_CK              '  for names to use to represent a specific call
MyCall(4)=ASCII_CM
MyCall(5)=ASCII_CV
MyCall(6)=ASCII_SP
MyCall(7)=ASCIINine     'APRS SSID number to append to call sign
                                'Can be ASCIIZero to ASCIIFifteen as listed
                                '  in constant table at beginning of program
                                'No dash or hyphen is required
```

*MyCall* is a seven byte array in which the user's call sign is embedded in the program. Shorter call signs should use ASCII_SP as fillers. The last item is always a number in the range of 0 to 15 represented by the named constants ASCIIZero to ASCIIFifteen.

**Fig 8—Putting your station call sign in the program. Follow the comments above to change an existing call sign in the program. There are several places requiring customization in the program. I've embedded instructions in the program for finding and changing these areas.**

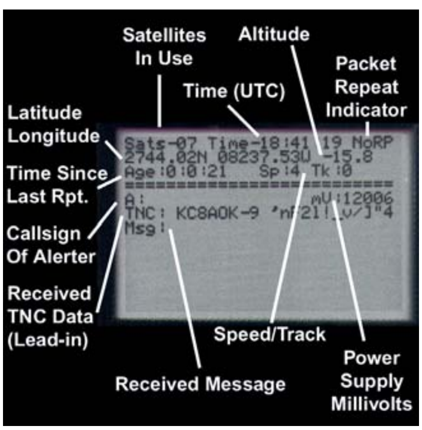


**Fig 9—This screen-shot of the outboard terminal, a Cybiko PDA-like device, shows the information that is listed in the course of running the tracker. There are many other screens that are used to prompt for messaging and changing UNPROTO paths as well as to set the smart beaconing timing.**

*ning several successful computer stores. Dennis believes the recent move back to Tucson following twelve years in Los Angeles will soon see him growing antennas in the desert on his eleven-acre site. Other activities include paragliding, photography and astronomy. Dennis can be reached at **w7kmv@arrl.net**.*

### Notes

[1]Information about APRS: **web.usna.navy.mil/~bruninga/aprs.html**.

[2]PicoPacket: **www.paccomm.com**.
TinyTrakIII: **www.byonics.com**.
TigerTrak: **www.gpstracker.com**.

[3]Basic Stamp, BASIC language programmable computer on a chip: **www.parallax. com**.

[4]NetMedia, Inc. BX-24: **www.basicx.com**.

[5]Insulation Displacement connectors are attached by routing flat cable or wire groups over a set of sharp "teeth" and squeezing a cover that pushes the individual wires into a groove in the "teeth". This displaces the insulation and makes a tight contact to the wire. The cover has locking tabs to keep the wires snugly in place. An example can be seen on this Web page: **www.kevinro.com/connections.htm**.

[6]The National Marine Electronics Association (NMEA) publishes standards for devices reporting positioning data. **www.nmea.org/pub/0183/index.html**.

[7]A new TNC is now available from W2FS—**www.john.hansen.net/PICTNC.htm**.

[8]The KISS TNC: A simple Host-to-TNC communications protocol—**people.qualcomm.com/karn/papers/kiss.html**.

[9]**www.u-blox.com**.

[10]An evaluation copy of Test Tone Generator is available to try at **www.esser.u-net.com/ttg.htm**.

[11]For a discussion of SmartBeaconing by the HamHUD inventors, see **www.hamhud.net/hh2/smartbeacon.html**.

[12]**www.ramtron.com**—makers of non-volatile high/unlimited cycle life memory chips that can replace EEPROMs. □□

# RF Power Amplifier Output Impedance Revisited

*This paper presents an analysis of vacuum tube RF power amplifiers, methods of calculating and measuring their output impedance and reasons for seeking a conjugate match.*

By Robert L. Craiglow

## Introduction

For over a decade, protagonists Walter Maxwell, W2DU,[1,2,3] and Warren Bruene, W5OLY,[4,5,6,7] have debated matters concerning impedance matching of vacuum tube radio frequency (RF) power amplifiers (PAs). Walt maintains that a conjugate match exists, or should exist, between a vacuum tube RF PA and its load—while Bruene maintains that there is no general reason for such a match to exist. Many others have taken one side or the other of the debate with no consensus to date. This paper dispels several commonly held myths and attempts to reconcile the two sides of this controversy.

A conjugate match exists between an RF PA and its load if and only if the PA's load impedance is the complex conjugate of the PA's output impedance. Ideally, stray reactances in the source and load are tuned out so that the source and load are purely resistive. Under these conditions, a conjugate match reduces to having the PA load resistance ($R_L$) equal to the PA's output or source resistance ($R_S$).

2204 Glass Rd NE
Cedar Rapids, IA 52402
**craiglowrl@juno.com**

Is there any reason to match the PA's load to its output impedance? How do you define, calculate, and measure an RF PA's output impedance? Does tuning and loading for maximum power output result in a conjugate match? Is Maxwell's load-variation method or Bruene's frequency-offset/directional-wattmeter method of impedance measurement valid?[1,2,6] Is the concept of "nondissipative resistance" necessary or useful?[2] These are crucial questions in this debate.

All the myths result from the misapplication of linear, ac circuit theory to RF PAs. The maximum available power theorem and Thevenin's and Norton's equivalent generator theorems apply only to linear circuits—not necessarily to RF PAs.

Considering the many conflicting factors in RF PA design, it is unlikely that an exact match would ever be achieved. However, there are conditions under which a conjugate match or near match are incidental to achieving other design objectives. There is insufficient room here to review all the arguments for and against a conjugate match.

[1]Notes appear on page 37.

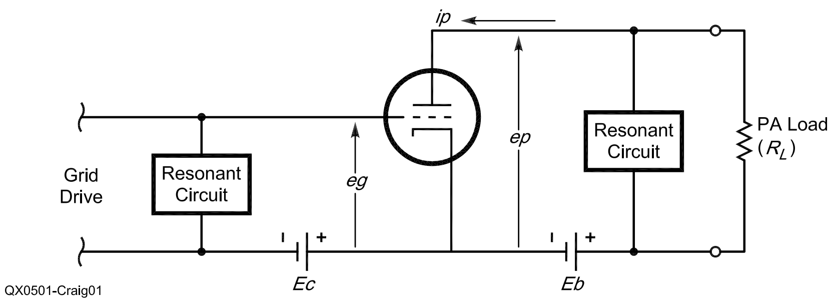


**Fig 1—Simplified diagram of a grounded cathode, RF power amplifier.**

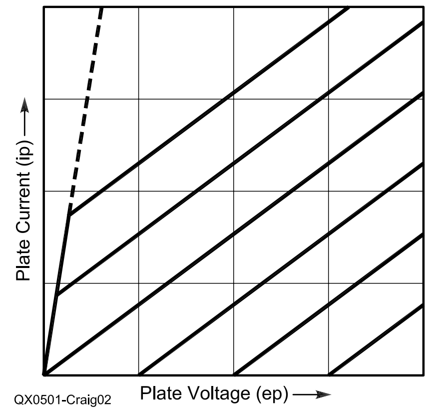


**Fig 2—Instantaneous plate current (*ip*) vs. plate voltage (*ep*) for an *ideal* tube. Solid lines are equally spaced, constant grid voltage lines.**

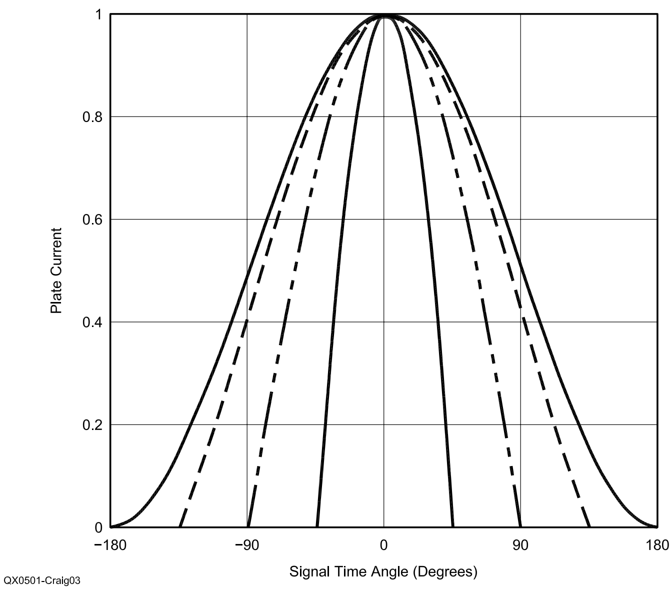


**Fig 3—Plate current waveform (*ip*) vs. time angle ($\phi$) for conduction angles ($\theta$) of 90°, 180°, 270°, and 360°.**

Rather, RF PA design, measurement and tune-up methods are examined to uncover conditions that would justify seeking a conjugate match.

### Simplifying Assumptions

Figure 1 is a diagram of a grounded-cathode, vacuum tube, RF PA. This analysis is based on the following simplifying assumptions.

- The tube has *ideal* characteristic curves with negligible electron transit time.
- Grid and plate voltages are sine waves due to the grid and plate resonant circuits.
- The grid and plate resonant circuits tune out all stray reactances.
- The PA load is purely resistive.
- Losses in the plate's resonant circuits are considered part of the PA's output load.

### Tube Model

Since all tube types and PA designs differ, neither mea-

## Appendix A—Plate Current Waveforms

Replacing *eg* and *ep* in Eq 1 with Eq 3 and Eq 4 gives:

$$ip = \frac{\mu \cdot Ec + \mu \cdot Eg \cdot cos(\phi) + Eb - Ep \cdot cos(\phi)}{rp} \text{ for } ip > 0 \text{ else } ip = 0 \qquad \text{(Eq A1)}$$

Since *ip* goes to zero when $\phi = \pm\theta/2$, one can solve for $\mu \cdot Ec + Eb$ by setting $\phi = \theta/2$ in Eq A1 to obtain:

$$\mu \cdot Ec + Eb = (Ep - \mu \cdot Eg) \cdot cos(\theta/2) \qquad \text{(Eq A2)}$$

Substituting $\mu \cdot Ec + Eb$ from Eq A2 into Eq A1 gives:

$$ip = \frac{1}{rp}[\mu \cdot Eg - Ep] \cdot [cos(\phi) - cos(\theta/2)] \text{ for } ip > 0 \text{ else } ip = 0 \qquad \text{(Eq A3)}$$

The maximum plate current ($ip_{max}$) occurs when $\phi = 0$ where Eq A3 becomes:

$$ip_{max} = \frac{1}{rp} \cdot [\mu \cdot Eg - Ep] \cdot [1 - cos(\theta/2)] \qquad \text{(Eq A4)}$$

Solving Eq A4 $(1/rp) \cdot (\mu \cdot Eg - Ep)$ for and substituting into Eq A3 gives:

$$ip = ip_{max} \frac{cos(\phi) - cos(\theta/2)}{1 - cos(\theta/2)} \text{ for } -\theta/2 \le \phi \le \theta/2 \text{ else } ip = 0 \qquad \text{(Eq A5)}$$

surement of an existing PA, nor mathematical analysis using a particular tube type or model, can prove or disprove the conjugate match hypothesis. Therefore, any general analysis will not be perfectly accurate. The classic, *ideal*, "linear" tube model is used here since it is simple, allows the derivation of closed form equations, and is a rough, useable model for all tube types.

A vacuum tube's instantaneous plate current ($ip$) is a function of its instantaneous grid and plate voltages ($eg$ and $ep$). *Ideal* characteristic curves are shown in Fig 2. The instantaneous plate current is given by:

$$ip \equiv f(eg,ep) = \frac{(\mu \cdot eg + ep)}{rp} \quad for \quad ip > 0\ .\ \ Else \quad ip = 0* \qquad \text{(Eq 1)}$$

where $f(eg, ep)$ is a function defining a particular tube's, instantaneous plate current ($ip$), ($\mu$) is the voltage amplification factor, and ($rp$) is the dynamic plate resistance.

A more accurate model is obtained by including the plate saturation resistance ($R_{sat}$), shown as a dashed line in Fig 2. Assuming that the RF PA is not driven into saturation, the minimum instantaneous plate voltage over the RF cycle ($ep_{min}$) is limited to:

$$ep_{min} \geq ip_{max} \cdot R_{sat} \qquad \text{(Eq 2)}$$

where $ip_{max}$ is the maximum instantaneous plate current. Other tube parameters of importance are the maximum plate and grid; voltage, current and power-dissipation ratings ($ep'_{max}$, $ip'_{max}$, $Pp'_{max}$, $eg'_{max}$, $ig'_{max}$, and $Pg'_{max}$) where the primes indicate maximum tube ratings.

**Power Amplifier Waveforms**

The grid and plate voltages are nearly perfect sine waves because of their parallel resonant circuits so that the instantaneous grid voltage ($eg$) is:

$$eg \equiv Ec + Eg \cdot cos(\phi) \qquad \text{(Eq 3)}$$

where ($Ec$) is the dc grid-bias voltage[8], ($Eg$) is the peak ac grid drive, ($\phi$) is the signal time angle with $\theta$ = w.t; where ($\omega$) is the radian frequency, and ($t$) is time.

Similarly, the instantaneous plate voltage ($ep$) is given by:

$$ep \equiv Eb - Ep \cdot cos(\phi) \qquad \text{(Eq 4)}$$

where ($Eb$) is the dc plate supply voltage and ($Ep$) is the peak ac plate voltage.

The dc plate voltage (Eb) is half way between the minimum and maximum plate voltages ($ep_{min}$ and $ep_{max}$) while the peak ac sine wave voltage ($Ep$) is one half the total swing or:

$$Eb = \frac{ep_{max} + ep_{min}}{2} \ \text{ and } Ep = \frac{ep_{max} - ep_{min}}{2} \qquad \text{(Eq 5)}$$

Eq 1 can be expressed in terms of the peak instantaneous plate current ($ip_{max}$) and the conduction angle ($\theta$), as shown by Eq A5 of Appendix A, as:

$$ip = ip_{max} \frac{cos(\phi) - cos(\theta/2)}{1 - cos(\theta/2)} \ \text{ for } -\theta/2 \leq \phi \leq \theta/2\,.$$

$$\text{Else } ip = 0 \qquad \text{(Eq 6)}$$

Plate current waveforms are shown for several conduction angles in Fig 3.

The dc and peak fundamental ac components of plate current ($Ip_0$ and $Ip_1$) are obtained by calculating the corresponding terms of the Fourier series expansion of Eq 6. Integration is taken over the range of $-\theta/2$ to $+\theta/2$ where the tube is in the conduction region since the plate current is zero otherwise.[9] Thus:

$$Ip_0 \equiv \frac{1}{2\pi} \int_{-\theta/2}^{+\theta/2} ip \cdot d\phi = ip_{max} \frac{2 \cdot sin(\theta/2) - \theta \cdot cos(\theta/2)}{2\pi \cdot [1 - cos(\theta/2)]} \qquad \text{(Eq 7)}$$

$$Ip_1 \equiv \frac{1}{\pi} \int_{-\theta/2}^{+\theta/2} ip \cdot cos(\phi) \cdot d\phi = ip_{max} \frac{\theta - sin(\theta)}{2\pi \cdot [1 - cos(\theta/2)]} \qquad \text{(Eq 8)}$$

The power output ($P_{out}$) is the *peak* ac plate voltage ($Ep$) from Eq 5 times the *peak* ac, plate current ($Ip_1$) from Eq 8 divided by 2 or:

$$P_{out} \equiv \frac{Ep \cdot Ip_1}{2} = \frac{ep_{max} - ep_{min}}{4} \cdot ip_{max} \cdot \frac{\theta - sin(\theta)}{2\pi \cdot [1 - cos(\theta/2)]} \qquad \text{(Eq 9)}$$

The dc plate input power ($P_{dc}$) is the dc plate voltage ($Eb$) from Eq 5 times the dc plate current ($Ip_0$) from Eq 7 or:

$$P_{dc} \equiv Eb \cdot Ip_0 = \frac{ep_{max} + ep_{min}}{2} \cdot ip_{max} \cdot \frac{2 \cdot sin(\theta/2) - \theta \cdot cos(\theta/2)}{2\pi \cdot [1 - cos(\theta/2)]} \qquad \text{(Eq 10)}$$

The plate efficiency ($Ef$), shown in Fig 4, is the ac power output ($P_{out}$) divided by the dc power input ($P_{dc}$) or:

$$Ef \equiv \frac{P_{out}}{P_{dc}} = \frac{1}{2} \cdot \frac{1 - (ep_{min}/ep_{max})}{1 + (ep_{min}/ep_{max})} \cdot \frac{\theta - sin(\theta)}{2 sin(\theta/2) - \theta \cdot cos(\theta/2)} \qquad \text{(Eq 11)}$$

Note that the effeciency depends only on the conduction angle and the ratio ($ep_{min}/ep_{max}$) and not on the load resistance ($R_L$). This is inconsistent with results obtained by applying the Thevenin or Norton theorem that result in efficiencies that vary with the load resistance and are only 50 percent for a conjugate match. The problem is that linear circuit theory does not necessarily apply to RF PAs. There is no need to invent the concept of "nondissipative" resistance to explain these results.[2]

The plate power dissipation ($Pp$) is the dc plate input

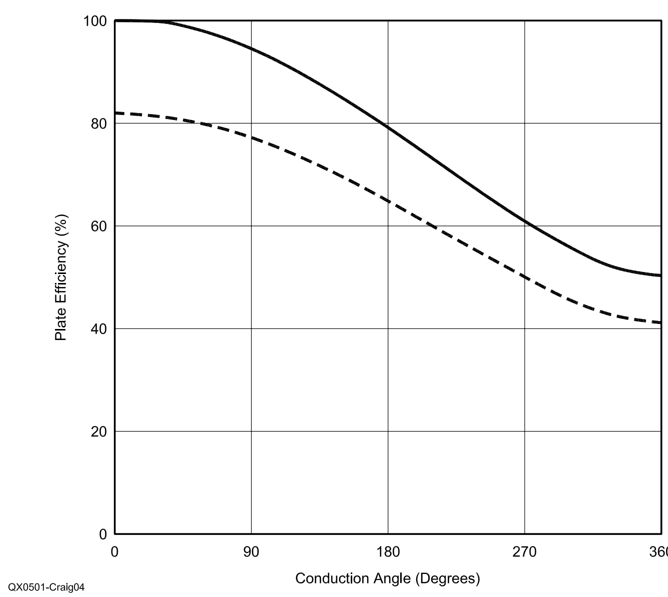


**Fig 4—Plate efficiency (*Ef*) vs. conduction angle (θ). $ep_{min}/ep_{max}$ = 0 (solid) and 0.1 (dashed).**

power ($P_{dc}$) less the ac output power ($P_{out}$). This can also be expressed in terms of the efficiency by dividing both terms by $P_{out}$ to obtain:

$$Pp = P_{dc} - P_{out} = P_{out} \cdot \left[ \frac{1}{Ef} - 1 \right] \quad \text{(Eq 12)}$$

**Design Procedure**

In most cases, the Amateur Radio designer will operate an RF PA tube according to the manufacturer's recommendations. However, if the application is atypical, it may be necessary to design from scratch based only on the manufacturer's tube ratings and characteristic curves. In this case it is useful to delve into some RF PA design theory.

The optimum PA design involves tradeoffs between many competing factors. Only the most obvious tradeoffs are addressed here and the procedure is, of necessity, over simplified. The design starts with the choice of a suitable tube type, conduction angle ($\theta$), and minimum instantaneous plate voltage ($ep_{min}$) that will give the desired tradeoff among linearity, efficiency, and power output.

If the goal is to achieve the maximum power output obtainable without exceeding the tube's instantaneous plate voltage and current ratings ($ep'_{max}$ and $ip'_{max}$), the designer tries a load line going from the maximum allowable instantaneous plate current ($ip'_{max}$) and minimum instantaneous plate voltage ($ep_{min}$) to the maximum allowable plate voltage ($ep'_{max}$). In addition, the load line must cross the zero plate current axis at the point that gives the desired conduction angle ($\theta$). This is the upper limit on the power output as determined by plate current and voltage ratings. The optimum PA load resistance in this case ($R_{Lp}$) is the maximum allowable ac output voltage ($Ep$) divided by the maximum allowable fundamental ac output current ($Ip_1$). Using this,

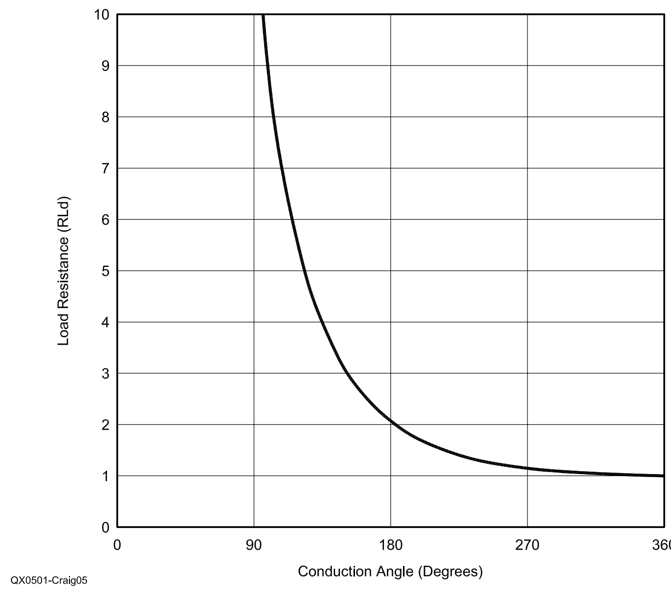


**Fig 5—Load ($R_{Ld}$) for maximum power output for a *fixed* grid drive voltage vs. conduction angle (θ). Multiply ordinate be *rp*.**

## Appendix B—Maximizing The Power Output For A Fixed Grid Drive Voltage

The maximum power output for a *fixed* grid drive voltage occurs when the partial derivative of the PA's power output with respect to the PA's load resistance is zero.[11]

Substituting Eq A4 into Eq 8 and simplifying gives:

$$Ip_1 = \frac{(\mu \cdot Eg - Ep) \cdot [\theta - \sin(\theta)]}{2\pi \cdot rp} \quad \text{(Eq B1)}$$

But the peak ac plate voltage is the peak ac plate current times the load resistance or:

$$Ep \equiv Ip_1 \cdot R_L \quad \text{(Eq B2)}$$

Substituting this into Eq B1 and solving for $Ip_1$ gives:

$$Ip_1 = \frac{\mu \cdot Eg \cdot [\theta - \sin(\theta)]}{2\pi \cdot rp + R_L \cdot [\theta - \sin(\theta)]} \quad \text{(Eq B3)}$$

Using Eq B3 for $Ip_1$, the PA's power output becomes:

$$P_{out} \equiv \frac{Ip_1^{\,2} \cdot R_L}{2} = \left[ \frac{\mu \cdot Eg \cdot [\theta - \sin(\theta)]}{2\pi \cdot rp + R_L \cdot [\theta - \sin(\theta)]} \right]^2 \cdot \frac{R_L}{2} \quad \text{(Eq B4)}$$

Taking the partial derivative of $P_{out}$ with respect to $R_L$ and simplifying gives:

$$\frac{\delta P_{out}}{\delta R_L} = \frac{[\mu \cdot Eg \cdot [\theta - \sin(\theta)]]^2}{[2\pi \cdot rp + R_L \cdot [\theta - \sin(\theta)]]^3} \cdot [2\pi \cdot rp - R_L \cdot [\theta - \sin(\theta)]] \quad \text{(Eq B5)}$$

$P_{out}$ is maximum when the derivative is zero. Setting Eq B5 to zero and solving for $R_L$ gives the optimum load resistance ($R_{Ld}$) as:

$$R_{Ld} = \frac{2\pi \cdot rp}{\theta - \sin(\theta)} \quad \text{(Eq B6)}$$

Dividing $R_{Ld}$ in Eq B6 by $R_S$ from Eq C8 gives the optimum $R_{Ld}/R_S$ ratio as:

$$\frac{R_{Ld}}{R_S} = \frac{\theta + \sin(\theta)}{\theta - \sin(\theta)} \quad \text{(Eq B7)}$$

substituting from Eq 5 and Eq 8, and simplifying gives:

$$R_{Lp} \equiv \frac{Ep}{Ip_1} = \frac{ep'_{max} - ep_{min}}{ip'_{max}} \cdot \frac{\pi \cdot [1 - cos(\theta / 2)]}{\theta - sin(\theta)} \qquad \text{(Eq 13)}$$

This is the load resistance for maximum power output if the plate power dissipation ($Pp'_{max}$) and the grid drive voltage, current, and dissipation ($eg'_{max}$, $ig'_{max}$, and $Pg'_{max}$) fall within ratings.

The load resistance, which maximizes the PA's power output for a *fixed* grid drive voltage, or equivalently, minimizes the grid drive voltage required for a *given* power output, is shown in Fig 5, and is given by Eq B6 of Appendix B as:

$$R_{Ld} = rp \cdot \frac{2\pi}{\theta - sin(\theta)} \qquad \text{(Eq14)}$$

This load resistance provides the maximum attainable power output if the power output is limited by the maximum available or maximum allowable grid drive rather than by the maximum allowable plate ratings. For some tubes $R_{Ld}$ may equal $R_{Lp}$, thus allowing optimization of both criteria simultaniously.

For still other tubes, the plate power disipation rating ($Pp'_{max}$) may limit the maximum attainable power output (see Eq 12). In this case, either the design maximum plate current ($ip_{max}$) or the design maximum plate voltage ($ep_{max}$) or both must be lowered with the accompanying necessary change in the PA load resistance ($R_L$).

**Tuning Procedure**

The tuning procedure used by Walt, when checking for a

## Appendix C—PA Output Impedance

The plate current changes instantaneously with changes in the grid and plate voltages. At any given instant in the PA's output cycle, the additional instantaneous plate current, $\Delta ip$, due to a small change in plate voltage ($\Delta ep$) caused by an external source is the slope of the constant grid voltage line ($\delta ip / \delta ep$) as a function of $\phi$ times $\Delta ep(\phi)$ or:

$$ip(\phi) = \frac{\delta ip}{\delta ep}(\phi) \cdot \Delta ep(\phi) \qquad \text{(Eq C1)}$$

Taking the partial derivative of *ip* given in Eq 1 with respect to *ep* gives 1/*rp* in the conduction region and zero otherwise so that:

$$\Delta ip = \frac{\Delta ep}{rp} \text{ for } -\theta / 2 > \phi > \theta / 2.\ Else\ \Delta ip = 0 \qquad \text{(Eq C2)}$$

Let the test voltage induced across the plate be $\Delta ep = \Delta Ep \cdot cos(\phi + \alpha)$ where $\alpha$ is the phase of the test signal relative to the PA's input voltage. Substituting this into Eq C2 gives:

$$\Delta ip = \frac{\Delta Ep \cdot cos(\phi + \alpha)}{rp} \text{ for } -\theta / 2 > \phi > \theta / 2 \quad \text{else } \Delta ip = 0 \qquad \text{(Eq C3)}$$

The peak, fundemental, *in-phase* component of incremental ac plate current ($\Delta Ip_i$) is:

$$\Delta Ip_i \equiv \frac{1}{\pi} \int_{-\theta/2}^{\theta/2} \Delta ip(\phi) \cdot cos(\phi + \alpha) \cdot d\phi = \frac{\Delta Ep}{\pi \cdot rp} \int_{-\theta/2}^{\theta/2} cos^2(\phi + \alpha) \cdot d\phi$$

$$= \frac{\Delta Ep}{2\pi \cdot rp} [\theta + cos(2\alpha) \cdot sin(\theta)] \qquad \text{(Eq C4)}$$

The PA output conductance (*Gs*) is the peak, fundemental, *inphase*, ac test current ($\Delta Ip_i$) divided by the peak ac test voltage ($\Delta Ep$) or:[12]

$$Gs \equiv \frac{\Delta Ip_i}{\Delta Ep} = \frac{\theta + cos(2\alpha) \cdot sin(\theta)}{2\pi \cdot rp} \qquad \text{(Eq C5)}$$

Similarly the peak, fundemental, *reactive* component of the test current ($\Delta Ip_q$) is:

$$\Delta Ip_q \equiv \frac{1}{\pi} \int_{-\theta/2}^{\theta/2} \Delta ip \cdot sin(\phi + \alpha) \cdot d\phi = \frac{\Delta Ep}{\pi \cdot rp} \int_{-\theta/2}^{\theta/2} cos(\phi + \alpha) \cdot sin(\phi + \alpha) \cdot d\phi = 0$$

$$= \frac{\Delta Ep}{2\pi \cdot rp} \cdot [sin(\theta) \cdot sin(2 \cdot \alpha)] \qquad \text{(Eq C6)}$$

Therefore the PA output suseptance (*Bs*) is:

$$Bs \equiv \frac{\Delta Ip_q}{\Delta Ep} = \frac{sin(\theta) \cdot sin(2\alpha)}{2\pi \cdot rp} \qquad \text{(Eq C7)}$$

When the test signal voltage is in-phase with the PA output voltage ($\alpha = 0$), the reactive component is zero. The source resistance from Eq C5 is then:

$$R_S\big|_{\alpha=0} = \frac{1}{G_S} = \frac{2\pi \cdot rp}{\theta + sin(\theta)} \qquad \text{(Eq C8)}$$

conjugate match, was to set the grid drive voltage at a convenient initial level and proceed to sequentially tune, load, and increase the grid drive until the required power output was achieved. At each step, the load is adjusted to give the maximum power output for the *fixed* grid drive voltage—but that was $R_{Ld}$. If the maximum available power theorem applied to an RF PA, this procedure would also lead to a conjugate match. This theorem does not necessarily apply to RF PAs. However, it will be shown that a conjugate match will provide maximum power output for a *fixed* grid drive voltage for operation at or near class-B.

**PA Output Impedance**

There has been no need to mention the PA output impedance in any prior discussion. All design criteria addressed so far, including "optimizing" the load resistance, can be addressed more simply and directly without reference to the source resistance. Therefore, a conjugate match is not a primary goal. However, to address the conjugate match conjecture, we must define and calculate or measure the source resistance $R_S$.

The PA's load impedance, $\boldsymbol{Z}_L = R_L + j0$, is linear, time-stationary, and passive and can be easily measured using conventional techniques. The impedance of a linear, passive circuit element is defined as the ratio of the ac phasor voltage across the circuit element divided by the ac phasor current into the circuit element, caused by the application of an *external* sine wave power source of the desired frequency.

An RF PA's output or source impedance, $\boldsymbol{Z}_S$, is not linear or passive. It must be measured while the PA is delivering full power output to its load without appreciably disturbing the PA's operation. For circuits having internal power sources that cannot be turned off, the impedance is defined as the change in the ac phasor voltage *across* the impedance ($\boldsymbol{\Delta Ep}$) divided by the change in the ac phasor current *into* the impedance ($\boldsymbol{\Delta Ip_1}$) caused by the application of an external sine wave power source or:

$$Zs = \Delta Ep \ \Delta Ip_1 \qquad \text{(Eq 15)}$$

This is the fundamental definition of impedance. Any valid calculation or measurement of $\boldsymbol{Zs}$ must be shown to conform to this definition.

In the case of an RF PA, the disturbances, $\boldsymbol{\Delta Ep}$ and $\boldsymbol{\Delta Ip_1}$, introduced by the *external* source must be small. Their frequencies must be exactly equal to that of the PA's output signal, and the PA load impedance must not be changed appreciably.

The PA's output impedance can have both resistive and reactive components depending on the phase ($\alpha$) of $\boldsymbol{\Delta Ep}$ with respect to the PA's output voltage ($\boldsymbol{Ep}$). Current flow into the tube occurs only during the conduction portion of the cycle. If the conduction is not in phase with the externally induced test voltage ($\boldsymbol{\Delta Ep}$), the current ($\boldsymbol{\Delta Ip_1}$) will lead or lag the test voltage and the source impedance ($\boldsymbol{Zs}$) will have a reactive component. Therefore, the phase angle ($\alpha$) must be specified and held constant during source impedance measurement.

It is more convenient to calculate the source admittance ($\boldsymbol{Ys} = Gs + j\,Bs$) rather than the source impedance ($\boldsymbol{Zs} = Rs + j\,Xs$). It is shown by Eq C5 and C7 of Appendix C that:

$$Gs = \frac{\theta + \cos(2\alpha)\cdot\sin(\theta)}{2\pi\cdot rp} \quad \text{and} \quad Bs = \frac{\sin(\theta)\cdot\sin(2\alpha)}{2\pi\cdot rp} \qquad \text{(Eq 16)}$$

Figure 6 shows *Gs* and *Bs* vs $\alpha$ for several values of $\theta$. For the *ideal* tube, the reactive component is zero, regardless of the test voltage phase angle ($\alpha$), when the conduction angle ($\theta$) is 180° and 360°.

The source resistance for $\alpha$ equal to zero is shown in Fig 7 and is given by Eq C8 as:

$$R_S\big|_{\alpha=0} = \frac{1}{G_S} = \frac{2\pi\cdot rp}{\theta + \sin(\theta)} \qquad \text{(Eq 17)}$$

For our *ideal* tube, the source resistance ($R_S$) depends only on the conduction angle ($\theta$) and the dynamic plate resistance ($rp$).

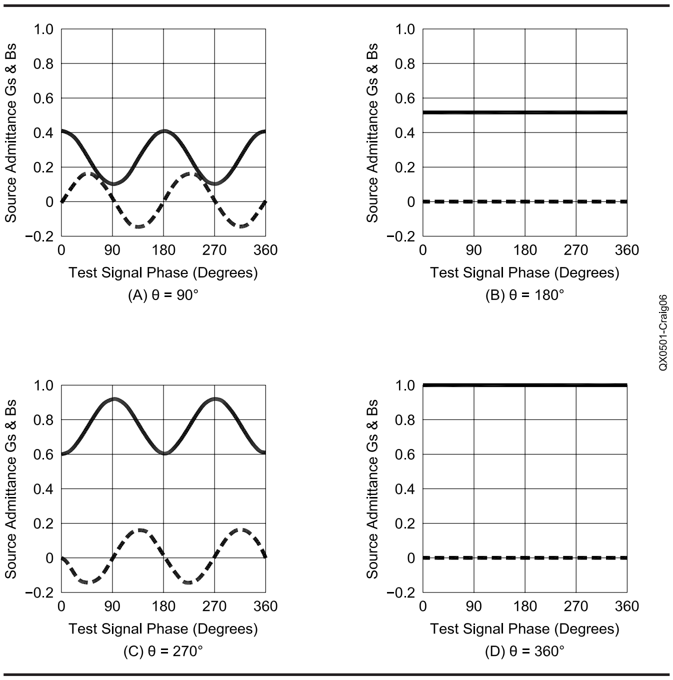


**Fig 6—Power amplifier source conductance, *Gs* (solid) and susceptance. *Bs* (dashed) vs. test signal phase angle ($\alpha$). Multiply ordinate by 1/ *rp*.**

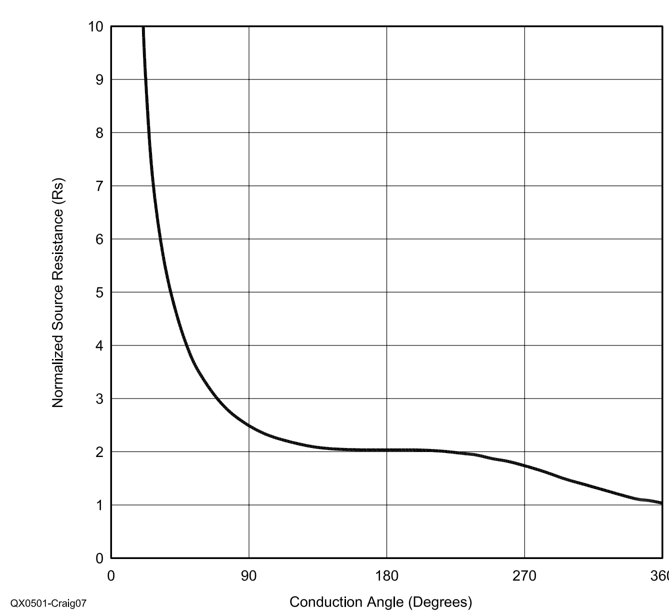


**Fig 7—Power amplifier source resistance (*Rs*) vs. conduction angle (θ) for a test signal phase ($\alpha$) equal to zero. Multiply ordinate by *rp*.**

### Match Conditions

The ratio of the optimum load resistance for maximum power output ($R_{Lp}$) of Eq 13 to the source resistance ($R_S$) of Eq 17 is:

$$R_{Lp}/R_S = \frac{ep'_{max} - ep_{min}}{2 \cdot ip'_{max} \cdot rp} \cdot \frac{[1 - cos(\theta/2)] \cdot [\theta + sin(\theta)]}{[\theta - sin(\theta)]} \qquad \text{(Eq18)}$$

This ratio depends on four unrelated parameters. It seems improbable that this ratio would be exactly equal to one as required for a conjugate match.

The ratio of the PA load resistance to the PA source resistance ($R_{Ld}/R_S$) that maximizes the power output for a *fixed* grid drive voltage, from Eq 14 and Eq 17, is:

$$R_{Ld}/R_S = \frac{\theta + sin(\theta)}{\theta - sin(\theta)} \qquad \text{(Eq 19)}$$

The solid curve of Fig 8 shows this relationship for the *ideal* tube. Note that this results in a conjugate match ($R_{Ld}/R_S = 1$) only for ideal class-A ($\theta = 360^\circ$) and class-B ($\theta = 180^\circ$) operation. This loading maximizes the power output for a *fixed* grid drive voltage. However, it does not provide the maximum power output that is obtainable from the tube if the output is limited by plate ratings rather than by the grid ratings or the available grid drive power.

### Other Tube Models

So far, we have considered only the classic, *ideal* tube model. These results are useful for rough calculations since the shape of the performance curves for all tube types are similar. More accurate results can be obtained by substituting tube equations for the particular tube's characteristic curve, using the general equations given here, and using numerical integration where necessary.

The Langmuir-Child's, or 3/2-power law tube model is based on space charge limited plate current and is closer to triode tubes than the *ideal* model as long as the grid voltage is not driven positive. The plate current for this model is given by:

$$ip = k \cdot (eg + ep/\mu)^{3/2} \qquad \text{(Eq 20)}$$

where $k$ is the perveance.

RF PA performance for this tube model has been calculated for comparison with the *ideal* model. The PA load to source resistance ratio ($R_{Ld}/R_S$) for maximum power output with a *fixed* grid drive voltage is shown in the dashed curve of Fig 8. There is very little difference in the two curves for conduction angles up to 230°. For conduction angles from 165° to 230°, the *optimum* load to source resistance ratio is between 1.3 and 0.7 or within ±30 percent of a conjugate match for both models. Therefore, for operation at or near class-B, a near conjugate match will be obtained when tuning for maximum power output with a *fixed* grid drive.

For Child's law and most other tube models, the source resistance changes with power output so that an exact conjugate match is obtained only at one specific power output level.

### Calculating and Measuring Output Impedance

For $\alpha$ equal to zero, a rough estimate of the PA's source resistance ($R_S$) can be calculated by Eq 17 based on the dynamic plate resistance ($rp$) obtained from a linear approximation of the tube's characteristic curves. More accurate estimates can be obtained using Bruene's method. [6]

Accurate measurement of an RF PA's[2] source impedance is a difficult task. Moreover, care must be taken to insure that the measurement technique rigorously conforms to the definition of impedance given by Eq 15. Some suggested means of measuring this impedance are conceptually flawed since they do not conform to this definition.

Most have assumed that the standard load-variation method of source impedance measurement applies to RF PAs. It does not. This method calculates a resistance ($R_X$) using the formula:

$$R_X = -\Delta Ep / \Delta Ip_1 \qquad \text{(Eq 21)}$$

where $\Delta Ep$ is the voltage change *across* the load resistance ($R_L$), and $\Delta Ip_1$, is the change in the current *into* the resistance due to a change in the load resistance ($\Delta R_L$). For linear circuits, $R_X$ is equal to the source resistance ($R_S$). It is also equal to the load resistance that delivers the *maximum available power* since $R_{Ld}=R_s$ for linear, time-stationary circuits.

For the *ideal* tube, $R_X$ is actually the *load* resistance that maximizes the power output for a *fixed* grid drive ($R_{Ld}$) rather than the *source* resistance ($R_S$) as most have assumed. This is shown in Appendix D.

In *Reflections II*, Walt states that he tuned and loaded the PA to maximize the power output for a *fixed* grid drive. Thus, he loaded the PA with $R_{Ld}$ and this is the impedance calculated using the load-variation method. He therefore thought that he was calculating $R_S$ while in fact he was calculating $R_{Ld}$ and therefore thought he had a conjugate match. This may explain Walt's belief that tuning for maximum power output with a *fixed* grid drive *always* results in a conjugate match. The true load to source resistance ratio is given by Eq 19.

Warren's method of measuring $R_S$ may give accurate results for operation at or near class-B but not for other classes of operation.[6] Since the frequency of the test signal is slightly offset from the PA's output frequency, the phase of the test signal with respect to the PA's output voltage ($a$), rotates slowly and the source impedance changes as shown in Figs 6 A and C. This method therefore measures some type of average source impedance rather than the true, in-phase, source resistance. However, Warren's method may give ac-

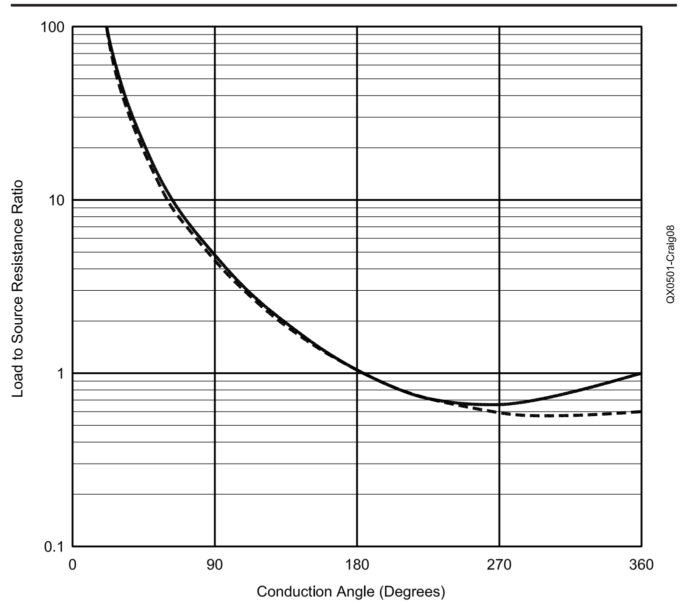


**Fig 8—PA load to source resistance ratio ($R_{Ld}/Rs$) for maximum output with *fixed* drive vs. conduction angle (θ). *Ideal* tube (solid). Child's law tube (dashed).**

## Appendix D—The Load Variation Method Of Impedance Measurement

The load-variation method is used to calculate the source resistance ($R_S$) of a generator by varying the load resistance by an increment, $\Delta R_L$, and measuring the resultant change in the voltage across the load ($\Delta V$), and the change in current *into* the load ($\Delta I$). This method calculates an impedance $R_X = -\Delta V / \Delta I$ . The maximum available power theorem states that the load resistance, which gives the maximum power output ($R_{Ld}$), is given by $R_{Ld} = R_S = R_X = -\Delta V / \Delta I$ . This method can be concidered either as means of *measuring* the source resistance ($R_S$) or *calculating* the optimum load resistance ($R_{Ld}$) for linear circuits since for this case $R_S \equiv R_{Ld}$ .

An RF PA is not linear and the above method does not apply. We will therefore derive the meaning $R_X$ for our ideal RF PA. The peak fundemental component of plate current ($Ip_1$), given by Eq B3, is:

$$Ip_1 = \frac{\mu \cdot Eg}{[2\pi \cdot rp]/[\theta - sin(\theta)] + R_L} \quad \text{(Eq D1)}$$

To simplify later calculations substitute $K$ for $[2\pi \cdot rp]/[\theta - sin(\theta)]$ in Eq D1 to get:

$$Ip_1 = \frac{\mu \cdot Eg}{K + R_L} \quad \text{(Eq D2)}$$

The change in $Ip_1$ with load resistance ($\Delta Ip_1$), is calculaed by subtracting Eq D2 from the same equation evaluated at $R_L + \Delta R_L$ so that:

$$\Delta Ip_1 = \frac{\mu \cdot Eg}{K + R_L + \Delta R_L} - \frac{\mu \cdot Eg}{K + R_L} = \frac{-\mu \cdot Eg \cdot \Delta R_L}{[K + R_L + \Delta R_L] \cdot [K + R_L]} \quad \text{(Eq D3)}$$

The volatage across the load ($Ep$) is:

$$Ep = Ip_1 \cdot R_L = \frac{\mu \cdot Eg \cdot R_L}{K + R_L} \quad \text{(Eq D4)}$$

The change in $Ep$ with load resistance ($\Delta Ep$) is calculaed by subtracting Eq D4 from the same equation evaluated at $R_L + \Delta R_L$ or:

$$\Delta Ep = \frac{\mu \cdot Eg \cdot (R_L + \Delta R_L)}{K + R_L + \Delta R_L} - \frac{\mu \cdot Eg \cdot R_L}{K + R_L} = \frac{\mu \cdot Eg \cdot \Delta R_L \cdot K}{[K + R_L + \Delta R_L] \cdot [K + R_L]} \quad \text{(Eq D5)}$$

Substituting Eq D5 and D3 into the load variation equation ($-\Delta Ep / \Delta Ip_1$) gives:

$$-\frac{\Delta Ep}{\Delta Ip_1} = -\frac{\mu \cdot Eg \cdot \Delta R_L \cdot K}{-\mu \cdot Eg \cdot \Delta R_L} = K \quad \text{(Eq D6)}$$

Finally substituting for $K$ gives:

$$-\frac{\Delta Ep}{\Delta Ip_1} = \frac{2\pi \cdot rp}{\theta - sin(\theta)} \quad \text{(Eq D7)}$$

But the right side of Eq D7 is the optimum load resistance for maximum power output for a *fixed* grid drive voltage as given in Eq B6—not the PA's source resistance as given in Eq C8. This explains Maxwell's experimental results. The fault was applying equations developed for linear circuits to nonlinear PAs.

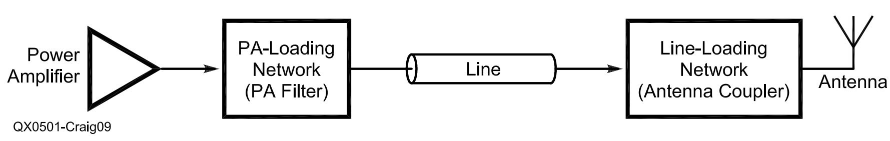


**Fig 9—RF power amplifier loading networks.**

curate results for conduction angles near 180° and 360° since the source impedance does not change appreciably with $\alpha$ as shown in Figs 6 B and 6 D,

### Power Amplifier Load

In our analysis, the PA load has been represented by a single resistive load ($R_L$). The real PA load consists of the tandem combination of the PA-loading network (PA filter), transmission line, line-loading network (antenna coupler), and antenna as shown in Fig. 9.[10] This cascade of devices can always be replaced by a single equivalent load impedance, as far as the operation of the PA is concerned, because all elements are linear.

There has been considerable discussion of the effects of these elements in regards to the conjugate match debate since the proper design and tuning of these devices has a great deal to do with the final radiated power. We will therefore examine the real purpose of the networks between the PA output and the antenna.

The purpose of the line-loading network is to present a load at the output of the transmission line that is equal to the line's characteristic impedance to avoid standing waves on the line and thus minimize transmission line losses. This also makes the line's input impedance independent of line length.

The purpose of the PA-loading network is to convert the transmission line input impedance to the *desired* or optimum PA load impedance. The purpose of each loading network is to provide the desired impedance to the driving device, not to provide a conjugate match. Introducing the details of the loading network only clouds the real issues regarding a conjugate match. The thing that counts is the load impedance presented to the PA—not the detailed composition of the loading network.

**Conclusions**

There is no direct reason to strive for a conjugate match. Optimizing the design does not require one to seek such a match. However, when operating at or near class-B, maximizing the power output for a *fixed* grid drive voltage does result in a near conjugate match. Depending on the plate and grid ratings of the tube this may or may not achieve the maximum power output capabilities of the tube.

The load-variation method of measuring an RF PA's source resistance does not necessarily apply to RF PAs and indicates that there is a conjugate match when none exists. Warren's[1,2] method of source resistance measurement gives correct results only when operating at or near class-B.[6]

Is there any reason for wanting to know the PA's output impedance? Warren has pointed out that the source resistance loads the antenna and its tuner, thus *de-Qing* the resonant circuits and increasing the overall bandwidth. This is the only obvious reason for wanting to know the PA source resistance.

**Notes**

[1]W. Maxwell, W2DU, *Reflections II—Antennas, and Transmission Lines*, Chap 19, pp 19.15-19.25.

[2]W. Maxwell, W2DU, "On the Nature of the Source of Power in Class-B and Class-C Amplifiers," *QEX* May/Jun 2001, pp 32-44.

[3]W. Maxwell, W2DU, "A Revealing Analysis of Mr. Bruene's RS," *WorldRadio*, Jan 2003, pp 16-20.

[4]W. Bruene, W5OLY, "RF Power Amplifiers and the Conjugate Match," *QST*, Nov 1991, pp 31-33, 35.

[5]W. Bruene, W5OLY, "The Elusive Conjugate Match," *Communications Quarterly*, Spring 1998, pp 23-31.

[6]W. Bruene, W5OLY, "Plate Characteristics of a Distortion-Free RF Amplifier Tube," *QEX*, Jul/Aug 2001, pp 48-52.

[7]W. Bruene, W5OLY, "On Measuring Rs," *QEX*, May/Jun 2002, pp 22-25.

[8]An artificial dc offset must be added to *Ec* when modeling tetrodes and pentodes.

[9]Sine wave terms in the Fourier expansion are zero since the plate current is symmetrical around $\phi = 0$.

[10]I have avoided the use of more conventional terms such as matching network because they might imply a conjugate match between the source and load.

[11]The equation for $P_{out}$ must be in terms of $R_L$ and the fixed parameters *Eg*, $\mu$, *rp*, and $\theta$ only, before taking the partial derivative of $P_{out}$ with respect to $R_L$.

[12]We solve for the PA's output admittance ($Gs + j\,Bs$) instead of the output impedance ($Rs + j\,Xs$) because the dynamic plate resistance (*rp*) goes to infinity during plate current cutoff. The PA output impedance is given by

$$Zs = Rs + j \cdot Xs = (Gs - j \cdot Bs)/(Gs^2 + Bs^2)\,.$$

*Bob Craiglow served during WWII in India and the Philippines as a part of the US Army Signal Corps, 3360th Signal Service Battalion, installing radio range stations. He graduated from Ohio State University in 1947 with a BEE degree and joined Collins Radio Co (later Rockwell Collins). There he worked as an electrical engineer until 1987. While at Collins he designed crystal oscillators, frequency standards, frequency synthesizers, digital MODEMS, speech signal processors, and VOCODERS. Later he worked in digital signal processing and system analysis. He contributed to sections of* Single Sideband Systems & Circuits *and* HF Radio Systems & Circuits *on analog speech modulation and intelligibility. Interest in the conjugate match debate was stimulated by conversations and correspondences with Warren Amfahr, WØWL, Warren Bruene, W5OLY and Jan Hornbeck, NØCS.* □□

# *Why Antennas Radiate*

*Antenna theory is a popular subject with hams. We love to read and talk about it. Now put on your thinking cap and fasten your safety belt for a review of the math and science behind it.*

By Stuart G. Downs, WY6EE

Mastering an understanding of electric and magnetic fields is not easy. The electric field E, the magnetic field B and the vector magnetic potential **A**, are abstract mathematical concepts that make practical presentations difficult. Those fields, however, have everything to do with why antennas radiate. Explanations for the qualitative and quantitative relationships between electric, magnetic and potential fields are presented.

All electromagnetic field equations are interrelated. Each represents a different aspect of the same thing. Indeed, we may derive one from another! Here we shall examine the dc case, and then move on to RF. First, we owe it to ourselves to cover the fundamentals.

11581 Aspendell Dr
San Diego, CA 92131

We shall begin with E and B. Assume that both fields are constant in magnitude (uniform) and observable. In our first example, they are produced by a single charged particle moving at a constant velocity **v** in a vacuum. Next, changing magnetic and electric fields produced by time varying antenna RF currents are discussed. In all cases, fields are produced both by stationary charge and charge in motion. All charge we assume to be connected through fields. We observe that the fields change when charge is in motion relative to an observer.

It is very important to realize that both constant and time-varying fields cause action at a distance. That is to say, an electron's field affects other electrons some distance away.

What is a field? No one really knows. Field lines were visualized by Michael Faraday. The idea came from the orientation of iron filings that he observed on top a piece of paper with a magnet (lodestone) placed beneath it. According to the Richard Feynman,[1] a field is a mathematical function we use to avoid the idea of action at a distance. We can state that a field connecting charged particles causes them to interact because the field exerts a force on charged particles.

Does this mean that all matter in the universe is connected through fields? As one so elegantly put it:

*All things by immortal power,*
*Near or far,*
*Hiddenly*
*To each other linked are,*
*That thou canst not stir a flower*
*Without troubling of a star...."*

[1]Notes appear on page 42.

From "Mistress of Vision" by English poet Francis Thompson (1857-1907)

### Charge in Motion Gives Rise to a Magnetic Field

All charged particles produce an electric field E. The E field can point inward or outward, depending on the sign of the charge, and is infinite in extent. The field causes action at a distance. See Fig 1. Because the field has both a magnitude and direction, we shall represent it as a vector. The same is true of a particle's velocity, so it is also a vector. Vectors are henceforth indicated by boldface letters.

The only magnetic field associated with a stationary charged particle is its spin magnetic dipole moment, but we shall ignore that for now. No other magnetic field is produced by stationary charged particles because the particle and its **E** field are not in motion relative to the observer.

When a particle with charge $q$ moves with velocity $v$, its **E** field changes: It becomes dynamic. The dynamic **E** field gives rise to a **B** field as seen by "Joe Ham," a stationary observer, in Fig 2. Joe observes that constant-magnitude electric and magnetic fields are present simultaneously. The magnitude of **B** depends upon the velocity **v** of the particle. The magnetic field that Joe observes is:[2]

$$\mathbf{B} = \frac{1}{c^2}\mathbf{v} \times \mathbf{E} \qquad \text{(Eq 1)}$$

where c is the speed of light in m/s, **v** is charge velocity in m/s and **E** is the E field in V/m. Note that if **v** = 0 then **B** = 0 (no magnetic field). If the velocity of the E field were c, then we would have **E**=c**B**, which is what we have with a freely propagating electromagnetic wave. The cross product, designated by x, between the velocity vector **v** and the **E** vector indicates that particle velocity is perpendicular to both the E and B fields. The B field in Eq 1 is bound to the moving charged particle, as observed by Joe. The B field comes from a relativistic transformation of the E field involving the ratio $v$/c. Einstein introduced the world to relativity 100 years ago, in 1905!

The **E** field multiplied by **v**/c² that transforms to the become the B field in Eq 1 is:[2]

$$\mathbf{E} = \frac{q}{4\pi\varepsilon_0 r^2}\frac{(1-\beta^2)}{(1-\beta^2 \sin\theta)^{3/2}}\hat{\mathbf{r}} \qquad \beta = \frac{v}{c} \qquad \text{(Eq 2)}$$

where $\varepsilon_0$ is the permitivity of a vacuum, $r$ is the distance from the particle's line of travel, θ is the angle between the **E** field and the particle's direction of travel, and $\hat{\mathbf{r}}$ is a vector of unit length pointing in the direction from the particle to the place where **E** is evaluated. The magnitude of **B** (see Note 2) is found by substituting Eq 2 into Eq 1:

$$B = \frac{q}{4\pi\varepsilon_0 r^2}\frac{v}{c^2}\frac{(1-\beta^2)\sin\theta}{(1-\beta^2 \sin\theta)^{3/2}} \qquad \text{(Eq 3)}$$

Therefore, for a moving charged particle in free space with no external influences, a portion of its E field gets transformed, becomes dynamic, and appears as the B field multiplied by the coefficient v/c². This means that if particle velocity increases, the magnitude of the B field increases proportionally. An observer sees both the B field and the E field at the same time with charge in motion. Note that the **B** vector is perpendicular to the **E** vector, to the velocity vector v. Einstein recognized this very fact by thinking about one of Maxwell's equations and the result was relativity. The picture assumes that θ in Eq 3 is 90°.

To summarize, the magnitude of the resulting magnetic field depends upon the velocity of the charge and the amount of charge. This means that the B field really is the relativistically transformed E field! The two fields must always change together and they do. If the B field source is the E field, can there be such a thing as a B field by itself without an E field? The answer may surprise you.

### Charge Moving at Constant Velocity Produces a Constant Magnetic Field

Charge flow in a wire is obviously very much different from that of an isolated charge moving in free space. However, exactly what is different and why?

Assume that there are no unmatched charges in our wire. That means the number of electrons (nega-

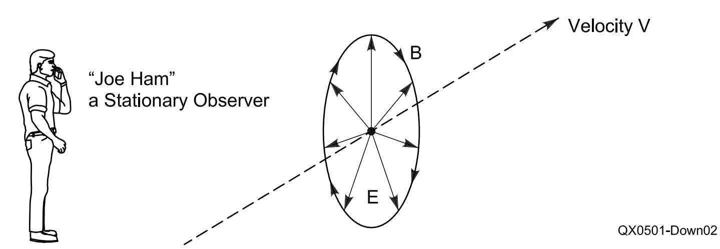


**Fig 2—The B and E fields of an electron moving with a constant velocity *v*.**

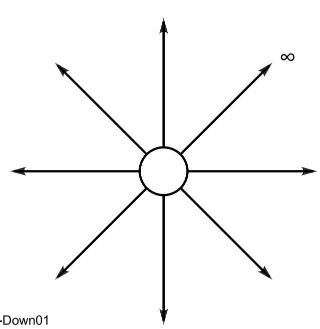


**Fig 1—An isolated charged particle with its E-field lines. E fields cause action at a distance. The effect is very small for small charges a great distance apart.**

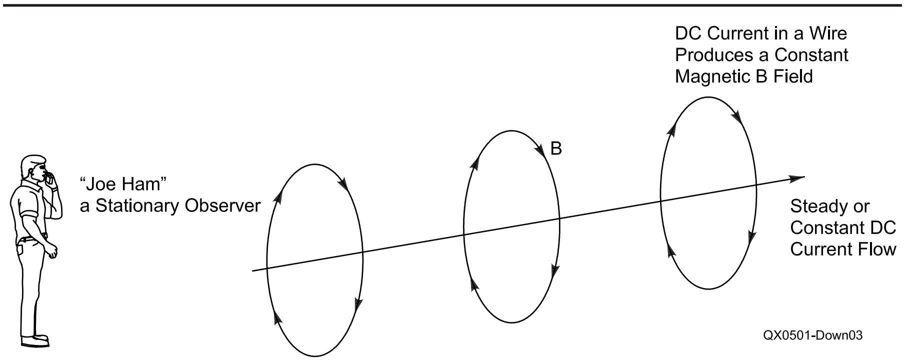


**Fig 3—Magnetic field lines around a wire with dc current.**

tive charges) equals the number of protons (positive charges) in the wire. Experiments have confirmed that current flow in such a wire produces only an observable magnetic B field at a distance *r* from the wire. The electrons' radial E fields are not observed at all. If Joe Ham were the observer, he would say there were no E fields present. The drift velocity of the moving charge is constant, so the B fields is just a function of the number of charges in motion and their velocity. See Fig 3.

Constant DC current in an infinitely long wire produces a uniform magnetic field along the wire's entire axial length. The magnitude of **B** everywhere along the axis at a distance *r* from the wire is the same. The magnetic field lines extend to great distances and they always close on themselves, unlike electric field lines, which always terminate at a charge.

Joe might ask the question, "If the B field came from the E field, then how is there now only a B field observable?" Perhaps we should state that there is no *net* E field present. Now I would like to propose another question: If there is no net E field present, is there an E-field energy density present?

**The Wire's Unobserved Net E Field**

Let's say that there is a moving radial E field that accompanies charge flow in a wire and it cannot be observed for some reason. We know that protons are fixed in the wire's metallic lattice and that the electrons are the charges that actually move. The proton static radial E field is uniform and produces no B field because there is no relative motion with respect to the observer. The electrostatic E field from all the wire's protons and electrons cancel and we are just left with the B field. The E fields of the protons and electrons, of the same magnitude but of opposite directions, must be zero or very close to it for Joe not to observe them.

Is there a basis for this in physics? The answer is yes. The big question is: How do we know this? The energy density of each field must be present. If this were not the case, then the law of superposition would be violated.

**Superposition of Like Field Quantities**

We know from the principle of field superposition that the net vector field produced by two separate vector fields of the same kind (either E or B), at the same time and place, is the vector sum of those individual fields. That may help additionally to explain why no net E field is observed when current flows in a wire. The E field from a fixed proton must exactly cancel the nonrelativistically transformed E field from the moving electrons.

The superposition principle also works for magnetic fields according to Feynman (See Note 2). That is to say, individual small amounts of magnetic field strength *d*B combine to produce the macroscopic strength that we observe. Is it possible to test for energy density where the net E field is zero and is not observable?

***Gauss's Law***

Let's use superposition and the concept of the closed surface to prove what we discussed earlier and what we saw in Fig 4. To do it, we extend the discussion to another term called flux. Flux is the electric field strength associated with each unit area through a surface. Feynman[3] relates flux and charge in the following way: "The E-field flux $\Phi$ through any closed surface is equal to the net charge inside that surface divided by the permittivity of free space." That is Gauss's law. The closed surface could be a sphere containing some charge, or any other shape so long as it fully encloses the charge. In mathematical terms:

$$\Phi_{total} = \frac{q_{total}}{\varepsilon_0} \qquad \text{(Eq 4)}$$

Thus the net E-field flux passing through the surface enclosing our wire, which has a net charge of zero, is zero.

It is interesting to note that if we used superposition to determine energy density (energy/volume) by summing the E-field energies of protons and electrons, the energy densities do not cancel, they add! The reason is that in the calculation of energy density, the E-field is squared. This yields two positive numbers so there can be no net density cancellation. The proof that field energy density is present is beyond the scope of this paper. I suspect that it has something to do with gravity. Didn't Einstein show us that matter and fields were both essentially forms of energy?

**The Biot-Savart Law**

It turns out that there is a law that may be derived from Eq 3 that supports the idea that all B fields arise from changing E fields. Everything about it is self-consistent. It is called the Biot-Savart law.

The Biot-Savart law allows determination of B a distance r away from a wire for a given dc current. To perform an actual calculation, one would break the wire into infinitesimally small segments *dl* and integrate along the entire length of the wire all the infinitesimally small *dB* contributions they produced at some distance *r* from the wire. The sum would be the magnetic field strength B at that distance.

To derive this law, we begin with Eq 3 and assume that the magnitude of B is changing with time. In the notation of calculus, the rate of change would be $dB/dt$, where *t* is time. Taking the time derivative of the magnetic field, we get:

$$\frac{dB}{dt} = \frac{d}{dt}\left[\frac{q}{4\pi\varepsilon_0 r^2}\frac{v}{c^2}\frac{(1-\beta^2)\sin\theta}{(1-\beta^2\sin\theta)^{3/2}}\right] \qquad \text{(Eq 5)}$$

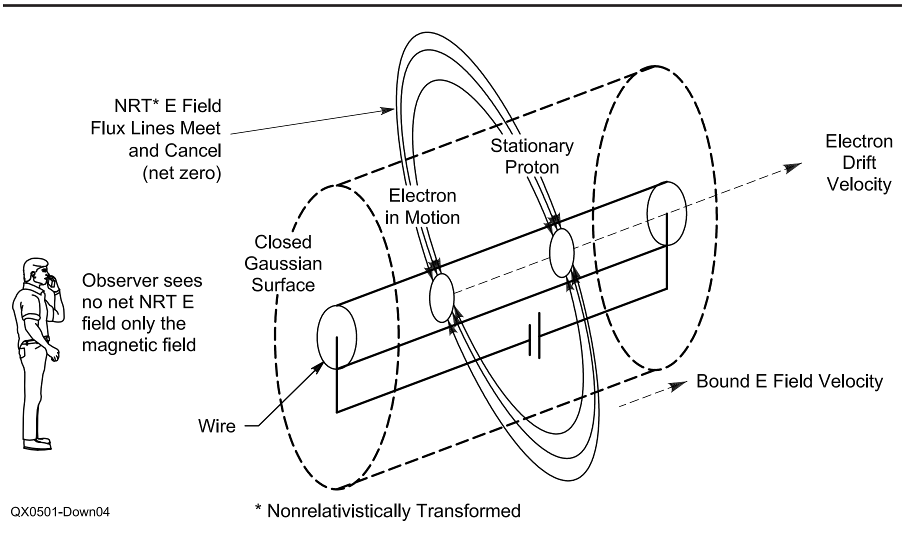


**Fig 4—Electron motion in a wire and particle E fields.**

Assuming $\theta = 90°$, it is easily shown that:

$$\frac{dB}{dt} = \frac{d}{dt}\left[\frac{q}{4\pi\varepsilon_0 r^2}\frac{v}{c^2}\frac{1}{(1-\beta^2)^{1/2}}\right] \quad \text{(Eq 6)}$$

Note that $\gamma = 1/(1-\beta^2)^{1/2}$ is a commonly used relativistic term. Using the binomial expansion theorem for the relativistic term and $\beta^2 = v^2/c^2$, we see that:

$$\left(1-\beta^2\right)^{1/2} \approx \frac{1}{\left(1-\frac{v^2}{c^2}\right)} \quad \text{(Eq 7)}$$

when $v$ is small with repect to c. Substituting in the relativistic gamma term $\gamma$, we see:

$$\frac{dB}{dt} = \frac{d}{dt}\left(\frac{v}{c^2}\frac{\gamma q}{4\pi\varepsilon_0 r^2}\right) = \frac{d}{dt}\left(\frac{v}{c^2}\gamma E\right) \quad \text{(Eq 8)}$$

The gamma function $\gamma$ stretches the electrostatic field $q/(4\pi\varepsilon r^2)$. Now substituting in Eq 7:

$$\frac{dB}{dt} = \frac{d}{dt}\left[\frac{v}{c^2}\frac{q}{4\pi\varepsilon_0 r^2}\left(1-\frac{v^2}{c^2}\right)\right] \quad \text{(Eq 9)}$$

Knowing that $v \ll c$, we use a simplification so that the inside term in parentheses of Eq 9, goes to zero. Additionally, we multiply both sides by $dt$ and we end up with:

$$dB = \frac{d}{dt}\left(\frac{q}{4\pi r^2}\frac{vdt}{\varepsilon_0 c^2}\right) \quad \text{(Eq 10)}$$

Lastly, we know that $vdt = dl$ (velocity times time equals distance); current $I = dq/dt$ (charge per unit time) and $\mu_0 = 1/\varepsilon_0 c^2$ (the permeability of a vacuum), we arrive at the magnitude form of the Biot-Savart law with $\theta = 90°$:[4]

$$dB = \frac{\mu_0 I dl}{4\pi r^2} \quad \text{(Eq 11)}$$

We derived the Biot-Savart law from charge in motion in free space. Biot and Savart experimentally deduced[4] this relationship that links a current segment in a wire to an infinitesimally small magnetic field $dB$ a distance $r$ away from the wire. It is taught in physics textbooks today[4, 5, 6] and forms the basis for magnetic induction. For example, Ampere's and Faraday's law can be derived from the Biot-Savart law. So magnetic fields are related directly to currents. See Fig 5.

***Electromagnetic Radiation***

Up to now, we have been looking at fields bound to or coupled to charges moving at constant velocities. We have also seen that a stationary observer sees only the B field for charge moving at constant velocity in a wire, and that velocity has been slow. Now what would happen if the charge velocity rapidly changed, as in the case of an RF signal? What if charge velocity were changing at a high rate?

When its velocity is changing, we say a particle is accelerating. Deceleration is just negative acceleration—it's just a matter of signs. Acceleration of charges is what launches radio signals. However, the E field here is one of a different color. We have seen that as field velocity goes to c, both E and B propagate together at the speed of light so that E=cB. However, how exactly does an antenna launch such an electromagnetic wave?

What really happens is that electrons in an antenna accelerate and decelerate because of the application of some time-varying electromotive force (EMF or voltage) to the antenna. A time-varying EMF implies the presence of a time-varying electric field E. Each electronic charge q in the antenna experiences force $F = qE$ and therefore accelerates and decelerates according to $F = mA$, where m is the mass of the electron and $A$ is acceleration.

Thus, we have an alternating current in the antenna. The simplest alternating current is sinusoidal since it consists of a single frequency. We have shown that a changing E field gives rise to a B field. The fields propagate with velocity c, but the drift velocity of the electrons in the antenna travel at some much lower velocity $v$. The magnitude of the fields must vary in a sinusoidal fashion from point to point along the wire's length. It is interesting to note that the electron speed and the wave speed appear to detach from each other.

The radiated B field is perpendicular to the antenna while the E field is

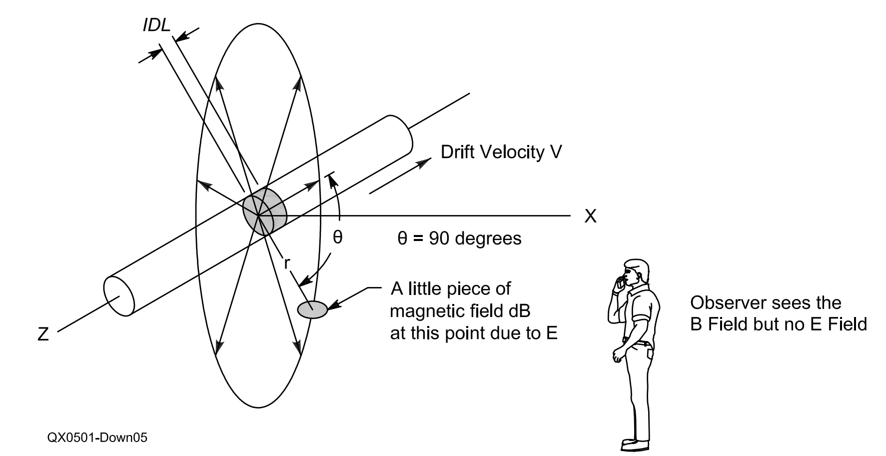


Fig 5—A pictorial representation of the Biot-Savart law.

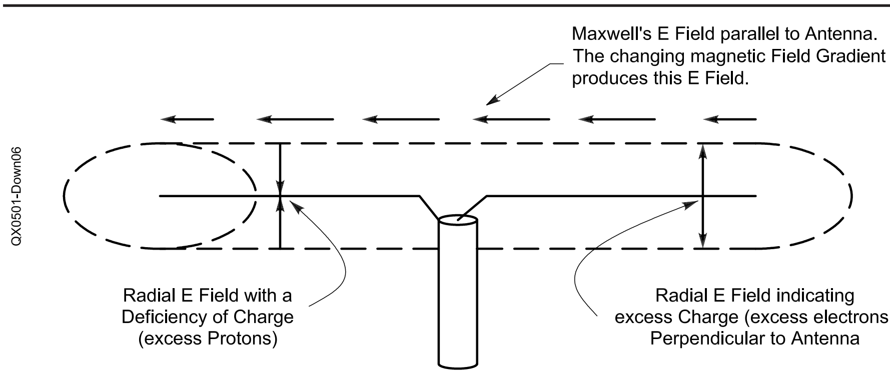


Fig 6—A dipole antenna and surrounding fields.

parallel to it. Both move outward from the antenna with speed c with respect to the antenna. See Fig 6. Nevertheless, how do we get a parallel E field when we know that the E-fields of the electrons themselves are perpendicular?

We saw above that in a wire having zero net charge, the E field caused by the electrons is not measurable macroscopically. Recall that is because the E field from the protons cancel it. All that is measurable outside the wire is the B field. But it has been shown that just as changing E fields produce B fields, the reverse is also true: Changing B fields produce E fields. The orientation of whichever field is so produced actually *counteracts* the change in the field producing it.

It might seem at first that this reciprocity would prevent anything from happening, since one effect tends to cancel the other, and that tendency is true. It's called Lenz's law and it is an essential physical fact, not just some arbitrary convention about signs or directions. It is an interesting manifestation of physical systems' resistance to change, akin to Newton's first law of motion. It implies that some energy must be added to the system to build fields. It is convenient to think of that energy as being stored in the field.

In our antenna, we start with only a B field outside the wire, but it is changing and propagating away from the wire at speed c. When the current in the wire alternates rapidly enough, the changing B field propagates away before the Lenz effect can cancel it. Since the B field is also alternating, it is accompanied by an alternating E field whose peak magnitude grows to its final value as the wave is launched. That first stage of wave formation takes place in what we call the near field.

The near field is generally considered within about 10 wavelengths. Outside the near field is the far field. In the far field, where the electromagnetic wave freely propagates outward, $E=cB$ at all times everywhere. Thus the near field is chiefly magnetic and $E<B$.

For more detailed discussion and mathematics surrounding the above topics, navigate to **www.arrl.org/qex/.** Look for 0501Downs.zip.

### Summary and Conclusion

The radial electrostatic field in motion around a current carrying wire is not observed. This is so because there is no net charge in the wire, and the net E field from all of the wire's protons and electrons cancel. To observe any net E field would violate Gauss's law.

In an electromagnetic wave, E drops off as $1/r$ in the far field whereas an electrostatic field drops off as $1/r^2$. Therefore, E in the travelling wave cannot be an electrostatic field. It is the changing field generated by the changing B field around the antenna. Likewise, E in the travelling wave is generated by the changing B field. Mutual recreation occurs perpetually and the wave travels at velocity c. James Maxwell proved it.

E and B fields are mathematical constructs we use to describe action at a distance. They are really manifestations of the same thing. There are particle theories of electromagnetic radiation, too, but we chose not to discuss them here.

### Acknowledgments

I am grateful to Glenn Borland, KF6ZVK, for his friendship and insight, which has helped with this paper's formulation. Indeed, over the years we have had many great conversations. A hardy thanks also to Julius Tolan and Santos Cota for their suggestions.

### Notes

[1]Feynman, Leighton, Sands, *The Feynman Lectures on Physics*, Volume II, Addison-Wesley, p 15-7.

[2]R.D. Field, University of Florida. Physics 2061 class notes, **www.phys.ufl.edu/~rfield/classes/fall02/images/relativity_21.pdf**

[3]Feynman, Leighton, Sands, *The Feynman Lectures on Physics*, Volume II, Addison-Wesley, 13-12.

[4]Halliday, Resnick, and Walker, *Fundamentals of Physics* Sixth Edition, Extended Version, Wiley 2001, pp 687-688.

[5]Fishbane, Gasiorowicz and Thornton, *Physics for Scientists and Engineers*, Prentice-Hall 1996, pp 819-896

[6]Hayt, *Engineering Electromagnetics*, Fifth Edition, McGraw Hill 1989, pp 216-224.

[7]Halliday, Resnick, and Walker, *Fundamentals of Physics* Sixth Edition, Extended Version, Wiley 2001, p 690.

[8]Feynman, Leighton, Sands, *The Feynman Lectures on Physics*, Volume II, Addison-Wesley, p 13-2.

[9]Hayt, *Engineering Electromagnetics*, Fifth Edition, McGraw Hill, 1989, p 251.

# *Low-Noise Frequency-Synthesizer Design*

*Use an* Excel *spreadsheet to design synthesizers with predictable performance.*

By Randy Evans, KJ6PO

There have been numerous articles and textbooks describing the advantages of low-phase-noise synthesizers, and any high-quality transmit/receive system requires their use for low jitter or low-noise sidebands to minimize signal degradation. Yet, the design of such synthesizers can be quite complex and confusing because of the multitude of tradeoffs that invariably occur during the design process.

This article describes a powerful, but simple-to-use, synthesis tool for designing low-noise frequency synthesizers using third-order Type 1 PLLs with charge-pump output to the loop filter or third-order Type 2 PLLs with a voltage-output phase detector. It is not meant as a theoretical treatise on phase-locked loops, because innumerable texts and articles have covered the subject in depth. This article gives practicing design engineers a tool for rapid and accurate designs that helps guide designers to optimum designs for the lowest-noise synthesizer design. Specific hardware implementations of PLL design are not covered in this article, but the circuit component requirements and design pitfalls are described for the hardware realization.

The design-synthesis tool is implemented in an *Excel* spreadsheet for ease of implementation and will calculate loop-filter component values, predict the loop phase margin, and plot the expected phase noise. The use of a spreadsheet allows the designer to change a single design value and immediately see the result of the change. This allows the designer to consider tradeoffs and perform "what if" analyses easily and rapidly.

Designing frequency synthesizers for low phase noise is more than just following "cookbook" design techniques available from numerous application notes and books available for PLL and synthesizer design. While such resources are certainly applicable and form the basis for much of this article, they seldom give the complete picture. Generally, application notes will generate the PLL-filter parameters for a given loop bandwidth and frequency step-size requirement, but they do not necessarily specify the optimum loop bandwidth for a given phase-noise requirement and the performance data requirements for circuit components. In particular, the designer often has given frequency step-size, settling time and phase-noise requirements to meet when only the loop bandwidth can be easily selected. Unfortunately, it may not be possible to meet all requirements with a given design. This article presents an approach to determine whether the synthesizer requirements can be met and offers alternative designs that may meet the system requirements.

Some background research may be desirable before diving into the frequency-synthesizer design-synthesis approach: A general model for all linear control theory is shown in Fig 1, which contains Eqs 1 and 2.

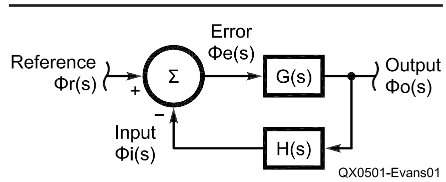


$$\phi e(s) = \frac{1}{1+G(s)H(s)}\phi r(s) \quad \text{(Eq 1)}$$

$$\phi o(s) = \frac{G(s)}{1+G(s)H(s)}\phi r(s) \quad \text{(Eq 2)}$$

**Fig 1—Linear-control theory model.**

A reference signal $\phi r(s)$ is used for comparison with the input signal $\phi i(s)$, a feedback version of the output signal $\phi o(s)$ transferred through $H(s)$ to a summing network, to generate an error signal $\phi e(s)$. The error signal is then filtered by the transfer functions $G(s)H(s)$ and fed back out-of-phase with the reference signal to reduce or, ideally, to cancel the error signal. The two most important equations, the closed-loop transfer and error-function equations, of the linear-control model are presented in Fig 1. Eq 1 describes the error signal output of the phase detector. Notice that if the loop gain


2688 Middleborough Circle
San Jose, CA 95132
**randallgrayevans@yahoo.com**

G(s)H(s) is large, the error signal is very small, indicating that the output signal is tracking the reference signal quite closely. Since G(s)H(s) for a linear control system is a frequency-dependent function with magnitude decreasing as frequency increases, the error signal will increase in magnitude with increasing frequency (because the denominator magnitude will decrease with frequency). Eq 2 shows that the output signal essentially follows the reference signal for G(s)H(s) >> 1. Conversely, the output signal no longer follows the reference signal as G(s) falls to very small values. Hence, the reference signal only controls the output signal within the loop bandwidth of the control loop.

This is fine, but how does it apply to frequency-synthesizer design? Well, let's move away from the generalized linear-control-theory model and go to a phase-locked-loop model as shown in Fig 2. Notice that this is the same general form as the linear-control-theory model. In this case, $\theta_{ref}$ is the phase of the reference signal, $\theta_{input}$ is the phase of the input signal from the frequency divider and $\theta_{error}$ is the phase error out of the phase detector, which represents the phase difference between the reference and input signals. G(s) consists of the phase-detector gain $K\phi$, the loop-filter function F($s$), and the VCO transfer function $K$vco/$s$. Therefore, G(s) = Kϕ*F(s)*Kvco/s and H(s) = 1/N. Several equations for PLL analysis are also shown, with Eq (6) being the very important closed-loop gain.

## The PLL Model

If we now redraw the PLL model as shown in Fig 3, we can now derive the final equations that we need to design and analyze a frequency synthesizer. $S_{out}(s)$ represents the phase spectral noise density of the output signal of the synthesizer versus frequency. Similarly, $S_{vco}(s)$ represents the free-running phase spectral noise density of the VCO, and $S_{ref}(s)$ represents the phase spectral noise density of the reference signal, noise(s) represents the spectral noise density of the frequency divider noise floor and the loop-filter op amp (if used). In order to derive the equations for $S_{out}(s)$, simply go around the loop and write the equations. Notice that $S_{out}(s)$ is a sum-

**Table 1—PLL Parameters**

| | |
|---|---|
| $K_{VCO}$—VCO sensitivity | 20 MHz/V |
| $K_{pd}$—Phase Detector Sensitivity | 5 mA/degree |
| $F_{ref}$—Frequency Reference | 200 kHz |
| N—Frequency Division | 4500 |
| Fp—loop bandwidth | 20 kHz |
| ϕm—Phase Margin | 45° |
| Atten—Excess reference frequency attenuation from loop filter | 10 dB |

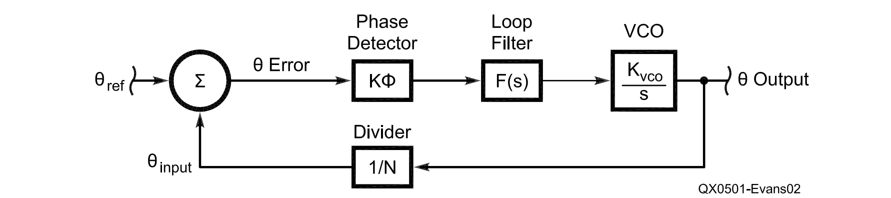


$$\textit{Forward Loop Gain} = G(s) = \frac{\phi o(s)}{\phi e(s)} = \frac{K\phi F(s) K_{vco}}{s} \quad \text{(Eq 3)}$$

$$\textit{Reverse Loop Gain} = H(s) = \frac{\phi i(s)}{\phi o(s)} = \frac{1}{N} \quad \text{(Eq 4)}$$

$$\textit{Open Loop Gain} = G(s)H(s) = \frac{\phi i(s)}{\phi e(s)} = \frac{K\phi F(s K_{vco})}{N s} \quad \text{(Eq 5)}$$

$$\textit{Closed Loop Gain} = \frac{G(s)}{1 + G(s)H(s)} = \frac{\phi o(s)}{\phi r(s)} \quad \text{(Eq 6)}$$

**Fig 2—PLL Model**

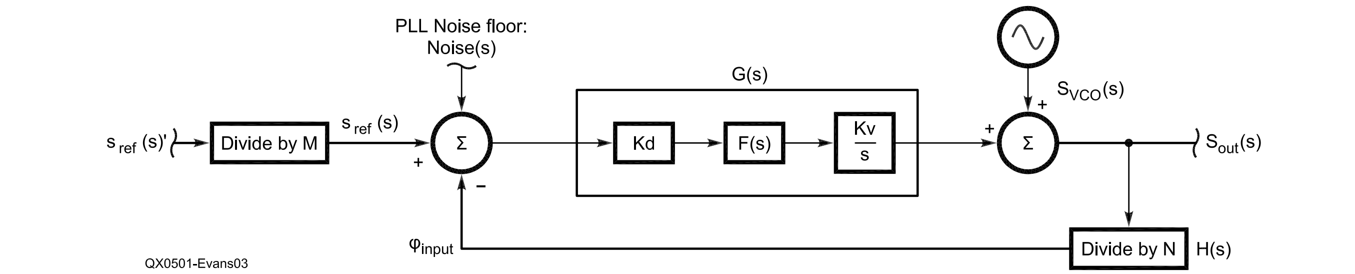


$$S_{out}(s) = S_{ref}(s)\, G(s) + \textit{Noise}(s)G(s) - S_{out}(s)G(s)H(s) + S_{vco}(s) \quad \text{(Eq 7)}$$

$$S_{out}(s) + S_{out}(s)G(s)H(s) = S_{ref}(s)G(s) + \textit{Noise}(s)G(s) + S_{VCO}(s) \quad \text{(Eq 8)}$$

$$S_{out}(s)[1 + G(s)H(s)] = S_{ref}(s)G(s) + \textit{Noise}(s)G(s) + S_{VCO}(s) \quad \text{(Eq 9)}$$

$$S_{out} = \frac{S_{ref}(s)G(s)}{1 + G(s)H(s)} + \frac{\textit{Noise}(s)G(s)}{1 + G(s)H(s)} + \frac{S_{vco}(s)}{1 + G(s)H(s)} \quad \text{(Eq 10)}$$

**Fig 3—PLL Linear-model equations.**

mation of four terms: $S_{ref}(s)$ times G(s), Phase Detector Noise times G(s), $S_{vco}(s)$ and $S_{out}(s)$ times –H(s) and G(s) as shown in Eq (7). Eqs (8) and (9) are simply collecting terms from Eq (7), and Eq (10) is the final description of $S_{out}(s)$.

### PLL Linear-Model Equations

Eq (10) shows that the phase-noise spectrum of the output signal is the result of the reference phase-noise spectrum, the VCO phase-noise spectrum and the phase-detector noise floor (resulting noise spectrum of the phase detector, frequency divider and loop filter). It also shows that the effects of the VCO phase noise are reduced by the 1 + G(s) H(s) denominator in the equation, so long as the magnitude of G(s)H(s) is greater than 1. Similarly, the reference phase noise and the noise sources are essentially controlling the output phase noise so long as the closed-loop gain magnitude, G(s)/[1 + G(s)H(s)], is greater than 1.

In order to get a better intuitive feel for what Eq (10) is really telling us, review the following diagrams. Both figures are based on an analysis of a PLL whose parameters are those summarized in Table 1. The PLL parameters shown are the same as those in National Semiconductor's application note AN1001. To compare

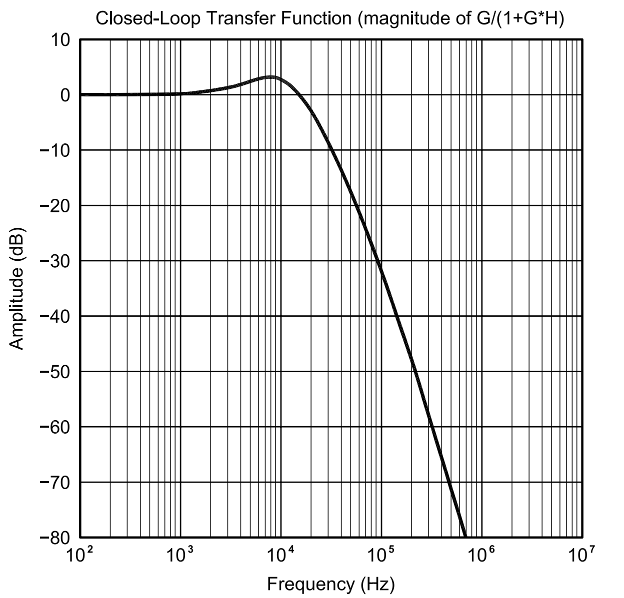


Fig 4—Closed-loop transfer function (magnitude of $\frac{G(s)}{1+G(s)H(s)}$ Eq A)

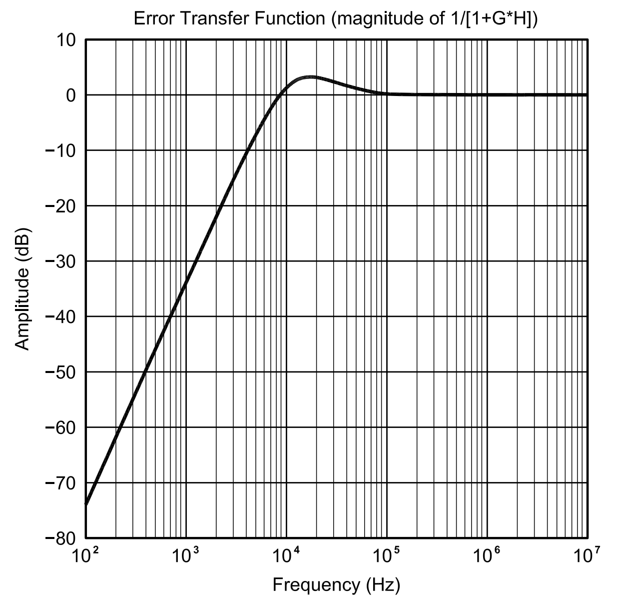


Fig 5—Error Function (magnitude of $\frac{1}{1+G(s)H(s)}$ Eq B)

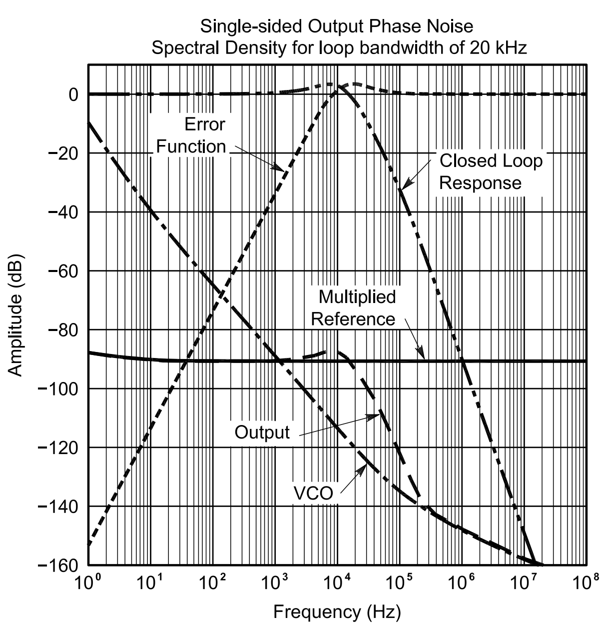


Fig 6—PLL Phase noise for a 20-kHz loop bandwidth.

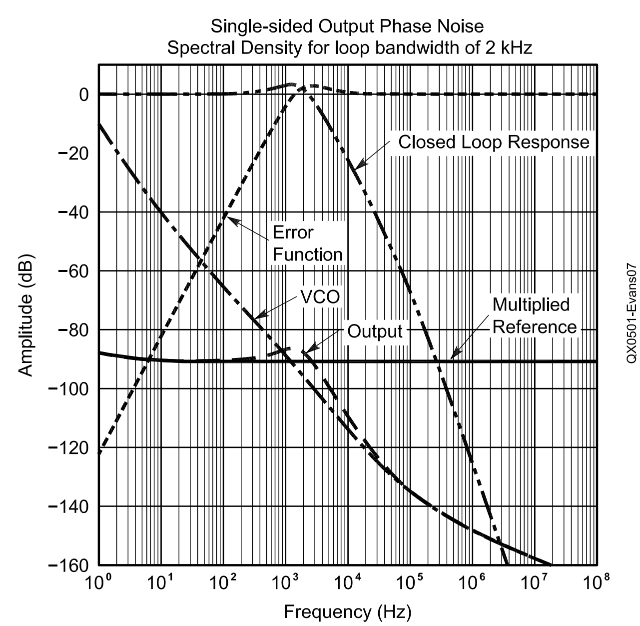


Fig 7—PLL Phase noise for a 2-kHz loop bandwidth.

**Table 2—Assumed Levels for Reference Oscillator Noise, VCO Spectral Density and the PLL Noise Floor**

| | | | | | | | | | | |
|---|---|---|---|---|---|---|---|---|---|---|
| Freq offset from carrier (Hz) | = | 1E0 | 1E1 | 1E2 | 1E3 | 1E4 | 1E5 | 1E6 | 1E7 | 1E8 |
| REF Phase noise level (dBc) | = | –80 | –110 | –135 | –150 | –155 | –158 | –160 | –162 | –164 |
| VCO Phase-noise level (dBc) | = | –10 | –40 | –65 | –88 | –114 | –135 | –148 | –158 | –165 |
| PLL Noise Floor | = | –164 dBc/Hz | | | | | | | | |

**Table 3—PLL Design Parameters**

| Symbol / Name | Units | Definition |
|---|---|---|
| Npd Phase Detector Noise Floor | dBc | Noise floor of the PLL due to phase detector, reference and output signal divider chains. |
| $K_{VCO}$ / VCO sensitivity | MHz/V | Frequency change of VCO output per volt change on the frequency-control input line to the VCO |
| $K_{pd}$ Phase Detector Sensitivity | mA/degree | Current change of the phase-detector output for a degree change in the phase difference between the signal input and reference signal input. |
| $F_{VCO}$ / VCO Output Frequency | MHz | VCO center frequency |
| $F_{ref}$ / Phase Detector Frequency Reference | kHz | Reference frequency into the phase detector. |
| *M* / Frequency Division | — | Division ratio for output frequency to phase detector reference input. |
| *N* / Frequency Division | — | Division ratio for reference source frequency to phase detector input. |
| Output Multiplier | — | Ratio of output frequency to the VCO frequency, which may be divided or multiplied by either “1/multiplier” or “multiplier,” respectively. |
| $F_p$ / loop bandwidth | kHz | Parameter to be optimized |
| ϕm / Phase Margin | degrees | This is typically 45° or more to insure loop stability. Notice that higher margins decrease ‘peaking’ in loop but increase loop settling time. |
| Attn_$F_{ref}$ / Reference Frequency attenuation | dB | This is the additional reference frequency attenuation required from the third pole in the loop filter. |
| Frequency Reference Spectral Noise Density | dBc/Hz | Spectral frequency plot of the phase noise versus frequency offset for the frequency reference. |
| VCO Spectral Noise Density | dBc/Hz | Spectral frequency plot of the phase noise versus frequency offset for the VCO. |
| Reference frequency divider noise floor | dBc/Hz | Noise floor of reference frequency divider output. |
| Output frequency divider noise floor | dBc/Hz | Noise floor of output frequency divider output. |
| Phase detector noise floor | dBc/Hz | Noise floor of phase detector output. |

results, the loop-filter values calculated were identical in AN1001 and the spreadsheet, as expected, for a ‘sanity’ check of the program.

Fig 4 represents the closed-loop transfer function, Eq (6), of the PLL, and it is clearly a low-pass filter function with a cutoff frequency near the loop bandwidth of the PLL. Therefore, when $S_{ref}(s)$ is multiplied by the closed-loop function in Eq (10), the output noise follows the reference phase noise and the noise sources up to the loop bandwidth, where the contributions from the reference phase noise and noise sources rapidly drop off.

Fig 5 represents the error function, Eq (1), of the PLL and is clearly a high-pass function. Therefore, when $S_{VCO}(s)$ is multiplied by the error function in Eq (10), the output noise follows the VCO phase noise above the loop bandwidth.

The summary of Eq (10) is that the

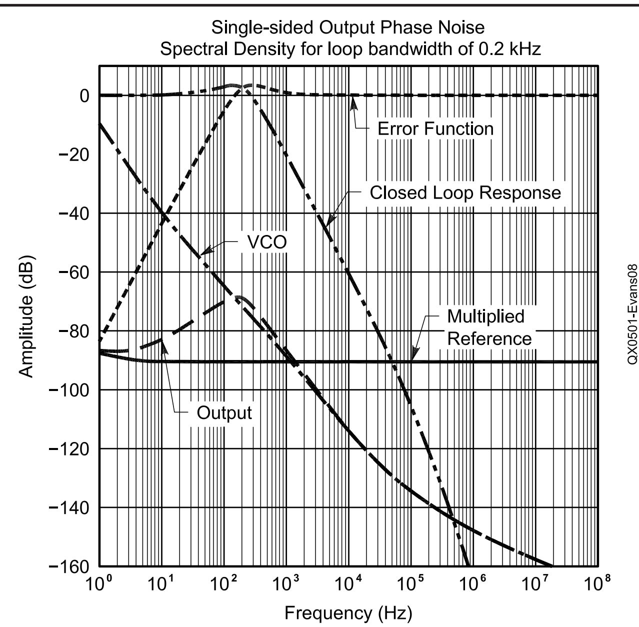


**Fig 8—PLL Phase noise for a 200-Hz loop bandwidth.**

reference phase noise and the PLL noise floor control the output phase noise up to the loop bandwidth, and the VCO phase noise controls the output phase noise beyond the loop bandwidth.

Now we will look at the effects of different loop bandwidths on a PLL when the other PLL parameters are held constant. Fig 6 shows the phase noise of the VCO, the reference frequency multiplied up to the output frequency, the output signal, and the transfer response for the error and closed-loop response functions, all superimposed on one graph for a loop bandwidth of 20 kHz. The VCO and reference phase-noise plots are based on published phase-noise data from commercially available VCOs and TCXOs.

The multiplied reference phase noise is used since Eq (10) shows that the output phase noise is a function of $S_{ref} \times G(s)/(1 + G(s)\,H(s))$. For $G(s) >> 1$, this simplifies to $S_{ref}(s) \times 1/H(s)$, which is equal to $S_{ref}(s) \times N$.

Notice that the VCO phase-noise plot and the multiplied reference phase-noise plot cross at approximately 1.4-kHz offset from the carrier. Therefore, the lowest phase noise would occur when the output phase noise tracked the multiplied reference phase noise up to 1.4 kHz and tracked the VCO phase noise beyond that point. This would imply a loop-bandwidth requirement in the 1.4 kHz area. As an example, Fig 6 shows the output phase noise for a loop bandwidth of 20 kHz. Notice the excess output noise *above the* VCO noise plot between approximately 1.4 kHz and 200 kHz offset from the carrier.

Fig 7 shows the output phase-noise plot for a loop bandwidth of 2 kHz. It is clear that there is less excess noise above the VCO phase noise. In particular, there is a much lower phase-noise-density level at 10 kHz offset from the carrier (–110 dBc/Hz for 2-kHz loop bandwidth versus –88 dBc/Hz for a 20 kHz loop bandwidth), which may be of concern if the designer is worried about reciprocal mixing in a receiver using this PLL as an LO.

Fig 8 shows the output phase noise for a loop bandwidth of 200 Hz. There is considerable peaking of the output phase noise because the output is starting to track the VCO phase noise well before it has dropped below the level of the multiplied reference phase noise. However, the phase-noise-density level drops to –114 dBc/Hz at 10 kHz offset.

The above plots are based upon analysis of a third-order PLL using a charge-pump with the parameters shown in Table 1, but varying the loop bandwidth. In addition, the parameters shown in Table 2 were also assumed for the reference oscillator and VCO phase-spectral-density levels and the PLL noise floor.

**Table 4—Spreadsheet input for the design example.**

| | | | |
|---|---|---|---|
| PLL Noise Floor | $N_{pd}$ | **–171** | dBc |
| Phase Detector Sensitivity | $K_{pd}$ | **0.0007958** | Amps/radian |
| VCO sensitivity | $K_{VCO}$ | **20** | MHz/Volt |
| VCO Output Frequency | $F_{VCO}$ | **77** | MHz |
| Reference Oscillator Frequency | $F_{osc}$ | **10000000** | Hz |
| Phase detector Ref Freq | $F_{ref}$ | **25000** | Hz |
| Output Multiplier | multiplier | **1** | |
| Phase Margin | PMdeg | **45** | degrees |
| Loop Bandwidth | BW | **2000** | Hz |
| Ref Freq Attenuation | $\mathrm{ATTN}_{-Fref}$ | **10** | dB |
| Output Multiplier Noise Floor | $So_{utput}$ | **–170** | dBc |

A third-order PLL is used for the design program, as shown in Fig 9, since this is the most prevalent and applicable design for most applications. (It can be argued that a second-order loop exists only on paper because high-frequency poles always exist at sufficiently high frequencies.) In each case, the 45° phase margin was met, thus insuring that the loops are stable.

We can conclude from the preceding discussion that we cannot arbitrarily select a PLL loop bandwidth if the minimum output phase noise is required and that the optimum loop bandwidth cannot be determined without a thorough analysis of the PLL, considering the parameters described in Table 3.

Most of the data described in Table 4 can be obtained from manufacturers' data sheets or from the design architecture. For example, the data sheet for the Analog Devices ADF4111 through ADF4113 PLL IC lists the phase-noise floor as –171 dBc/Hz for a 25 kHz phase-reference frequency and –164 dBc/Hz for a 200-kHz phase reference frequency. A note on the data sheet indicates that this was estimated by measuring the in-band spectral density in dBc/Hz on the output signal and subtracting 20log*N*, where *N* is the divider value. This number encompasses all the sources of noise described, but it assumes that the reference signal phase noise is much less than this. The 10 MHz TCXO phase noise data used in the previous analysis is –150 dBc/Hz at a 10 kHz offset from the carrier. Dividing the 10 MHz signal down to 25 kHz gives a –184 dBc/Hz value, which is below the thermal noise (–174 dBm/Hz ) for a 0-dBm reference output level. Therefore, the assumption that the reference phase noise is not contributing significantly to the output phase noise is likely true if a low-noise reference source is used. Similarly, the National Semiconductor LMX2310U through LMX2313U data sheet lists its phase detector noise floor as –159 dBc/Hz for a 200-kHz reference frequency, presumably using similar measurement techniques.

Similarly, the reference source and VCO phase-noise spectral-density plots versus frequency-offset from the signal can be obtained from the manufacturer if they are purchased items. If they are custom designs, the phase-noise spectral-density values must be measured by the designer before the analysis can be performed. Numerous articles have been written describing techniques to measure the phase noise. Several appear in a sidebar to this article. The simplest, albeit the most expensive, is to use a spectrum analyzer with the necessary software, if available: for example, the Agilent 8560 series spectrum analyzer with the *85671A Phase Noise Measurement Utility*.

**Phase-Noise Analysis Program**

Several manufacturers offer some very good free PLL design tools, but I have found them of limited use for several reasons:

- They are generally applicable only to their own PLL chips.
- They do not offer the flexibility I want, to vary design parameters so as to optimize the PLL design, and
- they do not allow users to customize the program for future requirements.

Therefore, to ease the design and analysis of PLLs, a *MATLAB* program was developed to perform the necessary calculations and plot the results for detailed analysis. Because many designers have no access to *MATLAB*, I developed an equivalent *Excel* spreadsheet that I discuss in this section. The spreadsheet allows the designer to quickly investigate the output phase-noise effects of changing many parameters:

- Changing the loop bandwidth,
- Using "quieter" reference oscillators or VCOs,
- Using VCOs with different tuning sensitivities,
- Using phase detectors with different sensitivities or noise floors,
- Changing reference frequency attenuation,
- Changing the phase-detector reference frequency,
- Changing the phase margin,
- Multiplying or dividing the PLL output.

Notice that the *Excel* spreadsheet uses far fewer frequency points (simply to minimize the size of the spreadsheet) than does the *MATLAB* program, hence *MATLAB* allows much finer resolution in the phase plots and loop-response plots. The result is more-accurate results for *MATLAB*, but the *Excel* spreadsheet results are still very accurate—even with fewer points. I have found it to be more than adequate for my synthesizer phase-noise analysis. The *Excel* spreadsheet could be easily extended to more points if desired.

I also find the *Excel* spreadsheet much easier and quicker to use than the *MATLAB* program because the *MATLAB* program requires the designer to open the program in an editor, change the values, and then run *MATLAB*. When Using *Excel*, it is only necessary to change a value and the results appear instantly.

The *Excel* "Analysis Toolpak" add-in must be installed before the spreadsheet can run. It requires complex-number functions that are not included in the standard *Excel* installation.

The program uses the PLL models shown in Fig 9 for the charge-pump PLL analysis model and those in Fig 10 for the voltage-output phase-detector PLL analysis model. The only differences between the two models are the loop filter and the phase-detector type.

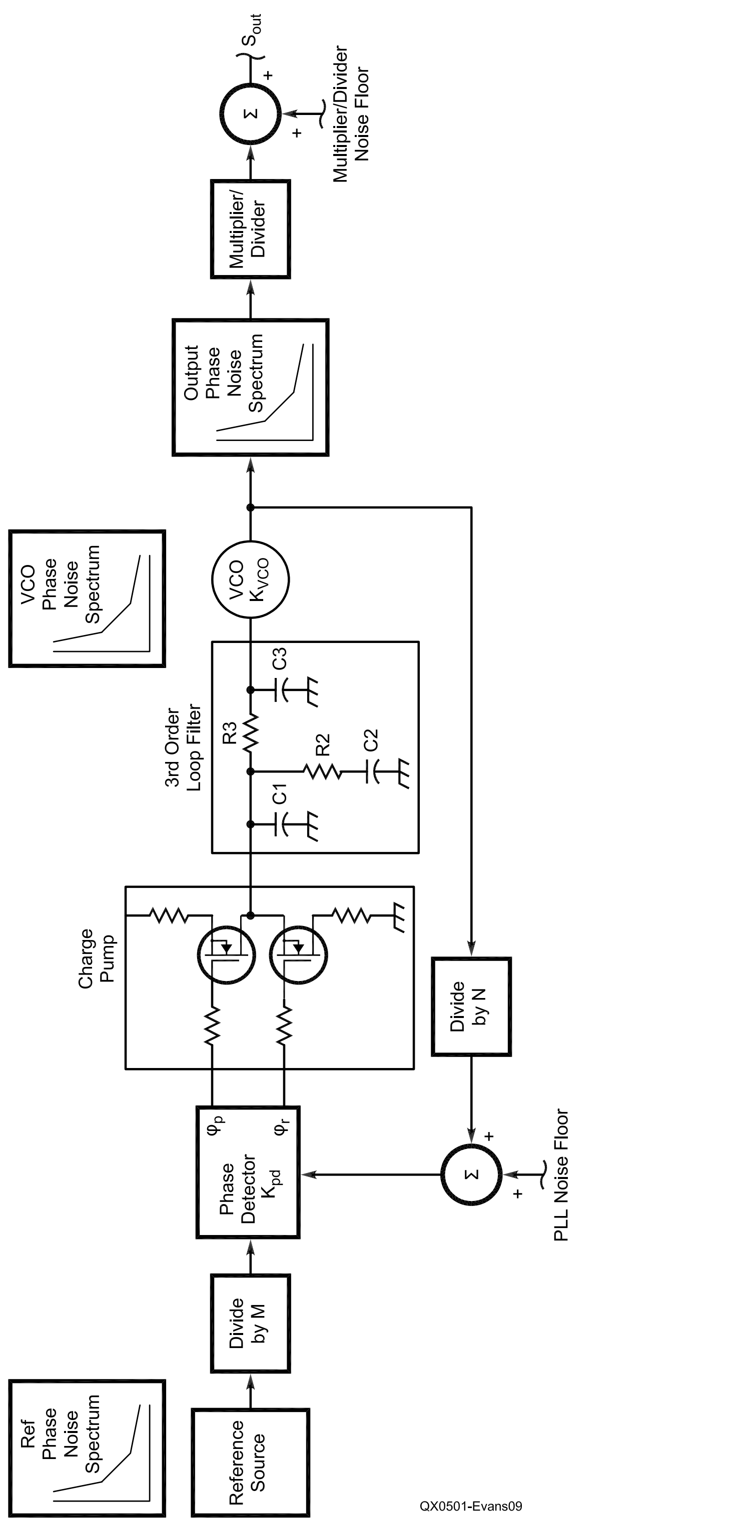


Fig 9—Analysis model of a charge-pump PLL.

## A Design Example

Here is a design example for a frequency synthesizer that is required to tune from 45 to 75 MHz in 25-kHz steps with a design goal of around –120 dBc/Hz phase-noise spectral density at 10 kHz from the carrier and spurious levels of less than –100 dBc beyond 10 kHz from the carrier. In addition, the synthesizer should be relatively immune to microphonics from a mechanical fan vibration of around 1800 Hz. The input section of the PLL design spreadsheet for this application is shown in Table 4.

The user enters the items shown here in bold. (They're yellow in the spreadsheet.—*Ed.)* The spreadsheet then calculates the loop-filter values and displays them in the *blue* boxes and plots the output spectral phase noise, the phase detector reference input spectral phase noise, the VCO spectral phase noise, and the normalized closed loop transfer function, as shown in Fig 11. By simply changing one of the input parameters, the designer can immediately see the effect (or lack of effect) on the output phase noise. It can be very enlightening to see what really impacts the output phase noise on a given PLL design.

The PLL chip selected for this design is the Analog Devices ADF4111A. The VCO is the Model V061ME01 from Z~Communications (**http://www.zcomm.com/home.htm**). The reference oscillator is the Compatible series of TCXOs from Wenzel Associates using an AT-cut crystal. The phase-noise data from the VCO and reference oscillator data sheets were

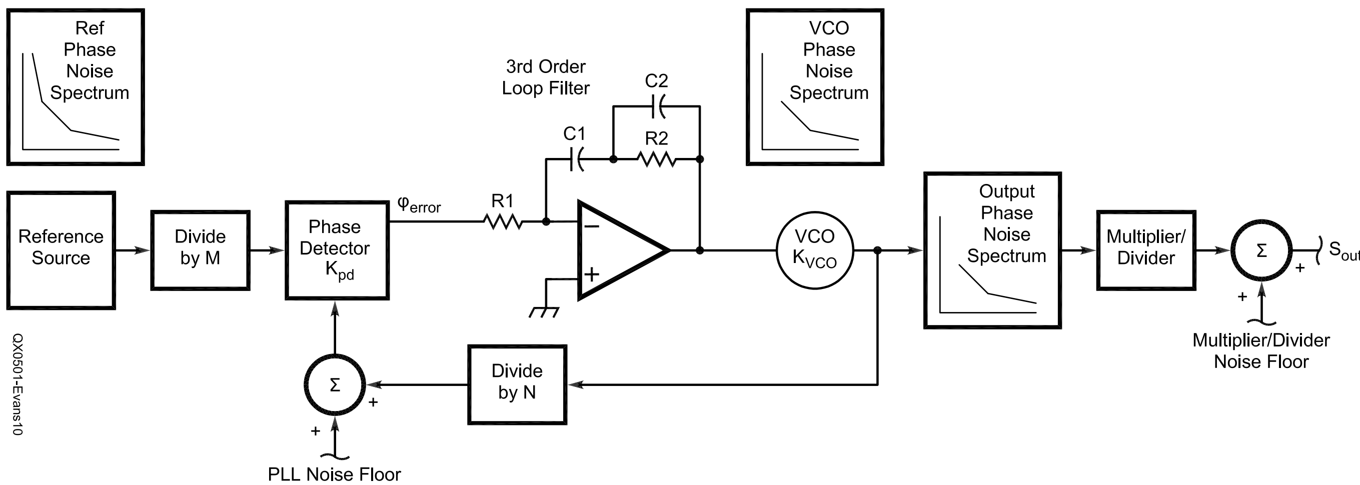


**Fig 10—Analysis model of a voltage-output phase detector.**

## VCO Tuning Line Sensitivity

The frequency voltage control line into the VCO can be a source of unexpected problems if it is not considered in the design of low-noise frequency synthesizers, particularly when the tuning sensitivity of the VCO is high. For example, if 10 $nV_{(P-P)}$ noise exists on the voltage tuning line of a PLL using a VCO with a sensitivity of 60 MHz/V, the noise will generate a frequency deviation of 0.6 $Hz_{(P-P)}$, or 0.3 Hz peak. The modulation index for frequency modulation is $\beta = \Delta F/fm$, where $\Delta F$ is the peak frequency deviation and fm is the modulation frequency. $\beta$ is also the phase deviation $\Delta\phi$ expressed in radians/sec. For small $\beta$, <<1, it can also be shown that the ratio of the amplitude of either modulation sideband to the amplitude of the carrier is

$$\frac{E_{SSB}}{E_c} = \frac{\beta}{2} = \frac{\Delta Fp}{2fm} \qquad \text{(Eq 11)}$$

where $E_{SSB}$ is the voltage single-sideband level of the modulation sideband and $E_c$ is the voltage level of the carrier. Expressing this ratio in decibels, we get

$$\left.\frac{E_{SSB}}{E_c}\right|_{dB} = 20\,log\,10\left(\frac{\Delta Fp}{2fm}\right) \qquad \text{(Eq 12)}$$

Since noise is generally measured in RMS, not peak or peak-to-peak, the sideband levels for an RMS measurement are

$$\left.\frac{E_{SSB}}{E_c}\right|_{dB} = 20\,log\,10\left(\frac{\Delta F_{RMS}}{\sqrt{2}fm}\right) \qquad \text{(Eq 13)}$$

where $\Delta F_{RMS} = \frac{\Delta F}{\sqrt{2}}$

If the noise voltage $V_n$ is measured in RMS, and the tuning sensitivity of the VCO is $K_{VCO}$, the sideband level of the noise relative to the carrier is

$$PSSB = 20Log10(K_{VCO}Vn_{\_RMS}) - 3 - 20Log(fm) \qquad \text{(Eq 14)}$$

In the example above, if the noise power were concentrated in a 1 Hz bandwidth around 10 kHz, the noise sideband level would be –87.4 dBc, much higher than our spec of –120 dBc for the design example. At 10 kHz offset, the loop error function is essentially 1, so the loop will not attenuate the noise sideband. Therefore, in order to meet the –120 dBc spec of the design example, it will be necessary to have a noise level at 10 kHz carrier offset of less than 230 $\mu V_{RMS}$/Hz, a real design challenge.

However, any noise on the VCO tuning line will be reduced by the PLL by the 1/ (1 + GH) factor for frequency components within the loop bandwidth, the same as the VCO phase noise. VCO line-noise frequency components beyond the loop bandwidth will be unaffected by the PLL.

The noise components on the VCO line can be from many different causes, such as signal coupling from adjacent circuits, DC supply noise, PLL op amp noise, etc. The circuit designer should be aware of any noise sources that may get into the VCO tuning line and mitigate the risks of the noise sources coupling into the VCO.

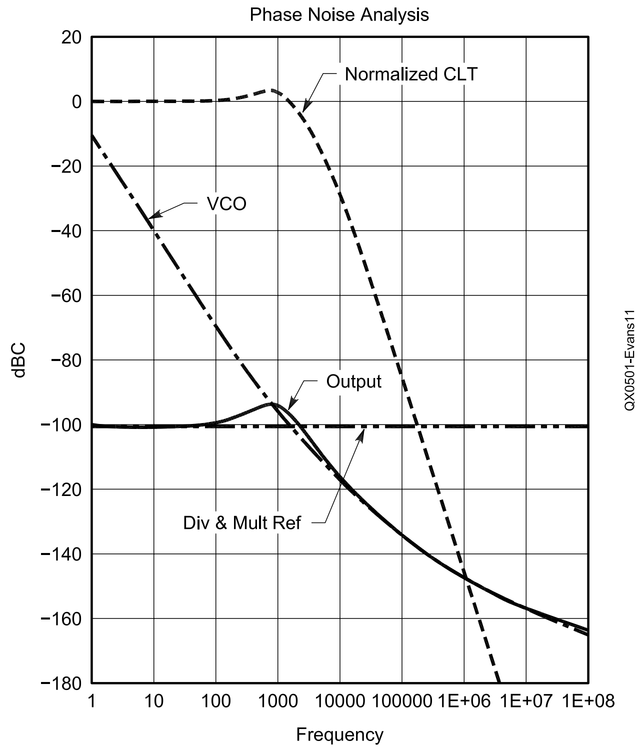


Fig 11—Output plot for a 2-kHz loop bandwidth (CLT=closed loop transfer function).

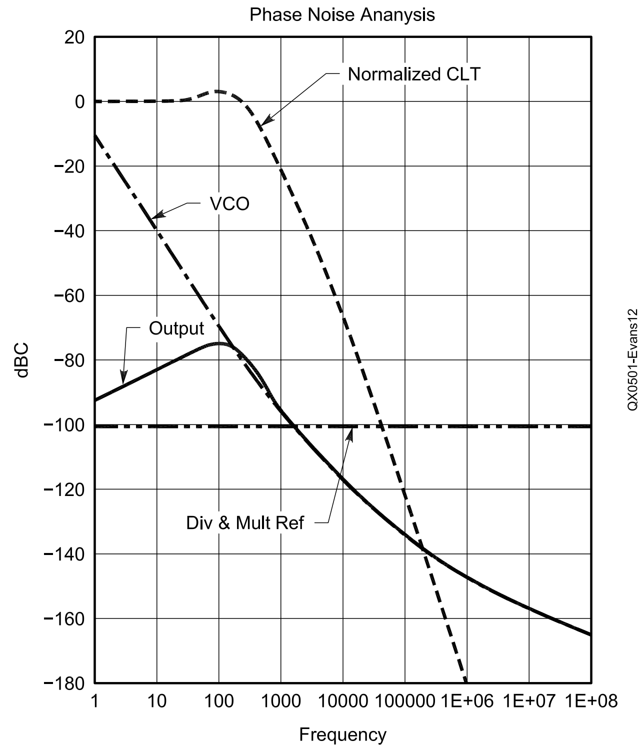


Fig 12—Output plot for a 200-Hz loop bandwidth.

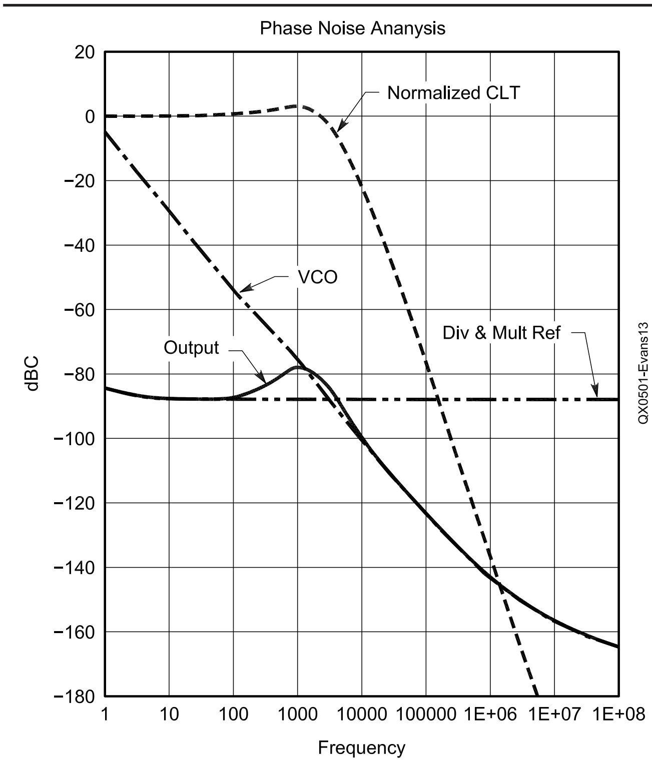


Fig 13—Phase-noise analysis for a 20x fequency synthesizer.

extrapolated to the range required for the spreadsheet.

In this PLL example, it can be seen that the 2-kHz loop bandwidth is just about optimal for the lowest output phase noise since the loop tracks the reference phase detector input signal just until the VCO phase noise drops below the multiplied phase detector reference signal noise level. The spectral noise density at 10 kHz offset is –118 dBc/Hz, and can't be made any better without a less noisy VCO. There is a peaking of the output phase noise just under 1kHz offset from the carrier due to peaking in the closed loop gain curve and the contributions of the reference and VCO phase noise in this loop transition region. Note that the attenuation of the 25 kHz reference frequency is approximately 50 dB as shown on the closed-loop-gain transfer curve, which may be too low to keep the reference sidebands at an acceptably low level.

**Table 5—Input Data for a 20×Synthesizer**

| | | | |
|---|---|---|---|
| PLL Noise Floor | Npd | **–164** | dBc |
| Phase Detector Sensitivity | Kpd | **0.000795775** | Amps/radian |
| VCO sensitivity | | **60** | MHz/volt |
| VCO Output Frequency | FVCO | **1500** | MHz |
| Reference Oscillator Frequency | Fosc | **10000000** | Hz |
| Phase detector Ref Freq | Fref | **250000** | Hz |
| Output Multiplier | multiplier | **0.05** | |
| Phase Margin | PMdeg | **45** | degrees |
| Loop Bandwidth | BW | **5000** | Hz |
| Ref Freq Attenuation | ATTN_Fref | **30** | dB |
| Output Multiplier Noise Floor | Soutput | **–165** | dBc |

### Output for 2 kHz Loop Bandwidth

For comparison, the loop bandwidth is changed to 200 Hz and the results are shown in Fig 12. The spectral phase noise density is still –118 dBc at 10 kHz offset. There is considerable peaking of the output phase noise between 1 Hz and 1000 Hz since the narrow loop bandwidth is forcing the loop to start tracking the VCO while it is still much higher than the multiplied reference phase noise. However, the closed loop attenuation has increased to approximately 87 dB at the 25 kHz reference frequency, but the narrow loop bandwidth has made the synthesizer more susceptible to microphonics since the loop cannot track out any mechanical vibrations (due to fans, etc) above the loop bandwidth.

**Output for 200 Hz Loop Bandwidth**

Note that the phase detector reference signal shown in the output plot for this example is relatively flat, although the reference oscillator shows a steadily decreasing noise density over the entire range. This is due to the 10 MHz reference oscillator being divided down by a factor of 400 to 25 kHz and the reference oscillator noise density is theoretically reduced by 20Log(400) or 52 dB for all frequencies (this ignores flicker, jitter, and thermal noise contributions from the reference signal divider chain and phase detector). For most of the frequency range, this is a phase noise level below the noise floor of the PLL circuits (-171 dBc for the ADF411X family of PLL chips), hence the phase detector noise floor is establishing the PLL's noise level. When the nearly constant PLL noise floor is multiplied up to the output frequency, it is also a constant level over the same range. In this case, the phase noise of the reference oscillator has little effect on the output phase noise. The spreadsheet easily allows the designer to see the effects, if any, on using a lower cost, higher phase noise reference oscillator.

The previous synthesizer design did not meet the requirement for immunity to microphonics (since the fan vibration frequency, assumed to be ~1800 Hz, is beyond the loop bandwidth) and low spurious (since the reference frequency attenuation is low). Therefore an alternative architecture is considered where the VCO operates at a frequency 10x required and the output frequency is divided by 10 to get the required output frequency. In this case, a Z~Communications V585ME30 VCO is proposed. It tunes over the range of 800 to 1600 MHz. Therefore, using a factor-of-20 divider on the output of the synthesizer would give a tuning range of 40 to 80 MHz, thus meeting our tuning range requirement of 45 to 75 MHz. In addition, the factor of 20 allows us to use a reference frequency of 250 kHz for the phase detector (this implies a PLL noise floor of –164 dBc/Hz using the data from the ADF1112A data sheet). Using the two phase-noise specs in the data sheet and extrapolating over the frequency range required for the spreadsheet, and trying an initial loop bandwidth of 5 kHz, as shown in Table 5, gives the results shown in Fig 13. Notice that the output and reference signal phase noise is shown after the divide-by-20 circuit (as specified by the 'Output Multiplier' value inserted in Table 5.

**Phase Noise Analysis for 20x Frequency Synthesizer**

Note that the phase noise spectral density at 10kHz offset is now –126 dBc/Hz and the loop bandwidth is 5 kHz, adequate to combat microphonics. In addition, the reference frequency attenuation is now over 100 dB. This analysis shows that all the design requirements can be met by this design. Of course, building the synthesizer and demonstrating that it meets the specs in practice is another matter, and is not detailed in this article. Suffice it to say that it is possible to build a practical synthesizer using this design with careful attention to providing the frequency synthesizer circuit with *very* clean DC power supplies, very low noise operational amplifiers (if active filters are used), careful PCB layout with ground planes and shielding, and very good signal bypassing around the PLL chip and VCO. The sidebar "VCO Tuning Line Sensitivity" describes the sensitivity of the PLL VCO to noise on the tuning line and must be considered, particularly when using a high sensitivity VCO such as this design requires.

## Phase-Noise-Measurement References

Articles listed here describe how to measure phase noise. The list is by no means comprehensive, but it is representative of what is available in the literature.


1. "Low Phase Noise Applications of the HP 8662A and 8663A Synthesized Signal Generators," Chapter 6: "Measuring SSB Phase Noise with the HP 8662A/8663A," Hewlett-Packard Application Note AN 283-3, pgs 19-25.
2. "Frequency Synthesizers," Section III—"Frequency Stability and Spectral Purity," Hewlett-Packard Application Note 96, pp 14-17.
3. "Some Aspects of the Theory and Measurement of Frequency Fluctuations in Frequency Standards", L. S. Cutler and C.L. Searle, *Proceedings of the IEEE*, Feb 1966.
4. "Low-Cost Phase Noise Measurement," Wenzel Associates, Inc; **www.wenzel.com/documents/measuringphasenoise.htm**
6. "Low Cost Phase Noise Tester for 50 MHz to 4.2 GHz Signal Generators", Andrew Baczynsky, Microwave Journal, Jan 1986.
7. "Phase Noise Measurement Using the Phase Lock Technique", Morris Smith, Motorola Semiconductor Application Note AN1639.
8. "Phase Noise Characterization of Microwave Oscillators, Phase Detector Method", Product Note 11729B-1, Hewlett Packard.
9. "Phase Noise Characterization of Microwave Oscillators, Frequency Discriminator Method", Product Note 11729C-2, Hewlett Packard.
10. "Choosing a Phase Noise Measurement Technique, Concepts and Implementation", Terry Decker and Bob Temple, RF & Microwave Measurement Symposium and Expedition, Hewlett Packard, Part Number 1000-1118.

References:

"Optimize Phase Lock Loops to meet your needs – or determine why you can't", Andrzej B. Przedprelski, Electronic Design, September 13, 1978.

Stanley J. Goldman, *Phase Noise Analysis in Radar Systems using Personal Computers*, John Wiley & Sons, Inc, 1989.

R. E. Best, *Phase Locked Loops, Design, Simulation, & Applications*, 3rd Edition, McGraw-Hill, 1997.

W. P. Robins, *Phase Noise in Signal Sources*, Peter Peregrinus Ltd, 1982

F. M. Gardner, *Phaselock Techniques*, Second Edition, John Wiley & Sons, Inc, 1979

J. A. Crawford, *Frequency Synthesizer Design Handbook*, Artech House, Inc, 1994

D. H. Wolaver, *Phase-Locked Loop Circuit Design*, Prentice Hall, 1991

W. F. Egan, *Phase-Lock Basics*, John Wiley & Sons, Inc, 1998

Ulrich L. Rohde, "All About Phase Noise in Oscillators", Parts 1, 2, and 3, *QEX* December 1993, January 1994, and February 1994.


[1]The colors show in the worksheet, which you can download from the *ARRLWeb* **www.arrl.org/qexfiles/**. Look for 0105Evans.ZIP.

# RF

By Zack Lau, W1VT

### A 10 GHz Waveguide Preamp

To obtain the ultimate in receive sensitivity at 10 GHz, it is worthwhile to use waveguide instead of coax. The lower losses of waveguide can result in significant signal-to-noise improvements. The loss of WR-75 waveguide is just 0.05 dB/foot. This is significantly better than semi-rigid UT-141 coax, which typically has a measured loss around 1 dB/ft. Advanced versions of UT-141 using foamed Teflon have claimed loss of 0.33 dB/ft at 10 GHz.[1] The loss is even lower with the larger WR-90, about 0.034 dB/ft.[2] This isn't surprising, as the waveguide is much larger than the coax—the coax being 0.141 inches in diameter and the waveguide having dimensions of 1.0 × 1/2 inches. The"90" refers to the interior h-field dimension of 0.90 inches. The loss of an SMA relay is typically 0.3 to 0.5 dB at 10 GHz, while a waveguide switch can have less than 0.07 dB loss.[3] Being able to reduce the 1/2 to 1 dB of switching and transmission line loss ahead of a mast mounted receive preamplifier may make a significant difference in weak-signal applications such as EME and long distance troposcatter.

While you could put an SMA-to-waveguide transition ahead of a preamplifier with a coaxial input, this is a rather inefficient way of designing a system. Not only does the transition have loss, coaxial input circuits to preamplifiers are quite lossy. In addition to providing the desired impedance transformation for low-noise operation, they also need to provide a DC block, since negative gate bias is almost a necessity at 10 GHz. I have yet to see anyone successfully implement a source-biased FET circuit at any amateur band higher than 3.5 GHz. It becomes increasingly difficult to maintain stability as you go up in frequency—UHF designs were only possible with careful computer modeling. Al Ward, W5LUA, showed how to source bias an ATF10135 up to 1.6 GHz.[4] Source grounding of this design is done with 1 mil copper foil. 36 mil × 250 mil copper strips are used to connect the source pads to the bottom ground plane.

Typically, the dc block is done with a high quality porcelain chip capacitor. In contrast to HF circuits, where a Q of 100 or more is typical, a Q of 13 or less is more likely at 10 GHz. The loss is significant—there is an improvement to be gained by omitting the dc blocking capacitor. This is easily done with a waveguide input—a simple probe sticking into the waveguide provides an excellent dc block with very low loss.

The device is the inexpensive NEC NE3210S01—available for around $2 from Down East Microwave. It may also be available from SHF Microwave. It may also be available from Mouser Electronics. They sold their initial stock and did not have any for a long time. As of October 11, 2004 they had 2792 on hand.

The first step in designing a preamplifier is to design the input and output matching networks. The usual priority is low noise figure. Next in line is output matching, followed by the input matching. Stability, while important, is usually handled later. At 10 GHz, the device is hardly unilateral—there is a considerable amount of interaction between the input and output networks. Similarly, the SMA connector on the output has a signifi-

[1]Notes appear on page 56.

225 Main St
Newington, CT 06111-1494
**zlau@arrl.org**

cant effect on the matching network—it is quite useful to model its effect from the very beginning. It is important to maintain the proper length to the SMA connector—while the line is 50 ohms, changing the length of the line will change the mismatch reflected back to the device.

I've had good luck cascading single stage preamplifiers with a two-stage MGF 1302 design published in the May 1993 *QST* (See Note 1). Alternatively, an isolator can be used to eliminate the effect of the output termination on preamplifier performance. Isolators can be very expensive new, but I've found cheap surplus ones that worked just fine.

I made the arbitrary choice of matching the input to 50 ohms—so I could design the waveguide transition and microstrip matching circuitry independently. I optimized the waveguide transition by trial and error, optimizing it with return loss measurements. I have a precision Narda directional coupler for making return loss measurements—the measurements I've made seem pretty reasonable.

The transition uses a 50-mil-diameter probe. I save the cut off center conductors from SMA panel mount connectors. They are gold plated and easy to solder. The magic probe length for a backstop distance is 264 mils, measured from the circuit board ground plane to the tip of the probe. The probe passes through a chamfered hole in the ground plane into the waveguide. The probe is the third item soldered to the board, after the two source ground foils.

The next challenge was attaching the waveguide to the circuit board. I'd like to maintain good electrical contact between the waveguide and the ground plane of the circuit board. While some experimenters have used silver epoxy, I've never actually tried this technique myself. Not only is it expensive, conductive epoxy has a very short shelf life—ill suited for the ham who works infrequently on projects. I've had good results using small screws. They need to be as close to the microstrip as possible to prevent quarter-wave choke effects. It is possible for the ground plane to be at a high-impedance $^{1}/_{4}$-wavelength away from the screw attachment points—this is just 0.28 inches. This could adversely affect the waveguide transition performance. They can't be too close, lest they short the microstrip to ground. Another problem I've often encountered in the past is the length of the screws. Short screws will strip out the threads. Long screws extend into the waveguide introducing a lossy material into the waveguide. A search yielded metric camera screws that are 2 mm long with 1.4 mm x 0.30 threads. Micro Tools sells these screws and matching taps. At $7 each, the taps aren't cheap, but we used to spend more on a single microwave FET than the cost of two taps and two dozen screws.

Now that I had the waveguide attachment sorted out, I could design the bias networks around the screws and waveguide. The bias lines are just long enough to clear WR-75 waveguide comfortably. I could make them longer to clear WR-90, but this increases the chance of unwanted waveguide modes in the box. A wide box can act as a waveguide, efficiently coupling the output of the amplifier back to the input. Absorber material can eliminate this problem, but it can be tough to find in small quantities. A possible source for this is SHF Microwave. I remember Chip, W1AIM, needing some microwave absorber to stabilize his gear for the 10 GHz contest. We scraped some off the lid of a dead 12 GHz microwave amplifier. Absorber is somewhat frequency sensitive—material from a

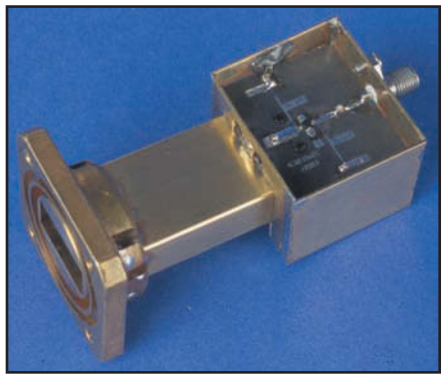

**Photo 1—Top view of the waveguide preamplifier.**

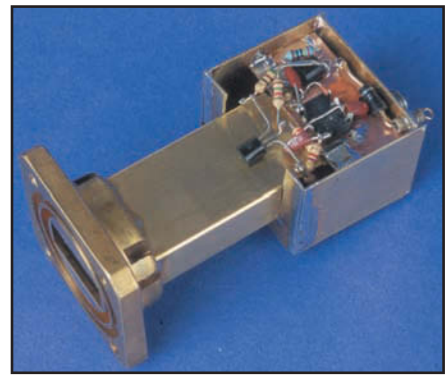

**Photo 2—Bottom view of the waveguide preamplifier.**

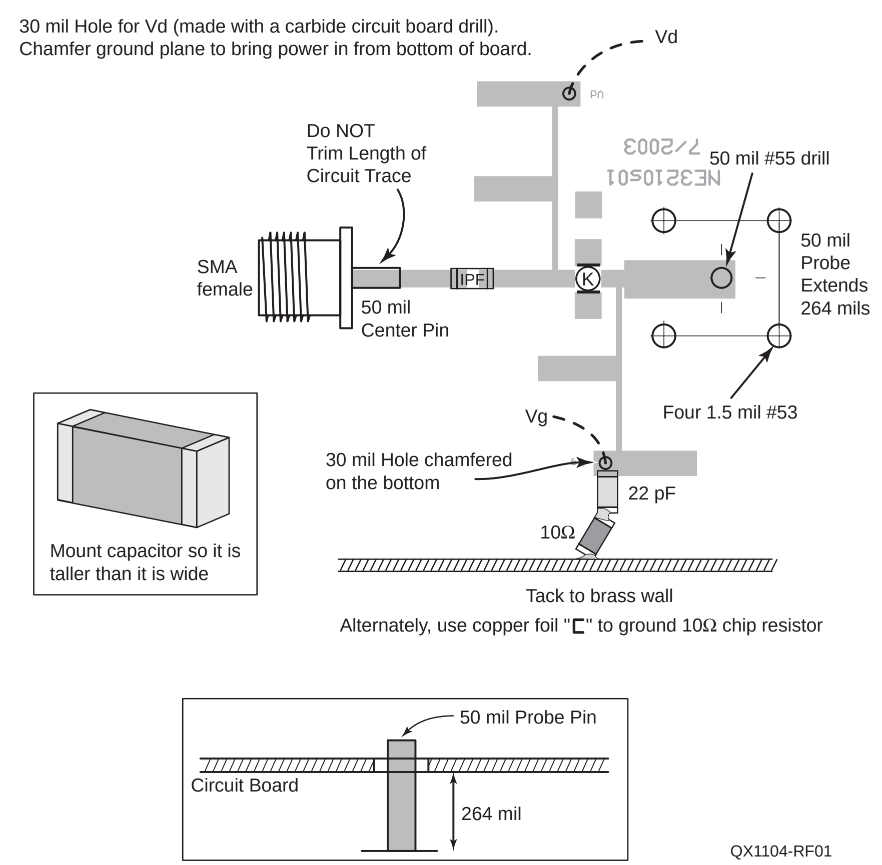


**Figure 1—Component layout of the 10 GHz waveguide preamplifier.**

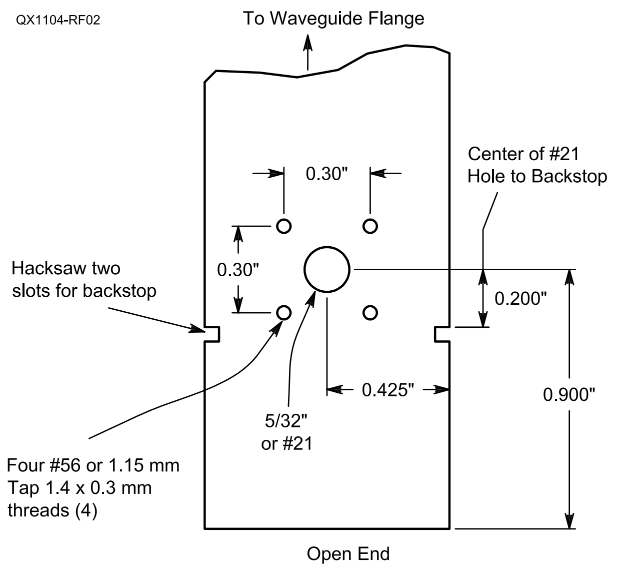


**Fig 2—Waveguide drilling and cutting details. The 0.850" x 0.475" backstop thickness is chosen to fit tightly in the slots.**

C band amplifier may not work as well. Surplus electronics can be a valuable resource for hard-to-find parts.

Originally, I designed this circuit using 10-mil-thick 5880 Duroid, but decided that the 15-mil-thick board was slightly easier to obtain. A thin circuit board is needed to avoid excessive radiation loss—30-mil-thick Duroid is a poor choice at 10 GHz when you need to cut losses to a minimum. 10-mil board is problematic in that 50-ohm traces get too thin for the center pins of standard SMA connectors—the pin is significantly larger than the trace width.

The FET wants to be biased at a relatively low voltage and current, 2 V at 10 mA. It also has fairly low maximums: 4 V for $V_{DS}$ and 3 V for $V_{SG}$. To prevent exceeding either while starting up the preamplifier, I opted to start off with a 2.6 V supply. An LM317L easily handles this chore. I then used an ICL 7660S to invert the 2.6 V, to generate the negative $V_{GS}$ required for modern microwave FETs. Pin 6 is grounded to bypass the internal regulator and improve low voltage operation. A 2N3906 PNP transistor is used as an active bias circuit; adjusting the exact gate-source voltage to set the drain current at 10 mA. I've successfully used this active bias circuit in dozens of preamps ever since Al Ward, W5LUA, published the design in the May, 1989, *QST*. R6 sets the drain current, while voltage divider of R4 and R5 set the drain voltage.

The last step of a good design is obtaining unconditional stability from dc to daylight. This means that it won't oscillate, no matter what sort of resistive load is connected to the input or output. It may oscillate when hooked up to another amplifier that acts as a source of negative resistance. The most common technique is resistive loading. A good textbook that covers stable amplifier design is *Introduction to RF Design* by Wes Hayward.

This amplifier had a stability problem below 3 GHz. I solved it by adding a simple RLC network to the bias network using a 10-ohm resistor, 22-pF capacitor, and 2 nH of stray inductance. The bias network provides good decoupling at 10 GHz. The effect of the lossy network on noise figure is negligible. A Microwave Harmonica model is available.[10] Table 1 shows the simulated performance, while Table 2

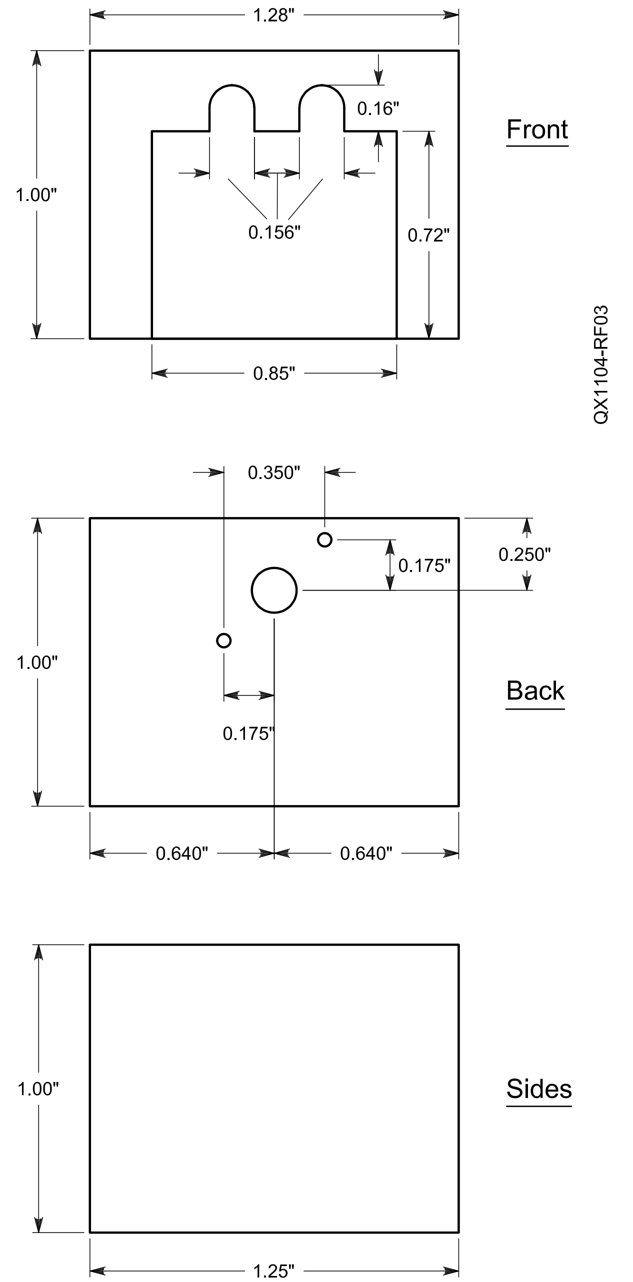


**Fig 3—Dimensions of the brass parts made out of brass strip.**

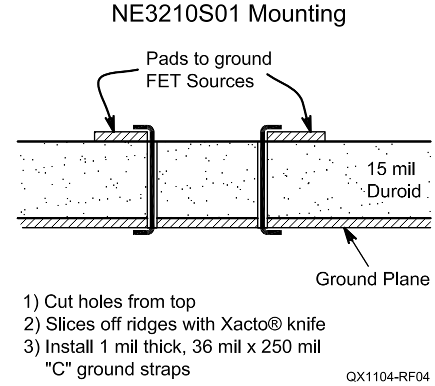


**Figure 4—Transistor mounting details.**

shows the measured performance. The NEC NE32684A was published in the December 1992 RF column of *QEX*—"The Quest for 1 dB NF on 10 GHz." This design is unusual in that many hams have had success in substituting different X-band FETs and obtaining good performance at 10 GHz.[6] Active device substitutions are normally quite difficult at microwaves. The component layout is shown in Fig 1.

**Construction**

Fig 6 shows the circuit board etching pattern. Inch markers are provided for those who wish to precisely scale the image to the proper size. When properly scaled, the 50-ohm output trace should have a width of 46 mils. The four mounting screws should be in a 0.300 by 0.300 inch square pattern. A mirror image is also provided—some homebrew circuit board processes are easier if you have a mirror image available.

I used brass WR-75 waveguide as the foundation to support the rest of the preamp. Fig 2 shows where to cut the slots and drill the holes. I'd hacksaw the two slots first—they set an important reference plane. The distance between the waveguide probe and surface of the backstop is important, as is the distance between the probe and the open end of the waveguide. If the distance to the open end of the waveguide is too long, you won't be able to mount the SMA connector properly. The thickness of the backstop should be chosen to fit tightly in the slot—I used 32-mil thick brass. You may need to adjust this, as the width of the slots may vary.

The next step is to prepare the circuit board. Not only should the 50-ohm microstrip be centered, but also the output microstrip line length should not be trimmed. The length is important for proper output matching. Cut the board into a rectangle with a width of 1.28 inches and a length of 1.15 inches. Ideally, the copper foil ground plane should extend all the way to the edge of the board to facilitate soldering. Slots also need to be cut for the ground returns. I forgot to cut the ground return for the stabilization network, so I soldered the chip resistor directly to the brass sidewall. I like to use a new No. 11 hobby knife to cut the slots—from the top of the board, then slice off the ridges that result on the bottom. Then I clean some 1-mil thick copper foil, so it solders easily. I cut the clean foil into 36 by 250 mil strips for the ground returns—threading them through the board and bending them flat against the board. It is important to minimize the length of the ground connections—long ground leads often result in the construction of an oscillator rather than an amplifier.

I then attached the 50-mil waveguide probe. The overall length is around 350 mils. When properly soldered into place, it extends 264 mils from the bottom surface of the ground plane so that it can stick into the waveguide. Dial calipers were used to accurately measure the distance.

It is important to mount the board in a stiff frame—flexing the soft Teflon

**Table 1—Simulated performance of the 10 GHz waveguide preamplifier.**

| *Freq GHz* | *MS11 dB AMP* | *MS21 dB AMP* | *MS22 dB AMP* | *K AMP* | *NF dB AMP* |
|---|---|---|---|---|---|
| 0.100 | –3.59 | –5.25 | –2.52 | 999.90 | 13.01 |
| 0.200 | –3.68 | –4.20 | –2.54 | 707.14 | 11.75 |
| 0.500 | –4.31 | –0.63 | –2.63 | 150.73 | 7.76 |
| 1.000 | –5.93 | 2.44 | –2.78 | 45.38 | 4.33 |
| 2.000 | –2.72 | –9.86 | –3.61 | 257.51 | 8.70 |
| 2.500 | –2.02 | –5.43 | –5.77 | 76.25 | 6.90 |
| 3.000 | –2.42 | 2.73 | –8.04 | 12.90 | 6.07 |
| 3.500 | –5.92 | –1.10 | –4.33 | 34.74 | 10.58 |
| 4.000 | –7.36 | 6.34 | –3.91 | 6.00 | 4.26 |
| 4.500 | –2.10 | 7.26 | –4.52 | 2.45 | 3.03 |
| 5.000 | –1.38 | 6.30 | –5.13 | 2.18 | 3.14 |
| 5.500 | –1.58 | 0.52 | –3.23 | 6.08 | 4.04 |
| 6.000 | –6.67 | –2.15 | –2.21 | 20.72 | 7.91 |
| 6.500 | –0.96 | 8.34 | –5.62 | 1.24 | 2.74 |
| 7.000 | –1.29 | 9.82 | –8.26 | 1.11 | 2.33 |
| 7.500 | –2.02 | 10.61 | –8.92 | 1.19 | 1.95 |
| 8.000 | –3.06 | 11.35 | –7.97 | 1.20 | 1.55 |
| 8.500 | –4.68 | 12.15 | –7.28 | 1.20 | 1.17 |
| 9.000 | –7.61 | 12.76 | –7.52 | 1.23 | 0.85 |
| 9.500 | –-11.80 | 13.02 | –8.95 | 1.23 | 0.62 |
| 10.000 | –12.90 | 12.92 | –11.33 | 1.21 | 0.50 |
| 10.368 | –10.08 | 12.65 | –13.57 | 1.18 | 0.48 |
| 10.500 | –9.19 | 12.51- | 14.45 | 1.17 | 0.49 |
| 11.000 | –6.99 | 11.86 | –17.27 | 1.19 | 0.56 |
| 11.500 | –5.87 | 11.29 | –17.02 | 1.18 | 0.70 |
| 12.000 | –5.41 | 10.82 | –14.53 | 1.18 | 0.87 |
| 12.500 | –5.17 | 10.48 | –11.62 | 1.16 | 1.05 |
| 13.000 | –5.18 | 10.27 | –9.30 | 1.17 | 1.22 |
| 13.500 | –5.30 | 10.18 | –7.69 | 1.18 | 1.37 |
| 14.000 | –6.00 | 9.85 | –6.59 | 1.28 | 1.67 |
| 14.500 | –7.18 | 9.91 | –12.76 | 1.37 | 2.41 |
| 15.000 | –19.71 | 11.56 | –20.67 | 1.22 | 1.49 |
| 15.500 | –8.27 | 10.42 | –9.30 | 1.23 | 1.73 |
| 16.000 | –2.74 | 5.25 | –3.67 | 1.57 | 2.72 |
| 16.500 | –2.11 | –11.35 | –3.58 | 35.82 | 10.75 |
| 17.000 | –2.08 | 0.60 | –4.30 | 6.01 | 4.13 |
| 17.500 | –3.45 | 2.85 | –3.01 | 2.01 | 2.63 |
| 18.000 | –2.07 | 1.60 | –2.78 | 1.79 | 3.27 |

**Table 2—Measured Performance of Preamplifiers**

| *Preamp* | *Freq Insertion* | *Gain* | *Noise Figure* |
|---|---|---|---|
| NE3210s01 | 10368 MHz | 12.6 dB | 0.68 dB |
| homebrew WG/coax transition with tuning screws | | | |
| NE3210s01 | 10368 MHz | 12.1 dB | 0.80 dB |
| untuned preamp with homebrew WG/coax transition | | | |
| NE32684A #1 | 10368 MHz | 11.3 dB | 0.80 dB |
| NE32684A #2 | 10368 MHz | 11.4 dB | 0.75 dB |

substrate isn't a good idea. Worst case, it can cause chip parts to become intermittent and unreliable. I used four pieces of 25-mil brass strip, 1-inch wide, to make the frame. The dimensions are shown in Fig 3. The back of the frame is drilled to hold an SMA female jack. The front has a 0.85-inch wide rectangle cut out so that it can snugly fit over the waveguide. I initially planned on sliding the waveguide through a hole in the frame, but this seemed to overly complicate the accurate mounting of the waveguide probe. Not only should it be perpendicular to the circuit board, but needs to set to a precise length for optimal matching. Notches also need to be cut in this front piece to clear two camera screws holding the circuit board to the waveguide. Fig 2 shows the suggested dimensions for the brass frame parts—they are a little smaller than the original.

The back of the frame, which holds the SMA connector, was soldered first. Attach the connector with screws and solder the center pin of the connector to the board. Tack solder the brass to the ground plane of the board. Back out the screw that interferes with the soldering and complete the soldering of the board to the rear wall. Then solder the front wall to the circuit board. Finally, solder both sidewalls, making sure that everything is square.

If everything is done properly, you should be able to set the frame over the waveguide and attach the board with the four camera screws. Then tighten up the SMA screw that was in the way of the soldering. Finally, a $^5/_8$-inch strip of thin fiberglass circuit board or brass can be tack soldered as a bottom support on the other side of the waveguide. This helps distribute stress from the SMA connector. Don't solder it in too well—just in case you want to remove it later.

### Testing

Verifying the proper performance of a very low noise figure preamplifier is difficult. A noise figure meter, such as the Agilent HP8970A, is quite expensive. Even if you can find one, it may not have the low 5 dB ENR noise source needed for testing modern preamplifiers. The commonly available 15 dB ENR source often yields results too inaccurate for amateur purposes. I'd like to have a calibrated low ENR source with a WR-75 waveguide flange, but must settle for testing with transitions. Ham radio gatherings with a strong microwave showing, such as the Microwave Update, Central States VHF Society, and Eastern VHF/UHF Conference, often have noise figure meters available to paid attendees.

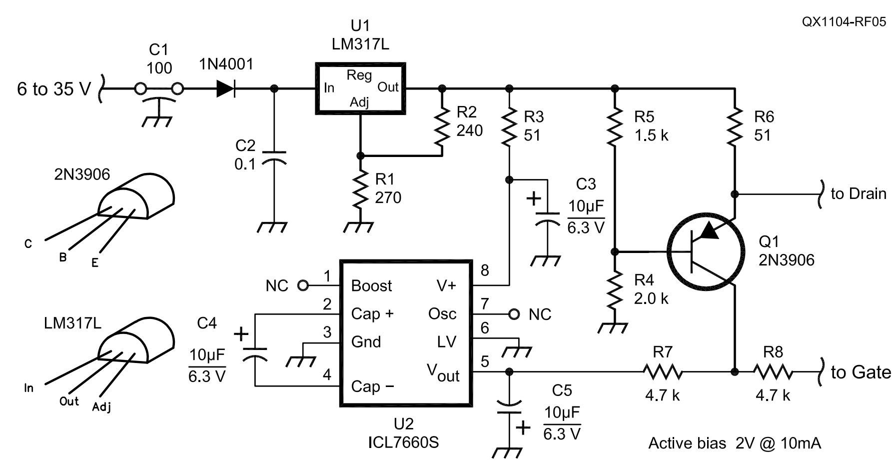


**Fig 5—Active bias circuit that generates the supply voltages for the FET.**

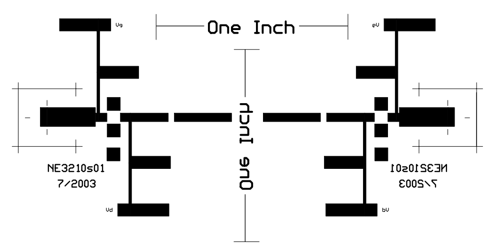


**Fig 6—Circuit board etching pattern. See download at www.arrl.org/qexfiles/. Look for 105RF.zip**

Sun-noise measurements may be worth making—they are useful for making overall system measurements. The DSP-10 software defined radio by Bob Larkin has programming to allow sun-noise measurements.[7] Paul Wade has also written an article describing more traditional sun-noise measurements.[8] If you are looking for 144 MHz gain blocks, I'd suggest looking at the amplifiers used in my 2 meter transmitter.[9] I designed the bandpass filters with a low pass stop band to maintain stability with modern MMICs. Casually implemented designs often have stability issues—unwanted oscillations can easily corrupt sun noise measurements.

Tuning the waveguide preamplifier for better noise figure can be done with a section of waveguide that has three 4-40 screw holes along the broad centerline spaced an eighth of a waveguide-wavelength apart. While a spacing of 0.219 inches is too close to put a screw in each of the holes, you should be able to find an optimum match using just one or two screws. Tuning can be somewhat of a challenge—the loss of the tuning screw will often drop as the threads become tightly engaged.

A wideband FM detector and a weak signal source can be useful for tuning preamplifiers. Relatively small changes in sensitivity can correspond to large changes in signal to noise ratio.

### Notes

[1]**www.micro-coax.com/semirigid/semirigid _lowloss.ht**. **www.micro-coax.com/semirigid/semirigid_mil17.htm**.

[2]**www.tallguide.com/tg134.html** Antennas for Communications sells low-loss waveguide—they provide the performance of WR-90 as a reference standard.

[3]**www.wavelineinc.com/catalog/cp50.htm** Waveline 679E WR-90 and 7579-E WR-75 waveguide switches have less than 0.07 dB of insertion loss.

[4]Application Note 1076 "Using the ATF-10236 in Low Noise Amplifier Applications in the UHF Through 1.7 GHz Frequency Range"**www.semiconductor.agilent.com/cgi-bin/morpheus/home/home.jsp**. The original article, "Low-Noise VHF and L-Band GaAs FET Amplifiers." *RF Design*, February, 1989, said the design could be scaled between 400 and 1600 MHz.

[5]Z. Lau, W1VT, "Home-Brewing a 10 GHz SSB/CW Transverter," *QST*, June 1993, pp 29-31.

[6]J. Swiniarski, K1OR, and B. Wood, N2LIV, "The 1 dB Quest Revisited," *Proceedings of the Microwave Update* 1996, pp 95-102.

[7]**www.proaxis.com/~boblark/dsp10.htm**.

[8]P. Wade, "More on Parabolic Dish Antennas, " *QEX*, December 1995, pp 14-22.

[9]Z. Lau, W1VT, "A 2-Meter Transmitter," RF, *QEX*, July 2003, pp 55-61.

[10]You can download this package from the ARRL Web **www.arrl.org/qexfiles/**. Look for 0105RF.zip.

# 2004 Index

*Issues 222 through 227*
*(All dates are 2004 unless otherwise indicated.)*

**Technical Articles**



**Tech Notes**



**Upcoming Conferences**

# Letters to the Editor

### ATX Adventures (Nov/Dec 2004)

***Doug and Phil,***

I greatly enjoyed this article. There is one possible glitch, however: The housekeeping windings on a high-power, square-wave transformer can produce a voltage more than twice the design [value]. The spikes from the leakage inductance of the big windings are peak-rectified. We burned up some 723s with 40 V when they were supposed to get only 17 V. I found this when I was repairing some 200-W, 10-V-output switchers with linear post-regulation. Can you think of a way to test for this effect?—*Sincerely, William Cross, KAØJAD, 7100 E Evans #411A, Denver, CO 80224*

***Dear Bill,***

We're glad you enjoyed the article. As to the glitches caused by leakage inductance in the transformer windings, I would want to 'scope the waveforms to see how large the voltage spikes were. Of course, snubber networks are normally employed to limit their excursion and a minimum load current may be necessary. You know that both those things tend to reduce efficiency; but absent another failure, properly implementing them should insure that the thing wouldn't blow up on its own!

You indicated you were repairing some switchers with linear post-regulators. Barring some design flaw, I would be surprised if straight component replacements did not restore the units to their original conditions. Motorola's MC1723 data sheet indicates that 40 V dc is okay on the input. Older 723s may not have been capable of that much without destruction.—*Regards, Doug Smith, KF6DX,* QEX *Editor*

### A New Approach to Modulating the Class-E AM Transmitter (Nov/Dec 2004)

***Dear Doug and Bob,***

Bob LaFrance's article is interesting and well done. Following are comments about the technology and Bob's article.

The full-bridge dc-dc converter (using four power transistors) shown in Fig 8 is best suited for dc output power of 300 W, or more, at the peak envelope power (PEP). Bob's application was for 300 W PEP, so his choice of a bridge converter is appropriate. Readers should be informed that a full-bridge converter still works well at lower values of PEP. Although, a dc-dc converter using only one or two power transistors will be sufficient, will cost less, be easier to build and occupy a smaller physical volume.

An undesirable parasitic side effect of the "resonating inductor" in Fig 4 (L2 in Fig 8) is overshoot of the reverse voltage on the rectifier diodes (D14 and D15 in Fig 8). The overshoot is caused by parasitic ringing of the diode capacitance and the "resonating inductor" when the power transistors switch. Because of the overshoot of reverse voltage, those diodes must be chosen for reverse-voltage ratings higher than would be needed if the overshoot could be prevented. The penalties that accompany the use of diodes with a higher reverse-voltage rating, as compared with using diodes rated for a lower reverse voltage are:

- Higher diode forward-voltage drop, hence higher diode power dissipation;
- Larger diode stored charge (from forward conduction) that must be removed by the power transistors during diode turn-off, resulting in additional power dissipation in the diodes and in the power transistors; and
- Higher diode cost and larger diode sizes if the designer tries to ameliorate the above penalties by using a larger-die diode.

A simple and inexpensive way to avoid the diode reverse-voltage overshoot is to add two small low-power clamp diodes, as shown in *U.S. Patent 5,198,969* issued March 30, 1993, held by my employer. The same text as in the patent can be found in R. Redl, N.O. Sokal and L. Balogh, "A Novel Soft-Switching Full-Bridge DC/DC Converter: Analysis, Design Considerations, and Experimental Results at 1.5 kW and 100 kHz," *PESC '90 Record of 21st Annual IEEE Power Electronics Specialists Conference*, San Antonio, Texas, June 1990, pp 162-172; and with corrections in *IEEE Transactions onPower Electronics*, vol. 6, no. 3, July 1991, pp. 408-418, reprinted in the book *Power Electronics Technology and Applications 1993*, IEEE Press, New York, New York, (1993)

Anyone using that patented circuit in conjunction with a Texas Instruments (formerly Unitrode) power-supply control IC (such as the UC3875N used by Bob LaFrance) is already licensed to use that patented technology, under a sub-license issued by TI, [in turn] under a license issued to TI by the patent owner. TI is the only semiconductor manufacturer that is licensed under that patent. Anyone using that patented technology *not* in conjunction with a TI power-supply control IC must obtain a license from Design Automation, Inc.

To avoid possible confusion in the names of the inductors: Bob LaFrance calls L2 of Fig 8 the "resonating inductor" and calls L1 of Fig 8 the "commutating inductor." The references given above call L2 the "commutating inductor" and do not use the inductor shown as L1 in Fig 8.

In the *QEX* article, p 49, column 1, penultimate paragraph, lines 7-13, Bob LaFrance mentions that the anti-parallel body diodes (also called "substrate" diodes by some people) of the power MOSFETs are useful and subsequently he explains why they are useful. Another undesired parasitic side-effect is associated with using those diodes: possible destruction of the power MOSFET by second breakdown of the parasitic bipolar junction transistor that is built into the power MOSFET at no extra cost. Details of that effect, as seen in a full-bridge DC-DC converter, and how to avoid the problem, can be found in Advanced Power Technology's *Application Note APT9804 Rev B*, "High-Voltage MOSFET Behavior in Soft-Switching Converters: Analysis and Reliability Improvements," available at **www.advancedpower.com** (reprinted from an INTELEC '98 paper by K. Dierberger, R. Redl, and L. Saro).

Additional information about non-obvious effects in the full-bridge converter are given in two papers by R. Redl, L. Balogh, and D. Edwards: "Switch Transitions in the Soft-Switching Full-Bridge PWM Phase-Shift DC/DC Converter: Analysis and Improvements," *Proceedings. INTELEC 1993*, pp. 350-357; and "Optimum ZVS ('Zero-Voltage Switching') Full-Bridge DC/DC Converter with PWM Phase-Shift Control: Analysis, Design Considerations, and Experimental Results," *Proceedings IEEE Applied Power Electronics Conference*, 1994, pp 159-165.

Bob LaFrance's circuit operates from 120 V ac power mains and imposes a peak voltage on the power MOSFETs equal to the rectified ac mains voltage (250 V at an ac-mains surge voltage of 170 V ac applied to the mains-voltage rectifier). For applications that operate from 230 V ac (used for higher power in North America—and the standard voltage in many other regions of the world—a high-voltage version of the bridge converter is available; it imposes on the four MOSFETs a peak voltage of *only half* of the rectified ac-mains voltage. For details, see I. Barbi, R. Gules, R. Redl, and N. O. Sokal, "DC-DC Converter for High Input Voltage: Four

Switches with Peak Voltage of $V_{in}/2$, Capacitive Turn-Off Snubbing and Zero-Voltage Turn-On," *IEEE Trans. Power Electronics*, vol. 19, no. 4, pp. 918-927, July 2004.

A typographical error and omission in the *QEX* article, p 52, col. 1, paragraph 2, lines 10-14: The "two series capacitors" at line 10 are C15 and C17 of Fig 8. "MOSFET C" at line 13 is MOSFET C in Fig 5, but is MOSFET B in Fig 8, which is the only figure that shows the "two series capacitors."

On p 52, col. 1, paragraph 2 explains why Bob recommends using L1 of Fig 8 to maintain ZVS, even when the converter's dc output voltage is low and the MOSFET currents are small. Under that low-voltage, low-current condition, the capacitance-discharge power dissipation will be very small, even if ZVS is not maintained, so the efficiency will not be sacrificed if ZVS is not maintained under that condition. Bob points out that maintaining ZVS will ensure low noise in the equipment, which he says is just as important as maintaining high efficiency. I respectfully suggest that low noise can be maintained, even if the power transistors are *not* operating at ZVS at low dc-supply voltage, by making the circuit layout so as to avoid injecting capacitance-discharge noise into the rest of the equipment. It seems that Bob's noise problem was at the node where Q1 source and Q2 drain are connected, because that is where he maintains ZVS by using L1. L1 does not maintain ZVS for Q3 and Q4, and there is no equivalent to L1 at the node Q3-Q4 that could maintain ZVS for Q3-Q4, if Bob would choose to do so. The absence of a "commutation inductor" (like L1) at the Q3-Q4 node suggests that Bob's circuit layout at Q3-Q4 does not inject capacitance-discharge noise into the equipment.

I respectfully suggest that Bob compare the physical layouts at the Q1-Q2 node and the Q3-Q4 node to see why there is a noise problem at the Q1-Q2 node, but apparently not at the Q3-Q4 node. If Bob can make the Q1-Q2 node not inject noise into the equipment (as apparently is the case at the Q3-Q4 node), Bob would be able to remove L1, C15 and C17.

Most bridge converters of this type don't use a dc-blocking capacitor like C1 of Fig 8. Probably Bob could safely replace C1 by a direct connection, unless there are unusually large differences in the duration of the "on" intervals among the four MOSFETs.

On page 47, column 3, line 1: Bob describes the application of this modulator as being for a "class-F" transmitter. I think he meant to say "class-*E*" transmitter, as in the title of the article. Similarly on page 54, column 2, last line, I think Bob means "class E" where the printed text says "class F."—*73, Nathan O. Sokal, WA1HQC, President, Design Automation, Inc., 4 Tyler Rd., Lexington, MA 02173, +1 (781) 862-8998* **www.advancedpower.com**

***Author's reply:***

***Nat,***

Thanks for your interesting comments and references. I'm sure readers will find them useful if they choose to experiment further with the full-bridge platform.

I agree that for lower power levels there are better ways to modulate. I might look towards a forward converter design driving a linear output stage. The Holy Grail for us AM radio types is 1500 W PEP. The full-bridge is just beginning to "wake up" here, and I expect it would do very well at multi-kW power levels. I thought it worthwhile to introduce the full-bridge resonant converter as an alternative to the hard-switched, open-loop, low-frequency designs presently talked about. My choice of power level had more to do with the RF deck available to test the modulator than any other factor.

I didn't have any noise problems with the design as the auxiliary commutating inductor was an integral part of the project from the outset. I had been talking over the idea with a Web acquaintance, and he suggested looking at the Beirante/Beatriz paper. When speaking of noise we should include audio as well. I found out that failing to maintain soft switching will cause the magnetics to "sing" at the audio modulating frequencies and it's very annoying. At the lower limits of the modulation envelope, the current is low to begin with, and there is a substantial time period where this freewheeling current is decaying when in a zero state. The auxiliary commutating inductor helps here, and it's well worth the buck or so I spent for the core. Without this inductor, I suspect it would be more than a difficult task to maintain resonant switching. Again, the problem is "transistioning" from a zero state into an active state, and not the other way around. Both poles do not need the forcing current. As far as electrical noise goes, my creed is to minimize it at the source, rather than to deal with it at the problem end. I spend most of my time designing large inverters in the hard-switched world, where switching noise tends to be a very real problem.

See my notes concerning choosing output rectifiers and eliminating the resonating inductor in favor of two auxiliary commutating inductors. These points, along with your reference concerning diode clamps, may go a long way toward scaling the design to larger power levels.

I agree that bridge converter designs might not use a dc blocking capacitor or a gapped core. Most designs are for a fixed dc output voltage—I'm not aware of the full bridge previously being used to modulate an RF deck. While traversing up and down the modulation envelope, there will always be some offsets developed in the core—probably more so than in a fixed supply. In any case, for now I'll consider it some very inexpensive insurance.

The RF deck I run is a push-pull design loosely modeled after a paper I had read from the Caltech group. Class-E RF decks should work as well with this design.

Thanks again for your valued insight.—*73, Bob LaFrance, N9NEO, 21 Moorland Dr, Uxbridge, MA 01569;* **yzordderrex@verizon.net**

**Coaxial Traps for Multiband Antennas, the True Equivalent Circuit (Nov/Dec 2004)**

***Dear Editor,***

DG1MFT's paper should certainly cause some head scratching regarding the true representation of coaxial traps. The original work, on which he bases his analysis, is "Optimizing Coaxial-Cable Traps," Bob Sommer, N4UU, *QST*, Dec 1984, p 37.

In a letter to *QST*'s "Technical Correspondence" column in August 1985, Mason Logan, K4MT, showed that the actual inductance achieved is four times that calculated by Sommer, and the capacitance is one-quarter of that calculated. The net result is the same resonant frequency but four times greater values of both XL and XC at resonance.

The discrepancy in the values of L, C and X would appear to be carried over into the VE6YP computer program, also mentioned by DG1MFT. Once again, the trap will resonate at the correct frequency.

To test this, I built a trap, designed from the Sommer article and the VE6YP program, for 7.15 MHz. I confirmed the resonant frequency with a dip meter. The program calculated the inductance as 3.762 µH and the reactance at resonance as 169 Ω.

The measured inductance, however, using an L/C Meter IIB (from Almost All Digital Electronics), was almost 15 µH, four times the calculated value, just as K4MT suggested it would be. I later verified this value of inductance using an HP 4815A Vector Impedance Meter operating at 500 kHz (the lowest frequency available) so as to minimize the effect on the reading of the trap capacitance.

The differences in the values of inductance can be better understood if you consider that the current in the trap flows first through the center conductor and then through the braid, in the same current sense. This gives twice as many turns and four times as much inductance, inductance being proportional to turns squared.

The different values of L and C should make a significant difference in the results obtained when using an antenna design program such as *EZNEC* for a multiband trapped antenna. When measured at 3.6 MHz, my trap showed an inductive reactance of about 450 Ω.

Regards—*Ken Grant, VE3FIT;* **ve3fit@rac.ca**

***Author's reply***
***Dear Doug,***

Thank you for forwarding Ken's response to my article. I am aware that I am not the first who measured C, L, impedance and resonance frequency of a coaxial trap. However, I had no knowledge of Mason Logan's letter to *QST* in August 1985.[1] After all, the wrong impedance is still, today, included in a widely used program for coaxial-trap design. I started my paper with the contradiction between the values of C, L and resonance frequency. As far as I see, it is not self-evident that a quarter of the capacitance is effective and not a quarter of the inductance, as it is assumed, for example, in the freeware design program offered by VE6YP.

Therefore, the main intention of my article is to derive an easily understandable equivalent circuit for the coaxial trap, explaining how C and L act together. As a byproduct, it is also applicable for VHF. To my knowledge, this equivalent circuit has not been published.—*73, Karl-Otto Müller, DG1MFT, Watzmannstr, 24A, D-85586 POING, Germany*

***Further exchange:***
***Hello Karl-Otto and Doug,***

I have just checked again to confirm my readings. My 7.15 MHz trap reads 450 Ω inductive at 3.6 MHz and 365 Ω capacitive at 14.3 MHz. In other words, it conforms to the measured readings shown for Karl-Otto's trap shown in his Fig 5.

I think that Karl-Otto is correct in stating that the trap capacitance is C/4. That being so, however, the trap inductance must be 4L. At least, then, we wouldn't have to re-invent the formula for resonance.—*73, Ken, VE3FIT*

***Hello Ken,***

Referring to your second paragraph, I would like to point out that the effective capacitance C is in fact a quarter of the value that can be measured or calculated from the value (pF/m) of the respective cable (RG-58: 101 pF/m). This is one of the topics of my paper and is understood by you correctly.

*Nevertheless,* the inductance is not 4L but just L, namely the value that is measured with an inductance meter across the trap. It is, of course, four times the calculated value, if the calculation is done on basis of the single number of turns of the trap, which is in fact not correct, because the effective number of turns is 2N.

Conclusion: To find the real resonance frequency of a coaxial-cable trap, measure (or calculate from pF/m) the cable C, divide it by 4, take this value together with the measured value of the L and insert both values into Thomson's formula.—*73, DG1MFT, Karl-Otto*

[1]You can download an image of this page from the ARRL Web**www.arrl.org/qexfiles/**. Look for 1X05Trap.zip.

**HSMM Radio Equipment (Nov/Dec 2004)**

***Dear OM,***

In this article (and also in the 2005 *Handbook*), the need for access control to keep non-ham users out of HSMM networks is rightly mentioned. Nevertheless, the solution described doesn't work. Fortunately, a solution does work and completely avoids any regulatory issues.

The FCC regulations only serve to muddle the picture, because they spell out a few limited cases where encryption is legal (such as space telecommand stations, 47 CFR 97.211), thereby implying that encryption is necessary for that sort of situation. In fact, encryption is *not* necessary and not even helpful for access control and control-link protection. Consider an example.

If I send a command—say, "Turn on rocket for 10 seconds"—to a satellite, does it matter if everyone knows that? No, it does not—so long as no unauthorized person can successfully issue that command.

Conversely, suppose that the command were encrypted. If that's all I did—hide the meaning of the command, exactly as 97.211 puts it—someone could record the command when I sent it, then retransmit it again at some later time. In the security community, that's called a "replay attack," and encryption alone does not prevent it. Replay attacks work just fine—even if the attacker has no idea what the message means.

So, what are the security services that are actually needed on a control link, or any other situation where you want to limit access to authorized parties only? They are:

1. Who is sending this message?
2. Is the message I received exactly what the sender sent?
3. Did the sender send that just now, or did someone record it yesterday and retransmit it?

The important observation for Amateur Radio is that *all* those security services are available today *without* the use of data encryption. That means that they are available to everyone in the service: repeater control operators, auxiliary stations, satellite control, HSMM network operators—the FCC exception in 97.211 is completely unnecessary.

The data-security technology that enables this is the "keyed message authentication code" or "keyed cryptographic hash." It is essentially a digital signature on a message; it proves the originator and that it was not modified along the way. When combined with sequence numbers or time stamps, you also get replay protection. Those checking data are attached to the message, but the message itself goes out "in the clear." It is not encrypted, and the meaning of the message is not obscured.

There is readily available, free software that does those things quite efficiently. The Internet standard "IPSec" (IP Security) does all that. IPSec is a standard component of recent versions of Microsoft *Windows* and Mac *OS X* operating systems. It's a free (open-source) package available for *Linux* and other free operating systems. The amount of code needed is relatively modest.

The computing power needed for IPSec protection of control links is quite modest. Even for HSMM links operating at several megabits per second, IPSec data integrity takes only a modest fraction of the power of a reasonably modern processor.

Finally, IPSec, unlike WEP, is highly secure. It was designed with the full-time participation of many of the world's leading experts in data security, and many of the implementations have gone through rigorous testing.—*73, Paul Koning, NI1D;* **ni1d@arrl.net**

**Empirical Outlook (Nov/Dec 2004)**

***Editor,***

On pages 2 and 62, you entitled

Sagan's proof as "*Reductio Ad Absurdium*." Perhaps your spell checker doesn't cover Latin very well, because the last word in the title should be "*absurdum*."—*Arthur C. Hupp, K4GSP;* **arthupp@adelphia.net**

***RECTUS*! de Doug, KF6DX**

### *In the next issue of* QEX/Communications Quarterly

In "Antenna Options," L. B. Cebik, W4RNL, concludes his "Tale of Three Yagis" by exploring some of the construction options available for building small three-element Yagis—whatever the selected design and element material. The focus will not be on commercial construction, but rather on what can be accomplished in a typical home shop. □□